

NUMERICAL ANALYSIS OF SINGLE/ DOUBLE SIDED VENTILATION FOR A
ROOM WITH THE INFLUENCE OF SOLAR RADIATION IN DHAKA CITY

By

GOLAM MOSTAFA

Roll No.: 1015093010P

Session: October 2015

MASTER OF PHILOSOPHY

IN

MATHEMATICS








DEPARTMENT OF MATHEMATICS

BANGLADESH UNIVERSITY OF ENGINEERING AND TECHNOLOGY

DHAKA-1000

This thesis entitled “NUMERICAL ANALYSIS OF SINGLE/ DOUBLE SIDED VENTILATION FOR A ROOM WITH THE INFLUENCE OF SOLAR RADIATION IN DHAKA CITY”, submitted by GOLAM MOSTAFA, Roll No.: 1015093010P, Registration No.: 1015093010, Session: October 2015, has been accepted as satisfactory in partial fulfillment of the requirement for the degree of Master of Philosophy in Mathematics on 7th November 2020.

BOARD OF EXAMINERS

- (i) 
Dr. Md. Abdul Hakim Khan (Supervisor) Chairman
Professor
Department of Mathematics, BUET, Dhaka
- (ii) 
Head (Ex-Officio) Member
13/12/2020
Department of Mathematics, BUET, Dhaka
- (iii) 
Dr. Mohammed Forhad Uddin Member
Professor
Department of Mathematics, BUET, Dhaka
- (iv) 
Dr. Salma Parvin Member
Professor
Department of Mathematics, BUET, Dhaka
- (v) 
Dr. Md. Abdus Samad (External) Member
Professor
Department of Applied Mathematics
University of Dhaka, Dhaka-1000

DECLARATION OF AUTHORSHIP

I, Golam Mostafa, declare that this thesis titled, “NUMERICAL ANALYSIS OF SINGLE/ DOUBLE SIDED VENTILATION FOR A ROOM WITH THE INFLUENCE OF SOLAR RADIATION IN DHAKA CITY” and the work presented in this thesis is the outcome of the investigation carried out by me under the supervision of Dr. Md. Abdul Hakim Khan, Professor, Department of Mathematics, Bangladesh University of Engineering and Technology (BUET), Dhaka-1000 and that it has not been submitted anywhere for the award of any degree or diploma.



Golam Mostafa

DEDICATION

This thesis is dedicated

To

All of my well-wishers

ACKNOWLEDGEMENT

First of all I want to express my gratefulness to Almighty Allah, the most merciful, benevolent to mankind, for enabling me to complete the work successfully.

I have the privilege to express my deep respect, gratitude, and sincere appreciation to my supervisor Professor **Dr. Md. Abdul Hakim Khan**, Department of Mathematics, Bangladesh University of Engineering and Technology, Dhaka, who initiated me into the realm of mathematical research. Without his valuable guidance, constant encouragement and generous help it would have been difficult to complete this thesis. I am grateful to him for giving me the opportunity to work with him as a research student and for every effort that he made to get me on the right track of this thesis.

I would like to express my hearty gratitude to Head, Department of Mathematics, BUET, and all respected teachers of the Department of Mathematics, BUET, for their valuable guidance and suggestions.

I am also deeply grateful to Md. Rakibul Hasan, Lecturer, Department of Mathematics, DUET for his help and assistance in this research. Special thanks also go to the Officials and Computational Lab attendants and other staff who were always available for technical support. My sincere thanks to my colleagues and the authority of Hamdard University Bangladesh for providing me the necessary support and facilities during my research works.

Finally, I would like to express my deep regards to my family and friends for their steadfast love and support.

Abstract

The energy consumption of the world has been increasing day by day due to the population growth, the industrial development, and the technological advancement. In addition, according to the annual report of the Bangladesh Power Development Board (BPDB), the domestic sector is the largest energy consumption sector in Bangladesh. Moreover, the result of the study which was conducted by the Bangladesh Meteorological Department (BMD) is that the average monthly temperature of Dhaka city is increasing significantly. The usage of different electrical equipment for cooling has been boosting up over time which is responsible for this large energy consumption. One of the approaches for saving energy is to utilize natural ventilation which is an alternative heat consumption efficient solution for decreasing the heat consumption in buildings and keeping a healthy indoor environment. In a living room, solar radiation has a pivotal influence on the heat balance in a number of ways. So, it is the demand of time to use natural ventilation in buildings with solar radiation. The focus of this study is to live healthily and reduce the consumption of the mechanical system as well as build an energy efficient city by examining the wind profiles and temperature distributions on the inside and outsides of the buildings. In this research, a single room with single/double opening/s on the windward wall and the leeward wall has been studied using the Computational Fluid Dynamics (CFD) based on the Finite Element Method (FEM) with the influence of solar radiation. Three dimensional computational model with a cubic room for four different configurations is calculated in the context of weather in Dhaka city. The Reynolds- Averaged Navier-Stokes (RANS) equation is applied to the natural ventilation in the computational domain. The standard k- ϵ turbulence model is used in this study. The physical model is solved by commercial software COMSOL Multiphysics. According to wind direction, the information about the airflow, ventilation rate and average room temperature are calculated and presented in this research work. The temperature inside the room maintains the American Society of Heating, Refrigerating and Air-conditioning Engineers (ASHRAE) standard for all configurations. Based on the air quality and the volume average temperature, double openings in the windward wall are more comfortable than the other opening/s.

CONTENTS

Board of Examiners	ii
Declaration of Authorship	iii
Acknowledgement	v
Abstract	vi
Contents	vii
Nomenclature	ix
List of Figures	x
List of Tables	xvi
Chapter 1: Introduction	1
1.1 Introduction	1
1.2 Ventilation	2
1.3 Categories of Ventilation	3
1.4 Natural Ventilation	4
1.5 Natural Ventilation Principles	5
1.5.1 Single-sided Ventilation	5
1.5.2 Cross Ventilation	5
1.5.3 Stack Ventilation	5
1.6 Statement of the Problem	6
1.6.1 General Problem	6
1.6.2 Specific Problem	10
1.6.3 Research Problem	11
1.7 Literature Review	17
1.8 Importance of the Present Thesis Work	19
1.9 Aim	20
1.10 Objectives of this Thesis	20
1.11 Scope and Limitations of the Research	20
1.12 Thesis Plan	21

Chapter 2: Mathematical Model on Natural Ventilation	22
2.1 Introduction	22
2.2 Physical Models	23
2.3 Mathematical Model	28
2.3.1 Governing Equations	29
2.3.2 Boundary Conditions	32
2.4 Discretization Methods	32
2.5 Meshing of the Physical Models	34
2.6 Code Validation	40
2.7 Conclusion	42
Chapter 3: Natural Ventilation without Solar Radiation Effect	43
3.1 Introduction	43
3.2 Results and Discussion	43
3.2.1 Velocity Distribution	44
3.2.2 Pressure	94
3.2.3 Ventilation Rate	95
Chapter 4: Natural Ventilation with the Influence of Solar Radiation	98
4.1 Introduction	98
4.2 Results and Discussion	99
4.2.1 Velocity Distribution	99
4.2.2 Temperature Distribution	99
4.2.3 Ventilation Rate	124
4.2.4 Radiosity	125
Chapter 5: Conclusion	128
5.1 Conclusion	128
5.2 Future Work	129
References	131

Nomenclature

J	Radiosity
K	Von Karman's constant
k	Turbulent kinetic energy
p	Pressure
s	Seconds
t	Time
T	Temperature
u, v, w	Velocity component
x, y, z	Cartesian coordinates
U	Streamwise velocity component
C_p	Constant specific heat
l_t	Turbulence length scale
P_k	Production rate of turbulent kinetic energy
\dot{Q}_i	Net heat transfer
T_i	Turbulence intensity
U_0	Reference velocity
U_{avg}	Average flow velocity

Greek symbol

ρ	Density of fluid
μ	Dynamic viscosity
ν	Kinematic viscosity
κ	Thermal conductivity
ε	Turbulent dissipation rate

Subscripts

avg	Average
o	Reference
i	Surface

Abbreviation

ASHRAE	American Society of Heating, Refrigerating and Air-conditioning Engineers
CFD	Computational Fluid Dynamics
HVAC	Heating, Ventilation, and Air-Conditioning
IEA	International Energy Agency
LES	Large-eddy simulation
RANS	Reynolds averaged Navier–Stokes equation
BMD	Bangladesh Meteorological Department

List of Figures

Figure No.	Name of the Figure	Page No.
Figure 1.1	Three basic ventilation principles	6
Figure 1.2	Consumption pattern in Bangladesh	7
Figure 1.3	Present installed generation capacity in Bangladesh	7
Figure 1.4	Consumer growth in Bangladesh	9
Figure 1.5	Net generation in Bangladesh	9
Figure 1.6	Category wise total expenses in Bangladesh	10
Figure 1.7	Location of Dhaka, Bangladesh	12
Figure 1.8	Average Temperature in Dhaka City	12
Figure 1.9	Maximum Temperature in Dhaka City	13
Figure 1.10	Minimum Temperature in Dhaka City	13
Figure 1.11	Seasonal wind direction at Dhaka based on wind speed data.	14
Figure 1.12	Wind Speed in Dhaka City	14
Figure 1.13	The absorption, reflection, and transmission of irradiation by a semi-transparent material	16
Figure 2.1	Schematic view of the building model	24
Figure 2.2	Two dimensional (2D) view of the computational domain and logarithmic wind profile	25
Figure 2.3	Three dimensional (3D) view of the computational domain	25
Figure 2.4	3D view of the computational domain for windward face ((a) case 1 and (b) case 3)	25
Figure 2.5	3D view of the location and arrangement of the opening/s for windward face ((a) case 1 and (b) case 3)	26
Figure 2.6	2D view of the location and arrangement of the opening/s for windward face ((a) case 1 and (b) case 3)	26
Figure 2.7	3D view of the location and arrangement of the opening/s for leeward face ((a) case 2 and (b) case 4)	27
Figure 2.8	2D view of the location and arrangement of the opening/s for leeward face ((a) case 2 and (b) case 4)	27

Figure 2.9	Computational domain (3D view of xy -plane)	28
Figure 2.10	Basic steps to perform a finite element analysis in this research	33
Figure 2.11	Meshing of windward wall with an opening (case 1)	35
Figure 2.12	Meshing of leeward wall with an opening (case 2)	35
Figure 2.13	Meshing of windward wall of double openings (case 3)	36
Figure 2.14	Meshing of leeward wall with double openings (case 4)	37
Figure 2.15(a)	Meshing of case 1 for 2D	37
Figure 2.15(b)	Meshing of case 1 for 2D, close view	37
Figure 2.16(a)	Meshing of case 2 for 2D	38
Figure 2.16(b)	Meshing of case 2 for 2D, close view	38
Figure 2.17(a)	Meshing of case 3 for 2D	39
Figure 2.17(b)	Meshing of case 3 for 2D, close view	39
Figure 2.18(a)	Meshing of case 3 for 2D	39
Figure 2.18(b)	Meshing of case 3 for 2D, close view	39
Figure 2.19	Locations of the vertical lines	40
Figure 2.20	Code validation of the model	41
Figure 3.1	Locations of velocity measurements	44
Figure 3.2	Velocity distribution at $t = 0.5$ s for single-sided ventilation with an opening on the windward wall (Case 1)	47
Figure 3.3	Velocity distribution at $t = 1$ s for single-sided ventilation with an opening on the windward wall (Case 1)	48
Figure 3.4	Velocity distribution at $t = 1.5$ s for single-sided ventilation with an opening on the windward wall (Case 1)	49
Figure 3.5	Velocity distribution at $t = 2$ s for single-sided ventilation with an opening on the windward wall (Case 1)	50
Figure 3.6	Velocity distribution at $t = 2.5$ s for single-sided ventilation with an opening on the windward wall (Case 1)	51
Figure 3.7	Velocity distribution at $t = 3$ s for single-sided ventilation with an opening on the windward wall (Case 1)	52
Figure 3.8	Velocity distribution at $t = 5$ s for single-sided ventilation with an opening on the windward wall (Case 1)	53

Figure 3.9	Velocity distribution at $t = 10$ s for single-sided ventilation with an opening on the windward wall (Case 1)	54
Figure 3.10	Velocity distribution at $t = 15$ s for single-sided ventilation with an opening on the windward wall (Case 1)	55
Figure 3.11	Velocity distribution along vertical direction at $t = 3$ s for single-sided ventilation with an opening on the windward wall (Case 1)	56
Figure 3.12	Velocity distribution at $t = 0.5$ s for single-sided ventilation with an opening on the leeward wall (Case 2)	57
Figure 3.13	Velocity distribution at $t = 1$ s for single-sided ventilation with an opening on the leeward wall (Case 2)	58
Figure 3.14	Velocity distribution at $t = 1.5$ s for single-sided ventilation with an opening on the leeward wall (Case 2)	59
Figure 3.15	Velocity distribution at $t = 2$ s for single-sided ventilation with an opening on the leeward wall (Case 2)	60
Figure 3.16	Velocity distribution at $t = 2.5$ s for single-sided ventilation with an opening on the leeward wall (Case 2)	61
Figure 3.17	Velocity distribution at $t = 3$ s for single-sided ventilation with an opening on the leeward wall (Case 2)	62
Figure 3.18	Velocity distribution at $t = 5$ s for single-sided ventilation with an opening on the leeward wall (Case 2)	63
Figure 3.19	Velocity distribution at $t = 10$ s for single-sided ventilation with an opening on the leeward wall (Case 2)	64
Figure 3.20	Velocity distribution at $t = 15$ s for single-sided ventilation with an opening on the leeward wall (Case 2)	65
Figure 3.21	Velocity distribution along vertical direction at $t = 3$ s for single-sided ventilation with an opening on the leeward wall (Case 2)	66
Figure 3.22	Velocity distribution at $t = 0.5$ s for single-sided ventilation with double openings on the windward wall (Case 3)	67
Figure 3.23	Velocity distribution at $t = 1$ s for single-sided ventilation with double openings on the windward wall (Case 3)	68
Figure 3.24	Velocity distribution at $t = 1.5$ s for single-sided ventilation with double openings on the windward wall (Case 3)	69

Figure 3.25	Velocity distribution at $t = 2$ s for single-sided ventilation with double openings on the windward wall (Case 3)	70
Figure 3.26	Velocity distribution at $t = 2.5$ s for single-sided ventilation with double openings on the windward wall (Case 3)	71
Figure 3.27	Velocity distribution at $t = 3$ s for single-sided ventilation with double openings on the windward wall (Case 3)	72
Figure 3.28	Velocity distribution at $t = 5$ s for single-sided ventilation with double openings on the windward wall (Case 3)	73
Figure 3.29	Velocity distribution at $t = 10$ s for single-sided ventilation with double openings on the windward wall (Case 3)	74
Figure 3.30	Velocity distribution at $t = 15$ s for single-sided ventilation with double openings on the windward wall (Case 3)	75
Figure 3.31	Velocity distribution along vertical direction at $t = 3$ s for single-sided ventilation with double openings on the windward wall (Case 3)	76
Figure 3.32	Velocity distribution at $t = 0.5$ s for single-sided ventilation with double openings on the leeward wall (Case 4)	77
Figure 3.33	Velocity distribution at $t = 1$ s for single-sided ventilation with double openings on the leeward wall (Case 4)	78
Figure 3.34	Velocity distribution at $t = 1.5$ s for single-sided ventilation with double openings on the leeward wall (Case 4)	79
Figure 3.35	Velocity distribution at $t = 2$ s for single-sided ventilation with double openings on the leeward wall (Case 4)	80
Figure 3.36	Velocity distribution at $t = 2.5$ s for single-sided ventilation with double openings on the leeward wall (Case 4)	81
Figure 3.37	Velocity distribution at $t = 3$ s for single-sided ventilation with double openings on the leeward wall (Case 4)	82
Figure 3.38	Velocity distribution at $t = 5$ s for single-sided ventilation with double openings on the leeward wall (Case 4)	83
Figure 3.39	Velocity distribution at $t = 10$ s for single-sided ventilation with double openings on the leeward wall (Case 4)	84

Figure 3.40	Velocity distribution at $t = 15$ s for single-sided ventilation with double openings on the leeward wall (Case 4)	85
Figure 3.41	Velocity distribution along vertical direction at $t = 3$ s for single-sided ventilation with double openings on the leeward wall (Case 4)	86
Figure 3.42	Velocity distribution for all cases (case 1: S W, Case 2: S L, Case 3: D W, case 4: D L) at $t = 3$ s	87
Figure 3.43	Velocity distribution along vertical direction for all cases (case 1: S W, Case 2: S L, Case 3: D W, Case 4: D L) at $t = 3$ s	88
Figure 3.44	Velocity distribution for all cases in computational domain (Dash dot dot line: Section A, Solid line: Section B, Dashed line: Section C) at $t = 3$ s	89
Figure 3.45	Velocity distribution for all cases in XY plane at $t = 15$ s	90
Figure 3.46	Air flow distribution in computational domain for all cases at $t = 15$ s	91
Figure 3.47	Air flow distribution in cubic building for all cases at $t = 15$ s	92
Figure 3.48	Velocity stream lines in computational domain for all cases at $t = 5$ s	93
Figure 3.49	Velocity stream lines in cubic building for all cases at $t = 15$ s	94
Figure 3.50	Pressure distribution for all cases in xy plane at $t = 15$ s	95
Figure 4.1	Temperature distribution in section A for four cases at $t = 3$ s	101
Figure 4.2	Temperature distribution in section B for four cases at $t = 3$ s	102
Figure 4.3	Temperature distribution in section C for four cases at $t = 3$ s	103
Figure 4.4	Temperature distribution in section A for four cases at $t = 5$ s	104
Figure 4.5	Temperature distribution in section B for four cases at $t = 5$ s	105
Figure 4.6	Temperature distribution in section C for four cases at $t = 5$ s	106
Figure 4.7	Temperature distribution in section A for four cases at $t = 10$ s	107
Figure 4.8	Temperature distribution in section B for four cases at $t = 10$ s	108
Figure 4.9	Temperature distribution in section C for four cases at $t = 10$ s	109
Figure 4.10	Temperature distribution in section A for four cases at $t = 15$ s	110
Figure 4.11	Temperature distribution in section B for four cases at $t = 15$ s	111
Figure 4.12	Temperature distribution in section C for four cases at $t = 15$ s	112

Figure 4.13	Temperature distribution in section A for four cases at $t = 30 s$	113
Figure 4.14	Temperature distribution in section B for four cases at $t = 30 s$	114
Figure 4.15	Temperature distribution in section C for four cases at $t = 30 s$	115
Figure 4.16	Temperature distribution in section A for four cases at $t = 60 s$	116
Figure 4.17	Temperature distribution in section B for four cases at $t = 60 s$	117
Figure 4.18	Temperature distribution in section C for four cases at $t = 60 s$	118
Figure 4.19	Temperature distribution in section A (Dash Dot Dot), section B (Solid line), section C (Dashed) for all cases at $t = 60 s$	119
Figure 4.20	Surface temperature in computational domain for all cases at $t = 60 s$	120
Figure 4.21	Surface temperature in building for all cases at $t = 60 s$	121
Figure 4.22	Isosurface in computational domain for all cases at $t = 60 s$	122
Figure 4.23	Isosurface in building for all cases at $t = 60 s$	123
Figure 4.24	Surface radiosity in computational domain for all cases at $t = 60 s$	126
Figure 4.25	Surface radiosity in building for all cases at $t = 60 s$	127

List of Tables

Table No.	Name of the Table	Page No.
Table 1.1	Year Wise Per Capita Consumption (Grid)	8
Table 1.2	Under-heated, comfortable and over-heated period in Dhaka	15
Table 1.3	Climate chart of Dhaka for 2018	17
Table 2.1	Constants for the Turbulence Model	31
Table 2.2	Meshing for case 1 in 3D	35
Table 2.3	Meshing for case 2 in 3D	36
Table 2.4	Meshing for case 3 in 3D	36
Table 2.5	Meshing for case 4 in 3D	37
Table 2.6	Meshing for case 1 in 2D	38
Table 2.7	Meshing for case 2 in 2D	38
Table 2.8	Meshing for case 3 in 2D	39
Table 2.9	Meshing for case 4 in 2D	39
Table 3.1	Ventilation rate for windward single opening (case 1)	96
Table 3.2	Ventilation rate for leeward single opening (case 2)	96
Table 3.3	Ventilation rate for windward double openings (case 3)	97
Table 3.4	Ventilation rate for leeward double openings (case 4)	97
Table 4.1	Volume Average Temperature (K) in the room at noon	124
Table 4.2	Ventilation Rate for all cases at noon	125

A fluid, according to Mc Donough, is a substance that is capable to flow, no matter how small the amount is. Though the work of Leonardo Da Vinci gave rapid advancement to the study of fluid mechanics more than 500 years ago, fluid behavior was much more available by the time of ancient Egyptians. Enough practical information had been gathered during the Roman Empire to allow fluid dynamics application. A more modern understanding of fluid motion was begun through Bernoulli's equation several centuries ago. Since then, many researchers have done numerous works on fluid mechanics. The aim of this study is to present the fundamentals of the flows that occur in buildings, to describe how they are set up and the effects they have on the occupants' comfort. The energy consumption of the building and the fluid mechanics of building ventilation are described in this chapter.

1.1 Introduction

The phenomenon of global warming is mainly caused by human activities. The change in the climate system, from macro-scale (continent or country size) to mesoscale (state or county) or even down to micro-scale (city block or garden), resulted from the global warming phenomenon and has become a serious issue that the mankind is facing, as it can seriously harm the economies, societies, and ecosystems worldwide [1, 2]. In order to avoid reversals in human development and catastrophic risks to future generations, it is necessary to act against global warming with a sense of urgency.

Energy consumption for heating, cooling, and ventilating buildings often accounts for the largest part of a country's energy usage, which is still mainly based on fossil fuels. There is a great global emphasis on reducing the reliance of buildings on fossil fuel energy and a move toward Nearly Zero Carbon Buildings (NZCB). This requires a major shift in the way buildings and their integrated heating, cooling, and ventilation systems are designed, operated, and maintained. Achieving this goal will require a rethink of the traditional designs and types of systems currently in use. The proportion of ventilation energy in comparison with the total energy use in a building is expected to increase as the building fabric energy performance improves and ventilation standards commend higher ventilation rates for improving indoor air quality (IAQ). At the same time, new building regulations are imposing air-tight construction, which will inevitably impact on IAQ, health (e.g., sick building syndrome), and human

productivity in some future buildings. Despite recent advances in building ventilation, it is evident that complaints about poor IAQ have increased in recent years. There is a need, therefore for assessing current methods of building ventilation and developing ventilation systems that are capable of providing good IAQ and energy performance to satisfy building occupants and meet new building energy codes.

Future Development in ventilation and air distribution, room air distribution, and ventilation techniques have greatly been improved in the last 40–50 years. However, this important field of heating, ventilation, and air conditioning (HVAC), which has a direct impact on people's health and productivity, has the potential for greater development as some commonly used methods are not always suitable for delivering the IAQ demanded by the building occupants and at the same time meeting stricter energy performance guidelines. As increased awareness of the impact of ventilation on human health and productivity is expected to become more topical, it is anticipated that more advances in the delivery of fresh air to occupants will be foreseen to meet people's aspirations. It would be expected therefore that:

- the unconventional methods of room air distribution will become more commonly used.
- wider application of demand control ventilation (DCV), i.e., a direct link of fresh air supply to IAQ will be expected.
- more reliance on using simulation tools for visualizing room air movement, such as computational fluid dynamics (CFD), to improve our prediction of the performance of ventilation systems at the design stage will be seen.
- there will be a move toward more energy efficient methods of room air distribution.
- there will be a demand for the improvement of the quality assurance and maintenance procedures for ventilation systems.

1.2 Ventilation

Ventilation is the intentional introduction of ambient air into space and is mainly used to control indoor air quality by diluting and displacing indoor pollutants; it can also be used for the purposes of thermal comfort or dehumidification. The correct introduction of ambient air will help to achieve desired indoor comfort levels although the measure of an ideal comfort level varies from individual to individual.

The intentional introduction of subaerial air can be categorized as either mechanical ventilation, or natural ventilation. Mechanical ventilation uses fans to drive the flow of subaerial air into a building. This may be accomplished by pressurization (in the case of positively pressurized buildings), or by depressurization (in the case of exhaust ventilation systems). Many mechanically ventilated buildings use a combination of both, with the ventilation being integrated into the HVAC system. Natural ventilation is the intentional passive flow of subaerial air into a building through planned openings (such as louvers, doors, and windows). Natural ventilation does not require mechanical systems to move subaerial air, it relies entirely on passive physical phenomena, such as diffusion, wind pressure, or the stack effect. Mixed mode ventilation systems use both mechanical and natural processes. The mechanical and natural components may be used in conjunction with each other or separately at different times of day or season of the year. Since the natural component can be affected by unpredictable environmental conditions it may not always provide an appropriate amount of ventilation. In this case, mechanical systems may be used to supplement or to regulate the naturally driven flow.

In many instances, ventilation for indoor air quality is simultaneously beneficial for the control of thermal comfort. At these times, it can be useful to increase the rate of ventilation beyond the minimum required for indoor air quality. Ventilation should be considered for its relationship to "venting" for appliances and combustion equipment such as water heaters, furnaces, boilers, and wood stoves. Most importantly, the design of building ventilation must be careful to avoid the backdraft of combustion products from "naturally vented" appliances into the occupied space. This issue is of greater importance in new buildings with more air tight envelopes. To avoid the hazard, many modern combustion appliances utilize "direct venting" which draws combustion air directly from outdoors, instead of from the indoor environment.

1.3 Categories of Ventilation

- **Mechanical ventilation** refers to any system that uses mechanical means, such as a fan, to introduce sub aerial air to a space. This includes positive pressure ventilation, exhaust ventilation, and balanced systems that use both supply and exhaust ventilation.
- **Natural ventilation** refers to intentionally designed passive methods of introducing sub aerial to a space without the use of mechanical systems.
- **Mixed mode ventilation** (or **hybrid ventilation**) systems use both natural and mechanical processes.

- **Infiltration** is the uncontrolled flow of air from outdoors to indoors through leaks (unplanned openings) in a building envelope. When a building design relies on environmentally driven circumstantial infiltration to maintain indoor air quality, this flow has been referred to as adventitious ventilation.

1.4 Natural Ventilation

Natural ventilation is the process of supplying air to and removing air from an indoor space without using mechanical systems. It refers to the flow of external air to an indoor space as a result of pressure differences arising from natural forces. There are two types of natural ventilation occurring in buildings: wind-driven ventilation and buoyancy-driven ventilation. Wind-driven ventilation arises from the different pressures created by wind around a building or structure, and openings being formed on the perimeter which then permits flow through the building. On the other hand, Buoyancy-driven ventilation occurs as a result of the directional buoyancy force that results from temperature differences between the interior and the exterior. Since the internal heat gains which create temperature differences between the interior and the exterior are created by natural processes, including the heat from people, and wind effects are variable, naturally ventilated buildings are sometimes called "breathing buildings". Natural ventilation, used to be the most common method of allowing fresh outdoor air to replace indoor air in a residence. Today, it is usually not the best ventilation strategy, especially for residences that are properly air sealed for energy efficiency. Natural ventilation also usually does not provide adequate moisture control. Natural ventilation occurs when there is uncontrolled air movement or infiltration through cracks and small holes in a residence—the same ones people want to seal to make their residence more energy efficient. Opening windows and doors also provides natural ventilation. Because of central heating and cooling systems, however, most people don't open windows and doors as often. Therefore, air infiltration has become the principal mode of natural ventilation in houses.

A residence's natural ventilation rate is unpredictable and uncontrollable, so it can not be relied on it to ventilate a house uniformly. Natural ventilation depends on a house's airtightness, outdoor temperatures, wind, and other factors. Therefore, during mild weather, some houses may lack sufficient natural ventilation for pollutant removal. On the other hand, tightly sealed houses may have insufficient natural ventilation most of the time, while houses with high air infiltration rates may experience high energy costs.

The American Society of Heating, Refrigerating, and Air-Conditioning Engineers (ASHRAE) recommends intermittent or continuous ventilation rates for bathrooms and kitchens instead of using windows (natural ventilation): 50 or 20 cubic feet per minute for bathrooms, and 100 or 25 cubic feet per minute for kitchens, respectively.

Natural ventilation can also be achieved through the use of operable windows; this has largely been removed from most current architecture buildings due to the mechanical system continuously operating. In Europe, designers have experimented with design solutions that will allow for natural ventilation with minimal mechanical interference. These techniques include building layout, facade construction, and materials used for inside finishes. European designers have also switched back to the use of operable windows to solve indoor air quality issues.

1.5 Natural Ventilation Principles

The driving forces in natural ventilation are thermal buoyancy and wind pressure on buildings. The design of the building, the form of window openings and location have a significant impact on the quality of the indoor climate. Natural ventilation is driven by three basic ventilation principles shown in Figure 1.1.

1.5.1 Single-sided Ventilation

Opening in a single side can create single-sided ventilation in a room. The amount of fresh air coming into the room is limited by single-sided ventilation.

1.5.2 Cross Ventilation

Openings in two or more facades can create cross-ventilation in a room. The ventilation is powered by difference in wind pressure on the facades in which the window openings are located. The easiest way to understand wind-based or wind-driven ventilation is to look at an open window. Fresh air comes in through one side, moves throughout the building, and then goes out through the opposite side, pushing the stagnant warm air that was in the building along with it.

1.5.3 Stack Ventilation

Caused by a height difference between openings, i.e. between facade and roof window. The ventilation is primarily driven by warm air rising to the top creating a pressure difference.

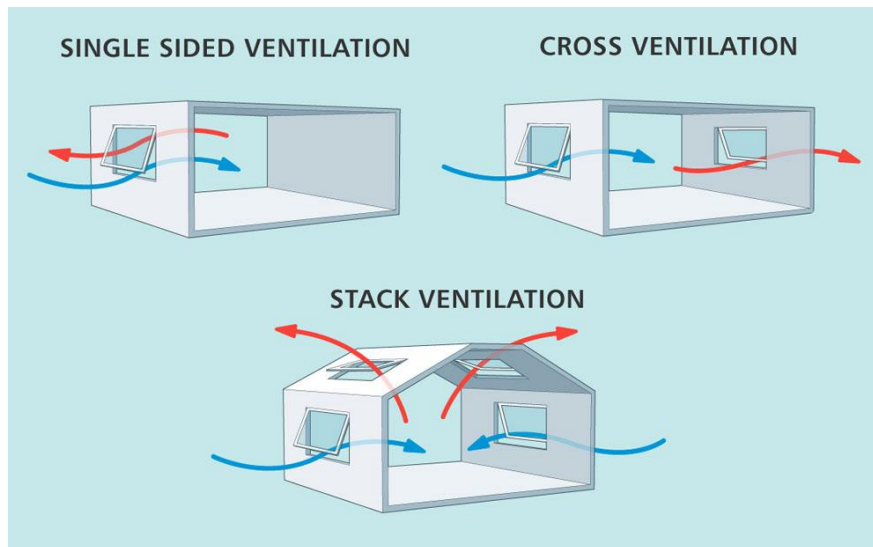


Figure 1.1: Three basic ventilation principles, source: www.tealproducts.com

1.6 Statement of the Problem

1.6.1 General Problem

Bangladesh is a low lying deltaic country of South Asia. It is a small but world's 8th-most populous country with nearly 163 million people and is the 92nd-largest country in land area, spanning 147,570 square kilometers. It is one of the most densely populated countries in the world with a density of 1116 people per square kilometer and the growth rate is 1.01%. Bangladesh has been identified as one of the most vulnerable countries in the world in terms of climate change. Some even argue, climate change is no longer a threat for Bangladesh, it has already affected the country [3-4]. Sea level rise, floods, drought, cyclone, salinity, waterlogging, and unplanned urbanization are some of the major environmental challenges that the country faces due to global climate change.

The heat consumption requirement has increased at a rate of 2 % per year for the past 25 years and it will increase continuously at the same rate if current heat consumption patterns persist, according to the International Energy Agency (IEA) [5]. Energy is used for heating and cooling purposes in most of the office and residential buildings in urban society. According to the Bangladesh Power Development Board (BPDB), the largest energy consumers in Bangladesh are the residential sector, followed by industries, commercial and agricultural sectors which are shown in Figure 1.2 and increasing day by day. There is an enormous demand for electricity, oil, gas, and natural resources in the agriculture, industry and service sector as well

as the daily life of Bangladesh. Now 95% of the total population of Bangladesh has access to electricity facilities.

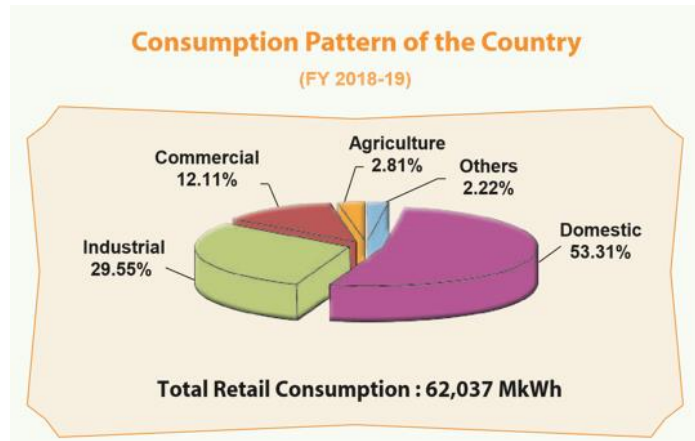


Figure 1.2: Consumption pattern in Bangladesh, source: BPDB

Electricity plays the most basic role in the economic growth through the sustainable structure as well as poverty eradication and security of any country. A reliable electricity supply is a vital issue for the world today. Future economic growth crucially depends on the long-term availability of electricity which is affordable, available, and environment friendly. Security, climate change, and public health are closely interrelated with electricity. Bangladesh Government has designed an extensive power generation plan to create sustainable growth in the power sector and for the overall development of the country's economy. Figure 1.3 shows the present installed generation capacity in public, private, and import sectors which is 18,961 MW generated from natural gas, furnace oil, hydro, diesel, and coal as in June 2019 [6].

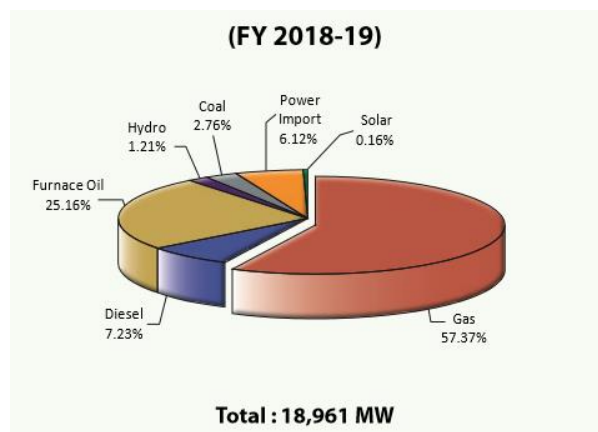


Figure 1.3: Present installed generation capacity in Bangladesh, source: BPDB

According to the Power System Master Plan (PSMP), the Government has set a target to increase installed electricity generation capacity to 21000 MW by 2021 and 57,000 MW by

2041. Table 1.1 shows the growth of electricity consumption per capita in Bangladesh from 2001-02 to 2018-19. The demand for electricity is increasing rapidly due to enhanced economic activities in the country with sustained GDP growth. At present, the growth of demand is about 10% which is expected to be more in the coming years shown in Figure 1.4.

Table 1.1: Year Wise Per Capita Consumption (Grid), source: BPDB

Year	Total Generation (GWh)	Per Capita Consumption (kWh)
2001-02	17,445	113.80
2002-03	18,458	122.43
2003-04	20,302	133.11
2004-05	21,408	139.68
2005-06	22,978	150.22
2006-07	23,268	149.97
2007-08	24,946	158.20
2008-09	26,533	165.32
2009-10	29,247	170.27
2010-11	31,355	180.08
2011-12	35,118	197.72
2012-13	38,229	213.15
2013-14	42,195	232.56
2014-15	45,836	249.16
2015-16	52,193	281.36
2016-17	57,276	308.22
2017-18	62,678	335.99
2018-19	70,533	374.62

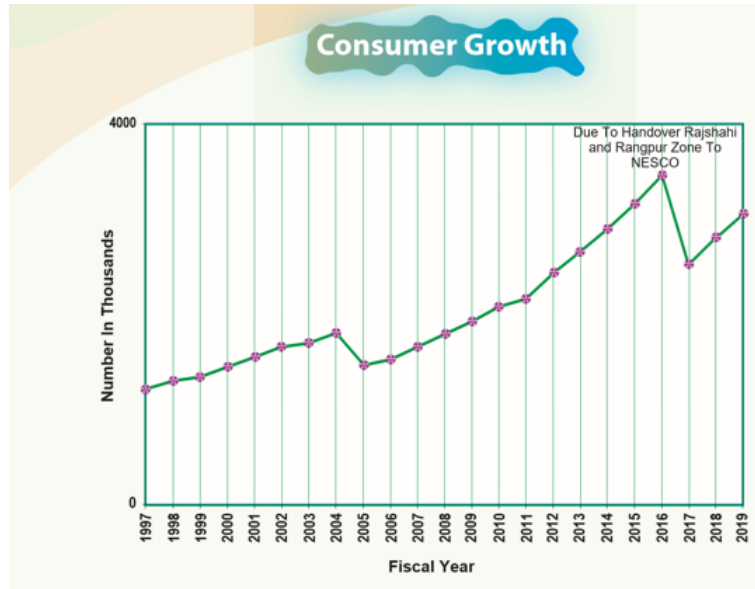


Figure 1.4: Consumer growth in Bangladesh, source: BPDB

Alam et al. [7] stated that Bangladesh has small reserves of oil and coal, but a large amount of natural gas resource. Figure 1.5 shows the total net energy generation in FY 2018-19 which was 70,533 MkWh. Net energy generation in the public sector was 35,107 MkWh and 28,640 MkWh was in the private sector (including REB). Another 6,786 MkWh was imported from India through the interconnection in Bheramara and Tripura. In Bangladesh, 48,306 MkWh (68.49%) of electricity is generated from natural gas, 11,426 MkWh (16.20%) from Furnace oil, 725 MkWh (1.03%) from hydro, 2,022 MkWh (2.87%) from diesel and 1,230 MkWh (1.74%) from coal.

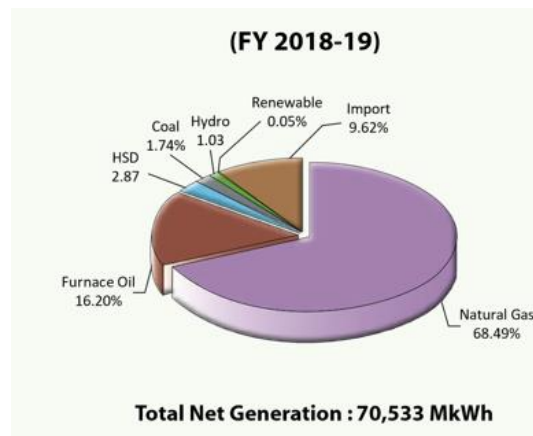


Figure 1.5: Net generation in Bangladesh, source: BPDB

During the peak summertime, from mid-March to mid-October, electricity use goes up to its highest level because of hot weather as well as a huge need for irrigation. Besides, electricity

demand is increasing whereas the available generation also increases against demand which creates a deficit. This deficit leads to extensive load shedding. Other problems in Bangladesh’s electric power sector include high system losses, delays in completion of new plants, low plant efficiencies, erratic power supply, electricity theft, blackouts, and shortages of funds for power plant maintenance. According to the annual report 2018-19 of Bangladesh Power Development Board (BPDB), the total expense is Tk. 42648.22 crores which are for electric purchase, distributions, maintenances, and others shown in figure 1.6.

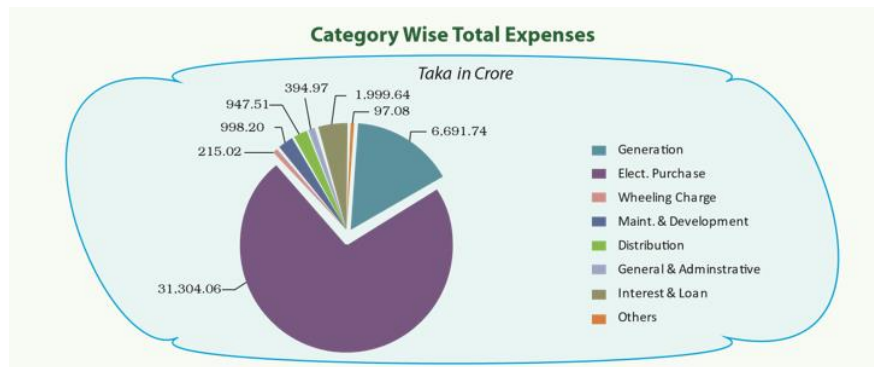


Figure 1.6: Category wise total expenses in Bangladesh, source: BPDB

1.6.2 Specific Problem

Dhaka, the capital and largest city of Bangladesh. It is the sixth-largest and sixth-most densely populated city in the world, with a density of 23,234 people per square kilometer within a total area of 300 square kilometers. The population of Dhaka in 2019 as per estimates is 20.628 Million. It is noticed that the population in the past 5 years has gone up by 3.94 Million. Also, each year the population increases by 0.788 Million as per aggregate. Dhaka city’s population is expected to grow at a rate of 3.6% annually and reach a total of 21005860 in 2020. According to the Department of International Development (DFID), migration is most prominent in Dhaka. Most of its population are rural migrants [8]. The adverse consequences of increased warming, climate variability for livelihoods, public health, food security, and water availability may also lead to migration. This migrated population is increasing day by day. Reza [9] stated that to accommodate the growing population, the Dhaka city would need new units/flats and these new units need more consumption of energy.

According to the annual report 2018-2019 of Dhaka Power Distribution Company Limited (DPDC) [10], the user of electricity is 1298733 and the maximum electricity demand is 1670.50 MW. At present, the monthly mean uses of electricity are 585 KWh per person, and the growth of demand is about 8.61% which is expected to be more in the coming years. The sector-wise

use of electricity in Dhaka City is residential (51.54%), industrial (23.38%), commercial (17.84%) and others (7.24%). Most of the increased demand for electricity is due to the increased standard of living among the wealthier income groups. One of the major factors in the increased use of electricity by the higher income group is the use of air conditioning units, which has only recently become quite popular [11]. Vangtook and Chirarattananon [12] have acknowledged that air conditioners are increasingly used in hot and humid regions to attain thermal comfort. However, they argue that air conditioning is highly energy intensive and suggests developing alternative energy efficient means to achieve comfort. Moreover, a study of the regulations in the national building code of Bangladesh shows that the building codes do not address the issues of energy efficiency in any building category. Architects and developers of residential buildings, too, have not considered ways in which energy use can be reduced.

The specific problems that signify the importance of energy efficiency in residential buildings are as follows:

- high-energy use of residential buildings in Dhaka,
- growing population and rising number of apartments,
- increased standard of living that would further add to energy usage and interrupted power supply due to power deficits.

1.6.3 Research Problem

Since the building sector is a major consumer of electricity, it is essential to evolve energy-efficient building designs that can be used to provide thermal comfort. So, it is important to analyze the climate scenario for Dhaka and understand the typical thermal behavior of buildings. Knowledge of the thermal behavior of the building envelope is crucial to control the amount of heat that goes into a building space. Buildings will cause thermal discomfort if an effective strategy is not adopted to reduce the extra heat going into it. According to Zain *et al.* [13], factors that influence thermal comfort in humans include outdoor air temperature, relative humidity, and airflow. Various strategies are needed to facilitate airflow for improving thermal comfort.

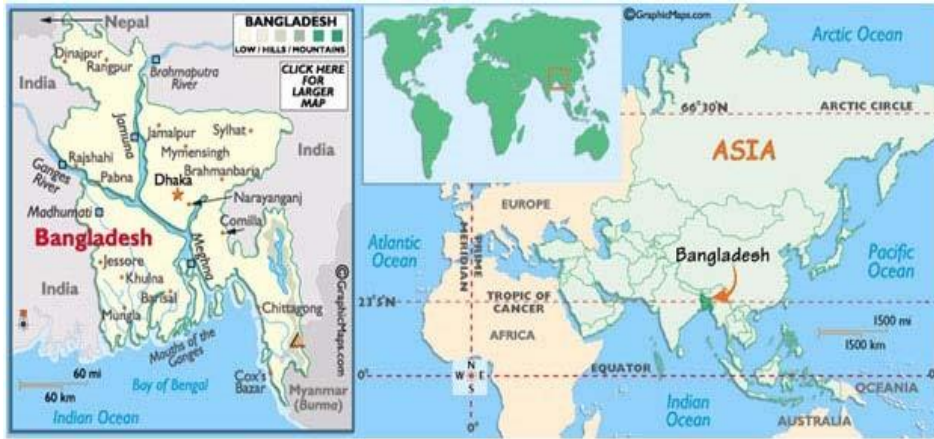


Figure 1.7. Location of Dhaka, Bangladesh, Source: World Atlas Travel

Figure 1.7 shows that Dhaka is located in central Bangladesh at $23^{\circ}42'0''N$ $90^{\circ}22'30''E$. The climate of Dhaka can be categorized as a tropical monsoon type with an annual average temperature of $26^{\circ}C$ and monthly means varying between $18.5^{\circ}C$ in January and $30^{\circ}C$ in June shown in Figure 1.8. The climate is characterized by high temperatures, high humidity most of the year, and distinctly marked seasonal variations in precipitation. According to meteorological conditions the year can be divided into four seasons, pre-monsoon (March–May), monsoon (June–September), post-monsoon (October–November), and winter (December–February).

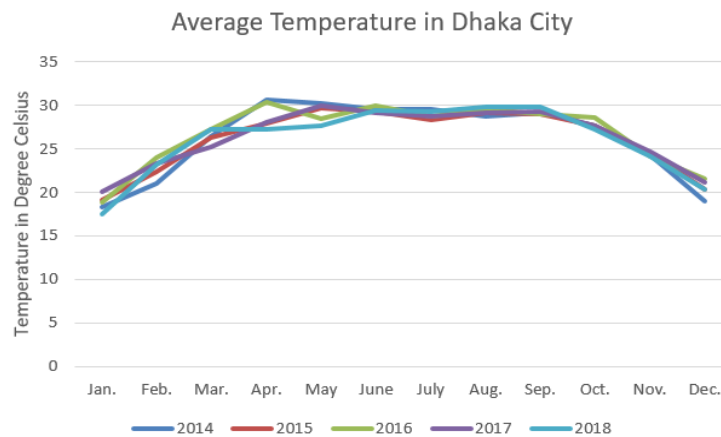


Figure 1.8: Average Temperature in Dhaka City

From Figure 1.9-1.12, it is clear that the pre-monsoon or summer season is generally hot and sunny. The hottest month is April. The mean monthly maximum temperature hovers around $37 - 38^{\circ}C$ and the mean monthly minimum varies around $19 - 20^{\circ}C$. Approximately 15% of the annual rainfall occurs in this season. During summer, winds are mainly from the southwest.

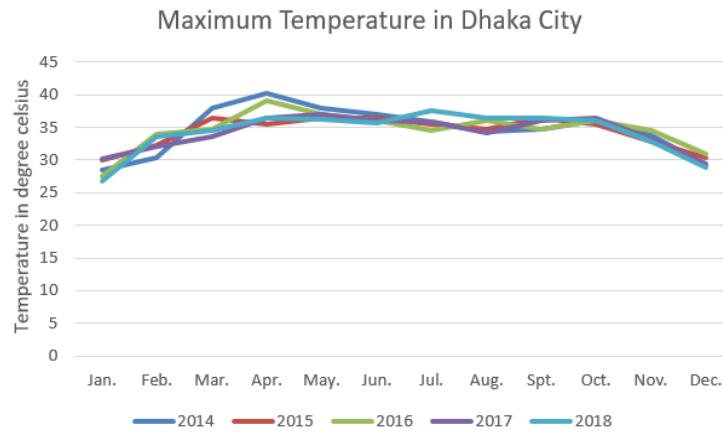


Figure 1.9: Maximum Temperature in Dhaka City

The monsoon or rainy season is characterized by high rainfall, humidity, and cloudiness. About 80% of the annual rainfall occurs in this period. The month of June is cool due to the cooling effect of the rains. This season experiences mean maximum temperatures of around 36.5°C and mean minimum temperatures of around 23.5 °C. Humidity is around 80%. During the monsoon or rainy season, winds are from the southeast.

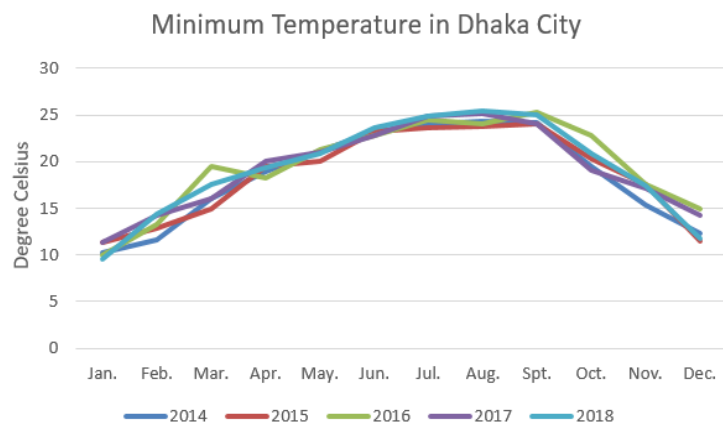


Figure 1.10: Minimum Temperature in Dhaka City

The post-monsoon is the transition period from monsoon to winter. In the post-monsoon season, the rainfall and relative humidity decrease along with the wind speed. In this period, the prevailing wind direction is from the northeast.

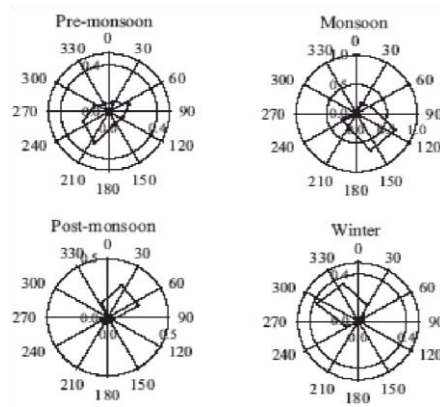


Figure 1.11: Seasonal wind direction at Dhaka based on wind speed data, Source: Khan et al. [14]

The winter or dry season is characterized by its low temperature, low humidity, and clear blue skies. The coldest month is normally January. The mean monthly maximum temperature lingers around 28.5°C and the mean monthly minimum varies between $10 - 11^{\circ}\text{C}$. About 5% of the annual rainfall occurs in this season. In winter, the general wind direction is from the northwest.

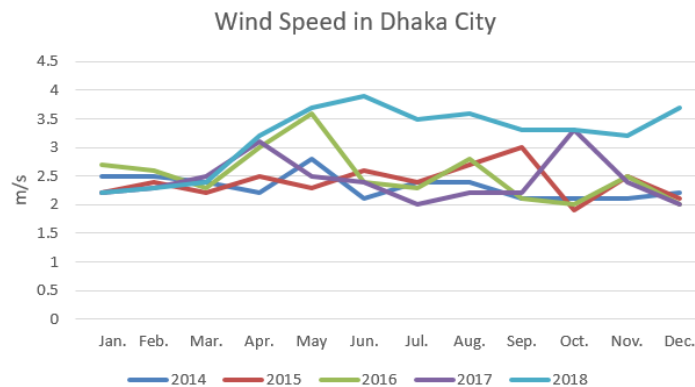


Figure 1.12: Wind Speed in Dhaka City

Ahmed [15] has compared diurnal temperature variations with the levels of monthly comfort zones in Dhaka to identify ‘over-heated’ and ‘under-heated’ periods. Ahsan [16] has defined an under-heated period as all hours that have temperatures below the comfort range, whereas over-heated periods include all hours with temperatures above the comfort range and concluded that identification of these periods enables the designer to pay special attention to the specific periods that do not fall in the comfort zone. Table 1.2 shows the duration of the over-heated and under-heated in the course of a year for Dhaka. It can be concluded that the overheated periods that cause discomfort persist for 10 hours a day on average (10 am in the morning to 8 pm at night).

Table 1.2: Under-heated, comfortable and over-heated period in Dhaka

Month	Hour											
	0-2	2-4	4-6	6-8	8-10	10-12	12-14	14-16	16-18	18-20	20-22	22-0
Jan	Under-heated					Comfortable	Over-heated					Under-heated
Feb	Under-heated					Over-heated					Comfortable	
March	Comfortable	Under-heated				Over-heated					Comfortable	
April	Comfortable	Comfortable	Under-heated			Over-heated					Comfortable	
May	Comfortable	Comfortable	Comfortable	Comfortable	Comfortable	Over-heated					Comfortable	
June	Comfortable	Comfortable	Comfortable	Comfortable	Comfortable	Over-heated					Comfortable	
July	Comfortable	Comfortable	Comfortable	Comfortable	Comfortable	Over-heated					Comfortable	
Aug	Comfortable	Comfortable	Comfortable	Comfortable	Comfortable	Over-heated					Comfortable	
Sept	Comfortable	Comfortable	Comfortable	Comfortable	Comfortable	Over-heated				Comfortable	Comfortable	
Oct	Comfortable	Comfortable	Comfortable	Comfortable	Comfortable	Over-heated				Comfortable	Comfortable	
Nov	Comfortable	Under-heated				Over-heated					Comfortable	
Dec	Under-heated					Comfortable	Over-heated			Comfortable	Under-heated	

Colour Index:

Under-heated periods	Comfortable periods	Over-heated periods
----------------------	---------------------	---------------------

Source: Ahmed, 1987

Sunlight is a major factor in creating heat generation. Every location on earth receives sunlight at least part of the year. The amount of solar radiation that reaches any one spot on the Earth's surface varies according to:

- Geographic location
- Time of day
- Season
- Local landscape and local weather

As sunlight passes through the atmosphere, some of it is absorbed, scattered, and reflected by:

- Air molecules
- Water vapor

- Clouds
- Dust
- Pollutants
- Forest fires

This is called diffuse solar radiation. The solar radiation that reaches the Earth's surface without being diffused is called direct beam solar radiation. The sum of the diffuse and direct solar radiation is called global solar radiation. Atmospheric conditions can reduce direct beam radiation by 10% on clear, dry days and by 100% during thick, cloudy days. Heat transfer due to the emission of electromagnetic waves is known as thermal radiation. For the gray body, the incident radiation (also called irradiation) is partly reflected, absorbed, or transmitted.

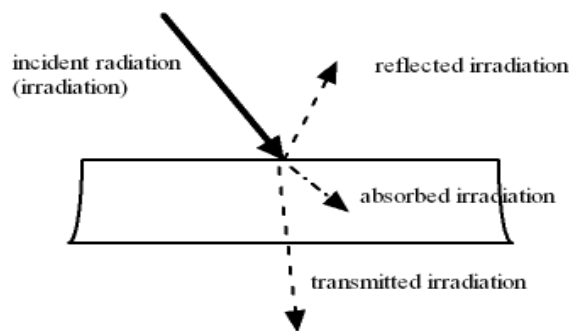


Figure 1.13: The absorption, reflection, and transmission of irradiation by a semi-transparent material, source: engineeringtoolbox.com

The emissivity coefficient is in the range $0 < \varepsilon < 1$, depending on the type of material and the temperature of the surface.

Bangladesh is a subtropical country, 70% of year sunlight drops in Bangladesh. Solar radiation varies from season to season in Bangladesh shown in Table 1.3. Bangladesh receives an average daily solar radiation of $4 - 6.5 \text{ kWh/m}^2$ [17]. Renewable Energy Research Centre (RERC), University of Dhaka is the only source that has got long term measured data of Dhaka. Solar radiation has an essential influence on the heat balance in a number of ways.

Table 1.3: Climate chart of Dhaka for 2018

Month	Temperature (°C)		Relative humidity (%)	Average sun hours	Radiation (kWh/m ²)	Wind speed and direction	
	Average	Record					
		Min					Max
January	17.5	9.5	26.8	68	232.5	4.36	2.2 W
February	23.2	14.4	33.6	61	207	4.92	2.3 W
March	27.3	17.5	34.6	59	324	5.59	2.4 S
April	27.3	19.4	36.5	69	325.5	5.76	3.2 E
May	27.6	20.8	36.3	79	347.5	5.30	3.7 S
June	29.4	23.6	35.6	81	300	4.53	3.9 S
July	29.3	24.8	37.6	81	268	4.23	3.5 S
August	29.8	25.4	36.5	78	302	4.29	3.6 S
September	29.8	25	36.5	77	292.5	4.02	3.3 S
October	27.3	20.8	36.1	72	238	4.32	3.3 N
November	24.2	17.4	32.8	68	210.5	4.28	3.2 WNW
December	20.3	11.8	28.9	66	206	4.21	3.7 NE

Source: Bangladesh Meteorological Department, RERC and WorldWeatherOnline.com

1.7 Literature Review

World energy consumption has been increasing rapidly for the last decades, mainly due to population growth and industrial and technological development. According to the Energy Information Administration [18], energy consumption in buildings accounts for more than 40% of the primary energy consumption. Now, the heat balance of a living room is inevitable from the energy consumption and the possible effect of solar radiation. Therefore, vast changes have to be made in the building sector, especially in the Heating, Ventilation, and Air-Conditioning (HVAC) systems, in order to reach the aforementioned targets. By reducing the need for electrical equipments and other cooling systems, energy can be saved and thus comfortable living environment can be enhanced. Tamami [19] described the relationship between heating and cooling load calculation, which is a starting point for building energy consumption analysis and equipment sizing. Jiang et al. [20] investigated the mechanism of

natural ventilation driven by wind force, large-eddy simulation (LES). In the meanwhile, detailed airflow fields, such as mean and fluctuating velocity and pressure distribution inside and around building-like models were measured by wind tunnel tests and compared to LES results for model validation. Three ventilation cases, single-sided ventilation with an opening in the windward wall, single-sided ventilation with an opening in the leeward wall, and cross ventilation, are studied. Camille Allocca et al. [21] studied single-sided natural ventilation by using a computational fluid dynamics (CFD) model, together with analytical and empirical models. The CFD model was applied to determine the effects of buoyancy, wind, or the combination of ventilation rates and indoor conditions. Jiang and Chen [22] investigated buoyancy-driven single-sided natural ventilation with large openings. Detailed airflow characteristics inside and outside of the room and the ventilation rate were measured. Joachim Seifert et al. [23] investigated a single-zone cubic building with two equal large openings using a computational fluid dynamics approach. They analyzed the driving forces and the ventilation flow rates due to wind as a function of the geometry, size, and relative location of the two openings. The ventilation flow rates are found to be affected by both wind flows around and through the building when the two openings are relatively large. G. Evola and V. Popov [24] applied the Reynolds averaged Navier–Stokes equation (RANS) to wind-driven natural ventilation in a cubic building. They determined the ventilation rate for single-sided and cross ventilation using the $k - \varepsilon$ turbulence model and renormalization group (RNG) theory and compared the results. Tine S. Larsen and Per Heiselberg [25] analyzed the wind direction which is an important parameter for single-sided ventilation. They also show that single-sided ventilation depends on the size, type, and location of the opening. Bangalee et al. [26] considered a building with multiple windows to investigate the wind-driven ventilation system using computational fluid dynamics (CFD), whose acceptance and accuracy are growing very fast. The Renormalization group (RNG) $k - \varepsilon$ turbulence model is chosen to simulate cross and single-sided ventilation with a specified accuracy after validating the methodology through a satisfactory comparison with an experimental result. Montazeri and Blocken [27] presented a systematic evaluation of 3D steady Reynolds-Averaged Navier–Stokes (RANS) CFD for predicting mean wind pressure distributions on the windward and leeward surfaces of a medium-rise building with and without balconies. It is shown that building balconies can lead to very strong changes in wind pressure distribution. Idris and Huynh [28] analyzed the air velocities in a single-sided naturally ventilated room along with an atmospheric zone into four different window locations and predicted air distribution inside the room. Staņislavs Gendelis and Andris Jakovics [29] considered the heat balance of a room and its dependence on solar

radiation and ventilation conditions. They analyzed the physical parameters of thermal comfort conditions, the airflow velocities, indoor temperatures, and their gradients. The distributions are calculated according to the solar radiation source through the window and the pressure difference between the opposite walls. It is shown that solar radiation has an essential influence on the heat balance of the room in a number of ways and on thermal comfort in the room.

In Bangladesh, the annual report 2018-2019 of Bangladesh Power Development Board showed that the domestic sector is the largest energy consumption sector and it is increasing day by day. M. Rounqu Ahmmad [30] analyzed the Wind Resources for Energy Production in Bangladesh. He estimated the wind power density, the annual mean wind power, and the annual mean wind speed. Hossain Mohiuddin et al. [31] analyzed the pattern of change of temperature of Dhaka city using the data of maximum and minimum monthly temperature of 1995 -2010 period collected from the Bangladesh Meteorological Department. This study reveals that the minimum average monthly temperature is showing a significant increasing pattern. Md. Rakibul Hasan [32] studied natural ventilation airflow and heat transfer calculation for a room of different flow paths and window configurations in Bangladesh.

In comparison to experimental investigation, temperature and average turbulent airflow distributions in the 2D and 3D model of a living room are modeled. Solar radiation has an essential influence on the heat balance of the room in a number of ways. Computational Fluid Dynamics (CFD) is cost-effective and easy to investigate the flow due to the change of geometry. So it is the demand of time to use the powerful tool CFD to model natural ventilation in buildings with solar radiation.

1.8 Importance of the Present Thesis Work

The prevalence of sustainable construction is increasing due to rising energy costs, improving life cycle cost, and design mandate. Engineers are utilizing more passive technologies to manage building heating and cooling demands. These approaches might take the form of low energy systems such as radiant heating and cooling, or thermally active building systems. Solar radiation is a form of thermal radiation having a particular wavelength distribution. Its intensity is strongly dependent on atmospheric conditions, time of year, and the angle of incidence for the sun's ray on the surface of the earth. So, solar radiation could play a vital role on the heat balance of the room in a number of ways. Nowadays' natural ventilation with the influence of solar radiation provides openings in the building facade to allow fresh air in the room.

1.9 Aim

The aim of this study is to analyze the criteria for energy efficiency, resulting in a series of feasible passive design solutions that can make a contribution in the field of architecture towards the knowledge of developing and designing energy-efficient residential buildings. The study also aims at identifying changes in the design process that can affect energy efficiency in residential buildings.

1.10 Objective of this Thesis

A review of earlier studies indicates that none has used solar radiation in such single or double-sided ventilation for a room in Dhaka city. The present study investigates the analyses of the indoor flow pattern without the mechanical system as well as for different window positions and different types of windows. The aim is to represent model geometrically and formulate mathematically using governing equations and boundary conditions. The target is to determine the standard thermal comfort inside the room for local weather conditions and to compare the result with others. The results will be displayed graphically. The specific objectives of the present research work are:

- To construct the physical model of the problem and then solve it using the Finite Element Method (FEM).
- To reproduce the result of Idris and Huynh by using Computational Fluid Dynamics (CFD).
- To determine the velocity distribution inside and around the building numerically and graphically.
- To describe the ventilation rate.
- To obtain standard thermal comfort inside the room for local weather conditions.
- To compare the result of the present investigation with similar published work.

It is expected that the present numerical and graphical investigation will contribute to the search for more efficient findings and to make a new dimension in the research area.

1.11 Scope and Limitations of the Research

Jones and Hudson [33] present that the energy use in modern buildings has occurred in five phases, namely, manufacture of building materials, transportation of building materials to the site, on-site construction activities, the operational phase, (running of the building) and finally, the demolition process of buildings and recycling of building materials. In terms of the various

categories of buildings that are there in Dhaka, the study was delimited to multi-unit residential buildings. This study confined itself in considering energy use at the operational phase of the building and it is also oriented towards the residential buildings inhabited by upper-middle-income groups in Dhaka.

The study is limited in the sense that it was not possible to identify a very good example of an energy-efficient residential building in all-season climatic context as of Dhaka city as well as Bangladesh. Another limitation has been the time of the year when the case study was considered. Habits and behavioral patterns that cannot be influenced by design and are related to energy efficiency have not been dealt with in this study.

1.12 Thesis Plan

Chapter 2 presents a geometrical description of the 2D and 3D models of the computational domain with a cubic building along with meshing. This chapter also provides the governing equation, solution procedure, and the justification of the proposed methodology. In order to investigate the flow pattern through the computational domain, and the room and also measured ventilation flow rates for all cases are arranged in Chapter 3. Solar radiation effects on natural ventilation where temperature distribution, radiosity as well as thermal comfort are discussed in Chapter 4. The main conclusions drawn from this research are summarized in Chapter 5, together with the main research contributions and the recommendations for future work.

Mathematical Model on Natural Ventilation

Natural ventilation depends on a home's air tightness, outdoor temperatures, wind forces, and other factors. Building simulation is a popular method for studying naturally ventilated building design. Thermal simulation and airflow network are two fundamental modules in building simulation method. Building simulation programs can be classified into two categories; design tools and detailed simulation programs. The design of the building, the form of window openings and location have a significant impact on the quality of the indoor climate. The effect of the outside natural environment on an indoor environment with single-sided natural ventilation is found more frequently in building designs. An overview of the separate and combined effects of temperature and wind forces on single-sided ventilation is given in this chapter. Issues relevant to single-sided natural ventilation design options are also presented in this chapter. This chapter has been devoted to detailed solution procedures for single sided natural ventilation to solve and analyze problems that involves fluid flow. Finally, an experimental single-sided ventilation case is validated.

2.1 Introduction

Single-sided ventilation depends on the interaction of physical parameters. The two major physical parameters affecting airflow in single-sided natural ventilation are the temperature difference across the opening/s and the wind forces. Most of the experimental methods have been applied to analyze the physical mechanisms of either buoyancy-driven or wind-driven flow through openings. Two particularly detailed studies have been performed to analyze the effects of both wind and temperature, separately and combined. The research of single-sided ventilation has been given more attention in building designs. It is, therefore, necessary to understand the study of single-sided ventilation in more detail. The related physical processes are complex, especially for the case of wind-driven flow, because of the variability in outdoor wind conditions and the turbulent motion of the wind. Experimental results have shown that the fluctuating effects of the wind are responsible for the airflow in the case of single-sided ventilation. Fluctuating flows are attributed to the turbulent characteristics of the incoming wind and/or to turbulence induced by the building itself [34]. Turbulence in the airflow along an opening causes simultaneous positive and negative pressure fluctuations of the inside air. This fluctuation of pressure distribution along the surface of an opening is a very important

driving force for the case of single-sided ventilation. However, for single-sided ventilation, the fluctuating nature of the wind produces continuously changing airflow patterns through an exterior opening. Therefore, a large number of simultaneous and highly accurate velocity measurements would be required to successfully predict the airflow rate for single-sided ventilation.

2.2 Physical Models

An important factor to select the site and building for simulation is the climatic characteristics. The climatic characteristics of Dhaka City differ from other cities of the country due to its location and rapid physical development in last few decades. Physical and environmental characteristics are further modified in different locations within the city. This is due to the density of built environment, building types, building heights and orientations, surface quality of the area – whether hard or soft depending on vegetal cover and presence of water bodies and ponds - materials used for construction, and other related factors. The criteria for site and building selection to determine the typical example office space was based on urban boundary, trend of typical office design, Building Construction Regulations of the City Authority, internal layout for daylight inclusion and distribution and scale and volume of the building.

In this study, single-sided natural ventilation has been presented for windward and leeward cases of three-dimensional model. Physical processes in a room with different heights and different location of windows are modelled using specialized computational fluid dynamics (CFD). Calculations are carried out in an empty room without any human or mechanical activity and compared with previous experimental measurements. Numerical analysis has shown distinct relationship between room dimensions (height in this case) and state of comfort in the room. The single-sided ventilation with opening/s on the windward wall and the leeward wall are considered. In this research, four different cases are considered and the cases are:

Case 1: single-sided ventilation with an opening on the windward wall

Case 2: single-sided ventilation with an opening on the leeward wall

Case 3: single-sided ventilation with double openings on the windward wall

Case 4: single-sided ventilation with double openings on the leeward wall

The positions of the single opening (case 1 and case 2) and double openings (case 3 and case 4) are considered on lower and middle of the building respectively. In this study, a cubic

building is considered whose walls are made of concrete. The dimension of the building-like model is $250\text{mm} \times 250\text{mm} \times 250\text{mm}$.

Two different building models are used: the first one is provided with a door-like opening sized $90\text{mm} \times 100\text{mm}$ (width \times height) for case 1 and case 2, and the second one is provided with window-like double openings both of them are sized $90\text{mm} \times 50\text{mm}$ (width \times height) for case 3 and case 4. All cases are used to study single-sided natural ventilation. The thickness of the walls is 5mm in both building models. [Figure 2.1](#) shows a schematic view of the building model. Furthermore, a logarithmic wind profile upwind of the building is considered in [Figure 2.2](#). The dimension of the computational domain are $3.25\text{m} \times 2.25\text{m} \times 1\text{m}$, displayed in [Figure 2.3](#), is chosen large enough in order not to disturb the air flow around the building. Three dimensional computational domain with opening/s of a cubic building for windward wall is shown in [Figure 2.4](#). Two dimensional and three dimensional views of the location and arrangement of the opening/s for windward wall of a building are shown in [Figure 2.5](#) and [Figure 2.6](#) respectively.

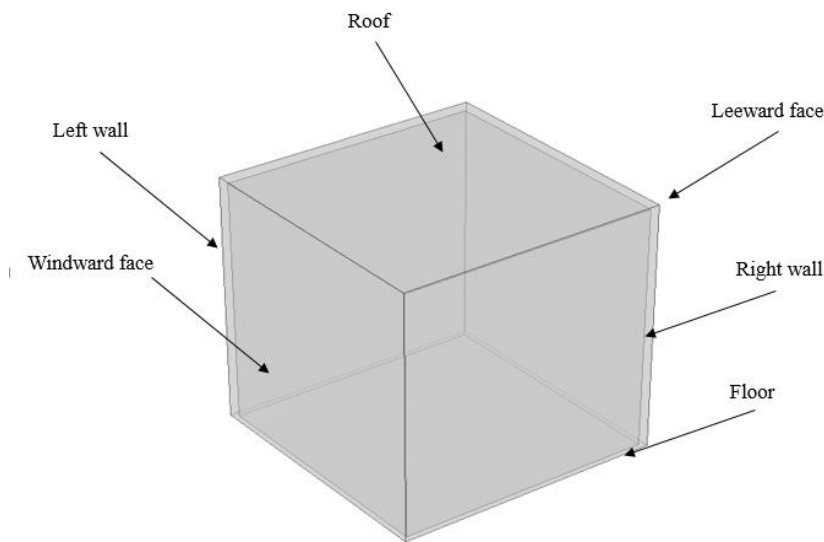


[Figure 2.1](#): Schematic view of the building model

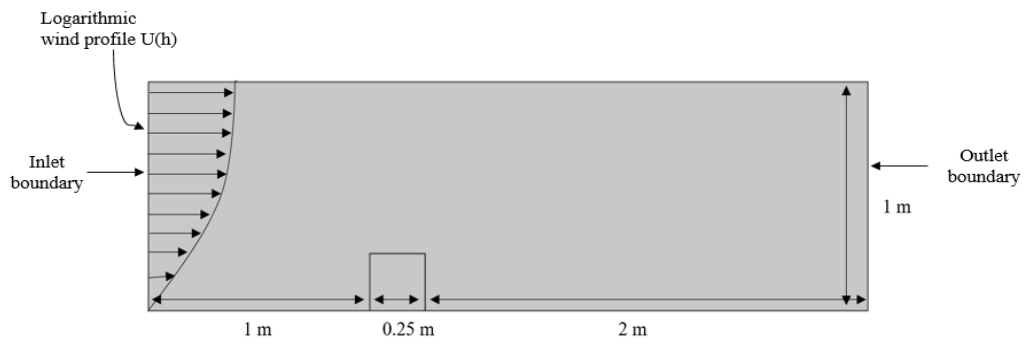


Figure 2.2: Two dimensional (2D) view of the computational domain and logarithmic wind profile

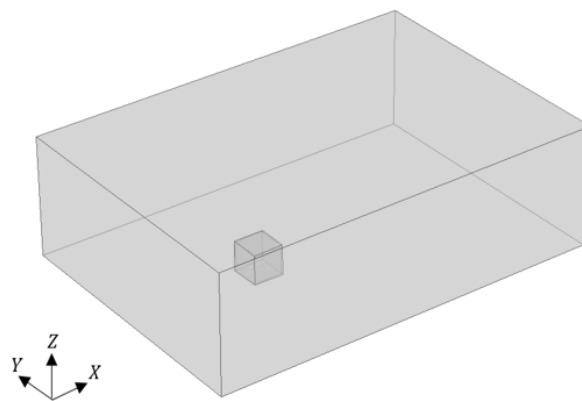


Figure 2.3: Three dimensional (3D) view of the computational domain

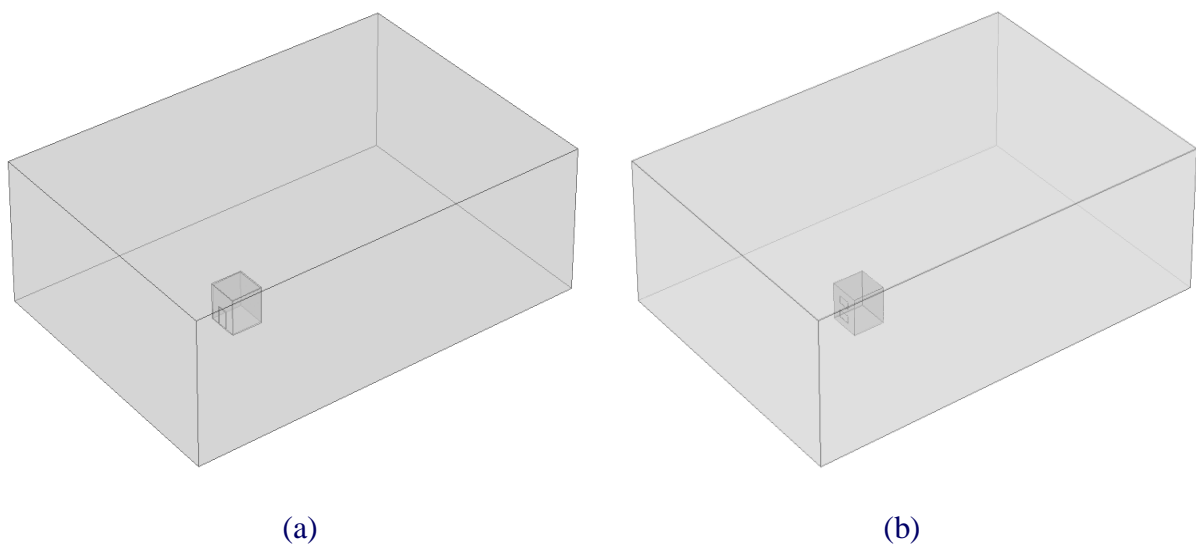


Figure 2.4: 3D view of the computational domain for windward face ((a) case 1 and (b) case 3)

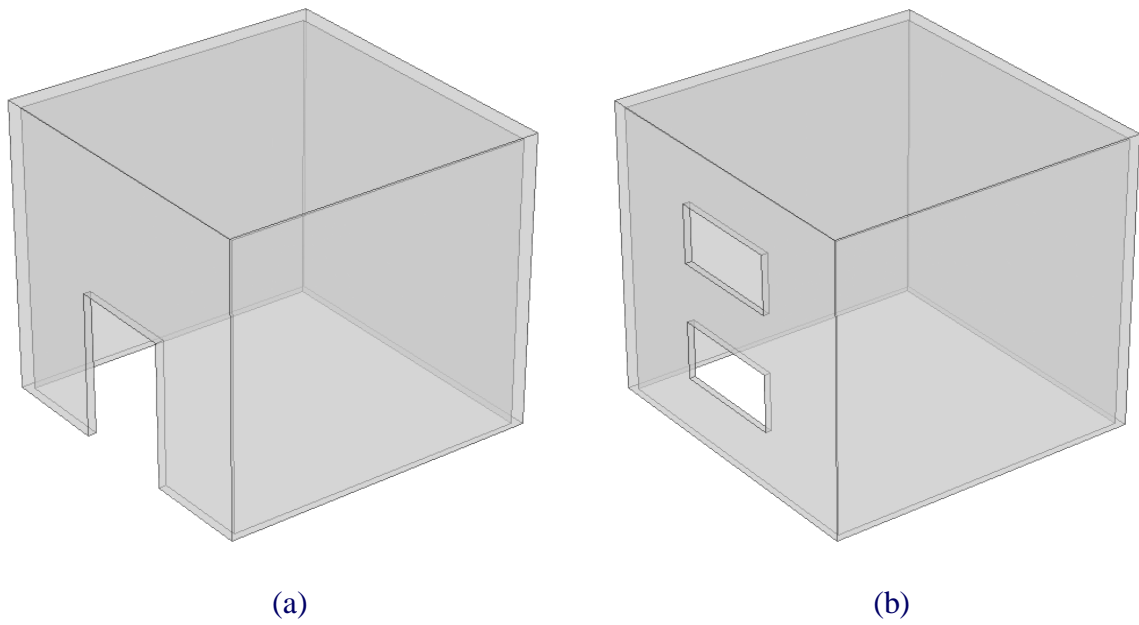


Figure 2.5: 3D view of the location and arrangement of the opening/s for windward face
 ((a) case 1 and (b) case 3)

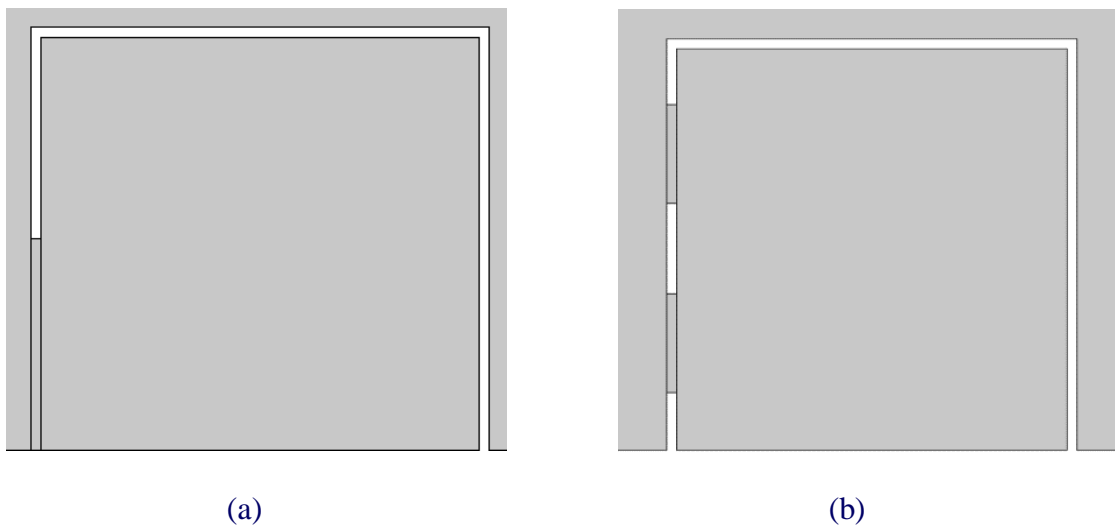


Figure 2.6: 2D view of the location and arrangement of the opening/s for windward face
 ((a) case 1 and (b) case 3)

Figure 2.7 and Figure 2.8 are also the location and arrangement of the opening/s for leeward wall of a building. Figure 2.9 shows the three dimensional view of computational domain's xy -plane. Since wind-driven ventilation depends on pressure difference, so physical model is a

very important factor for natural ventilation. In this study, details physical models are prepared to calculate the wind flow, temperature, radiosity, and ventilation rate.

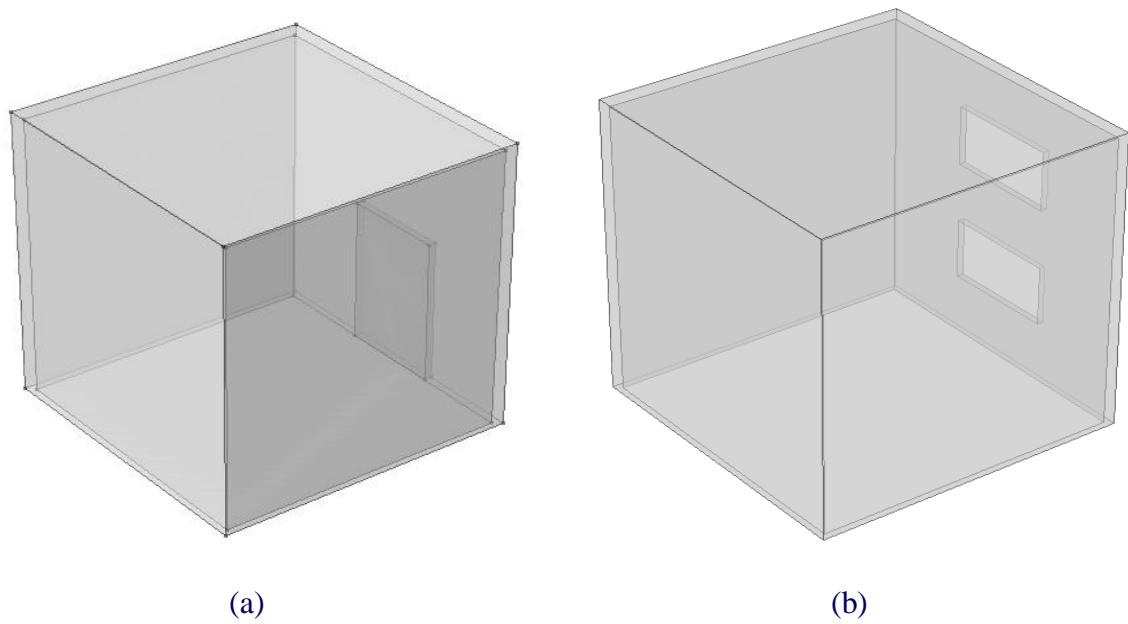


Figure 2.7: 3D view of the location and arrangement of the opening/s for leeward face ((a) case 2 and (b) case 4)

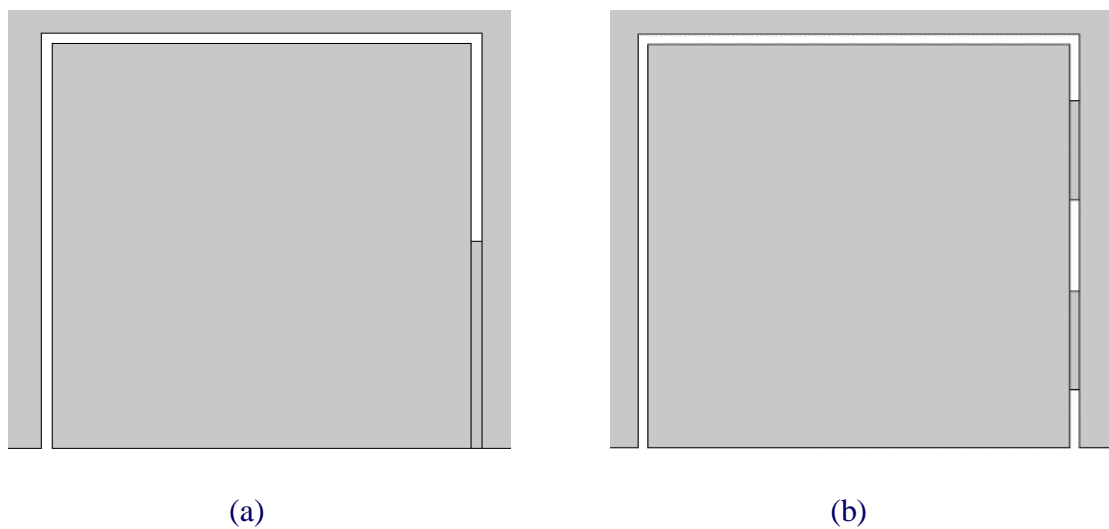


Figure 2.8: 2D view of the location and arrangement of the opening/s for leeward face ((a) case 2 and (b) case 4)

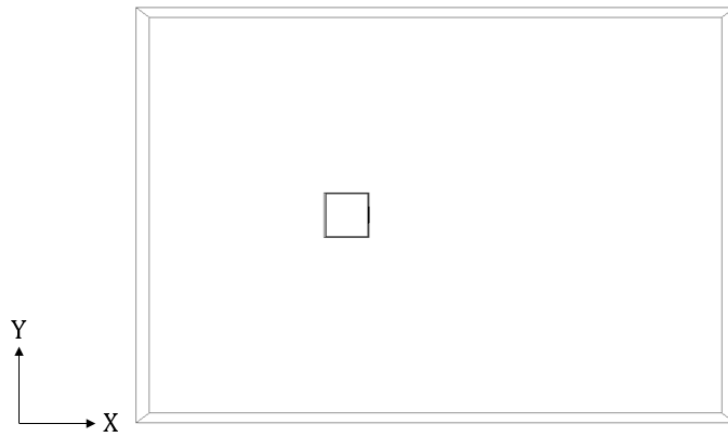


Figure 2.9: Computational domain (3D view of xy -plane)

2.3 Mathematical Model

Outdoor environment depends on natural forces. It is difficult to control and measure these unpredictable forces. A tool is needed that will enable designers to easily manipulate a building's design in order to observe trends and evaluate various potential designs. Full-scale tests [35], wind tunnel tests [25], and computational techniques are common procedures in studying a building and its surrounding outdoor environment. The full-scale test and wind tunnel test are usually time-consuming, expensive, and also may not be capable of capturing whole field information since there can only be a limited number of measuring points. The development of computational fluid dynamics (CFD) [36-40] allows the investigation of building wind environments, enabling the study of entire detailed flow fields in a timely and cost effective manner. So, CFD is a powerful tool for getting information about the air flow and pressure distribution around and inside the buildings. CFD is a branch of fluid mechanics that uses numerical methods and algorithms to solve and analyze problems that involve fluid flows. Its application becomes more and more popular as the computational power and technology have been increased and improved the turbulence modelling. Among the techniques studied by Chen, he agrees that CFD seems to be one of the most attractive technique for building environment design, since it is the most affordable, accurate, and informative method [41].

The common CFD techniques are direct numerical simulation (DNS), large-eddy simulation (LES) and Reynolds averaged Navier-Stokes (RANS) equation with turbulence models. Each technique handles turbulence in different ways [42]. Among those techniques, RANS is widely

used by most CFD software [43]. RANS solves the time-averaged Navier-Stokes equations by using approximations to simplify the calculation of turbulence flow. The present investigation is focused on the application of three dimensional RANS modelling on wind-driven natural ventilation of opening/s at single-sided buildings.

2.3.1 Governing Equations

The Navier-Stokes equations represent the fundamental governing equations for fluid flow. For incompressible Navier-Stokes equations in conservation form are

$$\frac{\partial u_i}{\partial x_i} = 0 \dots\dots\dots(1)$$

$$\rho \frac{\partial u_i}{\partial t} + \rho \frac{\partial}{\partial x_j} (u_j u_i) = - \frac{\partial p}{\partial x_i} + \frac{\partial}{\partial x_j} (2\mu s_{ij}) \dots\dots\dots (2)$$

where ρ is the density, t is time, p is pressure, μ is the dynamic viscosity of the fluid and the strain-rate tensor s_{ij} is given by

$$s_{ij} = \frac{1}{2} \left(\frac{\partial u_i}{\partial x_j} + \frac{\partial u_j}{\partial x_i} \right) \dots\dots\dots(3)$$

By the application of equation (1), the equation of motion can be written as

$$\rho \frac{\partial u_i}{\partial t} + \rho u_j \frac{\partial u_i}{\partial x_j} = - \frac{\partial p}{\partial x_i} + \frac{\partial}{\partial x_j} \left[\mu \left(\frac{\partial u_i}{\partial x_j} + \frac{\partial u_j}{\partial x_i} \right) \right] \dots\dots\dots (4)$$

In turbulent flows, the field properties become random functions of space and time. Hence, the field variables u_i and p must be expressed as the sum of mean and fluctuating parts as

$$u_i = U_i + u'_i, \quad p = P + p' \dots\dots\dots(5)$$

where the mean and fluctuating parts satisfy

$$\overline{u_i} = U_i, \quad \overline{u'_i} = 0 \dots\dots\dots(6)$$

$$\overline{p} = P, \quad \overline{p'} = 0 \dots\dots\dots(7)$$

with the bar denoting the time average.

We insert equation (5) into (1)-(4) and take the time average to arrive at the Reynolds- averaged Navier-Stokes (RANS) equations

$$\frac{\partial U_i}{\partial x_i} = 0 \dots\dots\dots(8)$$

$$\rho \frac{\partial U_i}{\partial t} + U_j \frac{\partial U_i}{\partial x_j} = - \frac{1}{\rho} \frac{\partial P}{\partial x_i} + \frac{\partial}{\partial x_j} \left[\nu \left(\frac{\partial U_i}{\partial x_j} + \frac{\partial U_j}{\partial x_i} \right) - \overline{u'_i u'_j} \right] \dots\dots\dots(9)$$

The quantity $\tau_{ij} = -\overline{u'_i u'_j}$ is known as the Reynolds stress tensor which is symmetric. A common method employs the Boussinesq hypothesis to relate the Reynolds stress to the mean velocity gradients

$$-\overline{u_i u_j} = \nu_t \left(\frac{\partial u_i}{\partial x_j} + \frac{\partial u_j}{\partial x_i} \right) - \frac{2}{3} k \delta_{ij} \dots\dots\dots(10)$$

where ν_t is the kinetic eddy viscosity assumed as an isotropic scalar quantity.

By the application of (10), equation (9) can be expressed as

$$\frac{\partial u_i}{\partial t} + U_j \frac{\partial u_i}{\partial x_j} = -\frac{1}{\rho} \frac{\partial p}{\partial x_i} + \frac{\partial}{\partial x_j} \left[\nu \left(\frac{\partial u_i}{\partial x_j} + \frac{\partial u_j}{\partial x_i} \right) + \nu_t \left(\frac{\partial u_i}{\partial x_j} + \frac{\partial u_j}{\partial x_i} \right) - \frac{2}{3} k \delta_{ij} \right] \dots\dots\dots(11)$$

Applying the first law of thermodynamics, the incident radiation must be equal to the sum of the absorbed, reflected, and the transmitted radiation [44-46]. The analysis of radiation exchange between surfaces is complicated because of reflection. This can be simplified when surfaces are assumed to be black surfaces. The solar energy reaching the edge of the earth's atmosphere is called the solar constant. The solar radiation undergoes considerable attenuation as it passes through the atmosphere. Radiation heat transfer between surfaces depends on the orientation of the surfaces relative to each other as well as their radiation properties and temperatures. Consider an enclosure consisting of N black surfaces maintained at specified temperatures. For each surface i , we can write

$$\dot{Q}_i = \sum_{j=1}^N \dot{Q}_{ij} = \sum_{j=1}^N A_i F_{ij} \sigma (T_i^4 - T_j^4) \dots\dots\dots(12)$$

where A_i is surface area and F_{ij} indicates the fraction of the radiation leaving surface i that strikes surface j directly.

Using the sign convention, a negative heat transfer rate indicates that the radiation heat transfer is to surface i (heat gain). Now, we can extend this analysis to non-black surfaces. It is common to assume that the surfaces are opaque, diffuse, and gray. Also, surfaces are considered to be isothermal. Also the fluid inside the cavity is not participating in the radiation. Radiosity J is the total radiation energy streaming from a surface, per unit area per unit time. It is the summation of the reflected and the emitted radiation. The radiosity of a blackbody is equal to its emissive power. For insulated or adiabatic surfaces, the net heat transfer through them is zero. In this cases, the surface is called reradiating surface. There is no net heat transfer to a reradiating surface.

In an N-surface enclosure, the conservation of energy principle requires that the net heat transfer from surface i to be equal to the sum of the net heat transfers from i to each of the N surfaces of the enclosure.

$$\dot{Q}_i = \sum_{j=1}^N \dot{Q}_{ij} = \sum_{j=1}^N \frac{J_i - J_j}{R_{ij}} \dots\dots\dots(13)$$

where $R_{ij} = \frac{1}{A_i F_{ij}}$ is called the space resistance to radiation and J_i and J_j are the radiosity for the surface i to j .

So, in radiation problems the conservation of energy is given by:

$$\frac{\partial T}{\partial t} + U_j \frac{\partial}{\partial x_j} (T) = \frac{\kappa}{\rho C_p} \frac{\partial^2}{\partial x_i^2} (T) + \frac{1}{\rho C_p} \dot{Q}_i \dots \dots \dots (14)$$

where T is the temperature of the fluid, κ is the thermal conductivity, C_p is the specific heat of the fluid at constant pressure and \dot{Q}_i is the net heat transfer from surface i .

The standard $k - \varepsilon$ turbulence model is used in this study, which assumes that the flow is fully turbulent and the effects of molecular viscosity are negligible. The turbulent kinetic energy, k , and its rate of dissipation, ε , in the flow field are calculated from two additional transport equations. The model transport equation for k is derived from the exact equation, while the model transport equation for ε was obtained using physical reasoning and bears little resemblance to its mathematically exact counterpart. The $k - \varepsilon$ transport equations are:

$$\frac{\partial k}{\partial t} + U_j \frac{\partial k}{\partial x_j} = \frac{\partial}{\partial x_j} \left[\left(\nu + \frac{\nu_t}{\sigma_k} \right) \frac{\partial k}{\partial x_j} \right] + \frac{1}{\rho} P_k - \varepsilon \dots \dots \dots (15)$$

$$\frac{\partial \varepsilon}{\partial t} + U_j \frac{\partial \varepsilon}{\partial x_j} = \frac{\partial}{\partial x_j} \left[\left(\nu + \frac{\nu_t}{\sigma_\varepsilon} \right) \frac{\partial \varepsilon}{\partial x_j} \right] + C_{\varepsilon 1} \frac{\varepsilon}{k} P_k - C_{\varepsilon 2} \frac{\varepsilon^2}{k} \dots \dots \dots (16)$$

where σ_k and σ_ε are turbulent Prandtl (Pr) numbers for k and ε respectively.

In equations (15) & (16), P_k is the production rate of turbulent kinetic energy, which depends on the turbulent viscosity and the velocity distribution. In Table 2.1, the values of all the constants for the turbulence model are provided.

Table 2.1: Constants for the Turbulence Model [24]

Constants	Values
C_μ	0.09
$C_{\varepsilon 1}$	1.44
$C_{\varepsilon 2}$	1.92
σ_K	1.0
σ_ε	1.3

In this research, two types of study are considered. They are:

- (i) natural ventilation without solar radiation effect
- (ii) natural ventilation with the influence of solar radiation

2.3.2 Boundary Conditions

In this study, the finite element method (Galerkin weighted residual method) has been used to solve the set of equations provided by $k - \varepsilon$ models. In the case of vertical wind direction, the computational domain was constructed that had a height of $4H$, width of $9H$ and length of $13H$ where $H = 0.25 \text{ m}$. The ability to accurately model outdoor airflow around buildings is necessary to provide the correct boundary conditions for the indoor building environment that is naturally ventilated. As far as the boundary conditions are concerned, at the inlet of upwind boundary a logarithmic profile (Figure 2.2) of the stream wise velocity component U has been applied: $U(h) = \frac{U_0}{K} \ln\left(\frac{h}{h_0}\right)$; where h is the distance from the ground, $K = 0.41$ is the Von Karman's constant, U_0 and h_0 have been determined through the best fit of the available data and experimental data. The velocity components along with vertical and span wise direction were equated to zero. In addition, as the distribution of k and ε on the inlet boundary was unknown, the following relations have used: $k = \frac{3}{2}(U_{avg} \cdot T_i^2)$;

$\varepsilon = c_\mu^{3/4} \frac{k^{3/2}}{l_t}$; where U_{avg} is the average flow velocity, T_i the turbulence intensity and l_t is the turbulence length scale. To solve turbulence conditions $T_i = 1\%$ [47] and $l_t = 0.4 \text{ m}$ [24] have been used in this research. A constant pressure is assumed at the outlet of the computational domain, while the gradients of all the dependent variables have assumed to vanish. The ambient conditions for pressure and temperature are considered here. For all cases, heated air entered into the region through the inlet. Standard wall functions are used and the no-slip velocity boundary condition is applied for the fluid-wall interaction. The wall of the room is modelled as adiabatic for study (i) and heat transmittance concrete material with emission $\varepsilon = 0.85$ for study (ii) respectively. All objects except the transparent window are modelled as grey bodies for study (ii). Owing to the ellipticity of the earth's orbit, the actual solar constant changes throughout the year within $\pm 3.4\%$. As a result the solar radiation reaching the earth's surface is around 1000 W/m^2 on a clear day and much less on a cloudy day, in the wavelength band 0.3 to $2.5 \mu\text{m}$. The thermal expansion coefficient of the air is based on the ambient temperature.

2.4 Discretization Methods

The description of the laws of physics for space and time dependent problems are usually expressed in terms of partial differential equations (PDEs). For the vast majority of geometries and problems, these PDEs cannot be solved with analytical methods. Instead, an approximation

of the equations can be constructed, typically based upon different types of discretization. These discretization methods approximate the PDEs with numerical model equations, which can be solved using numerical methods. The solution to the numerical model equations are, in turn, an approximation of the real solution to the PDEs. The finite element method (FEM) is used to compute such approximations. The Galerkin method is one of the many possible finite element method formulations which can be used for discretization by a commercial software which is performed by the following procedural flow as viewed in Figure 2.10.

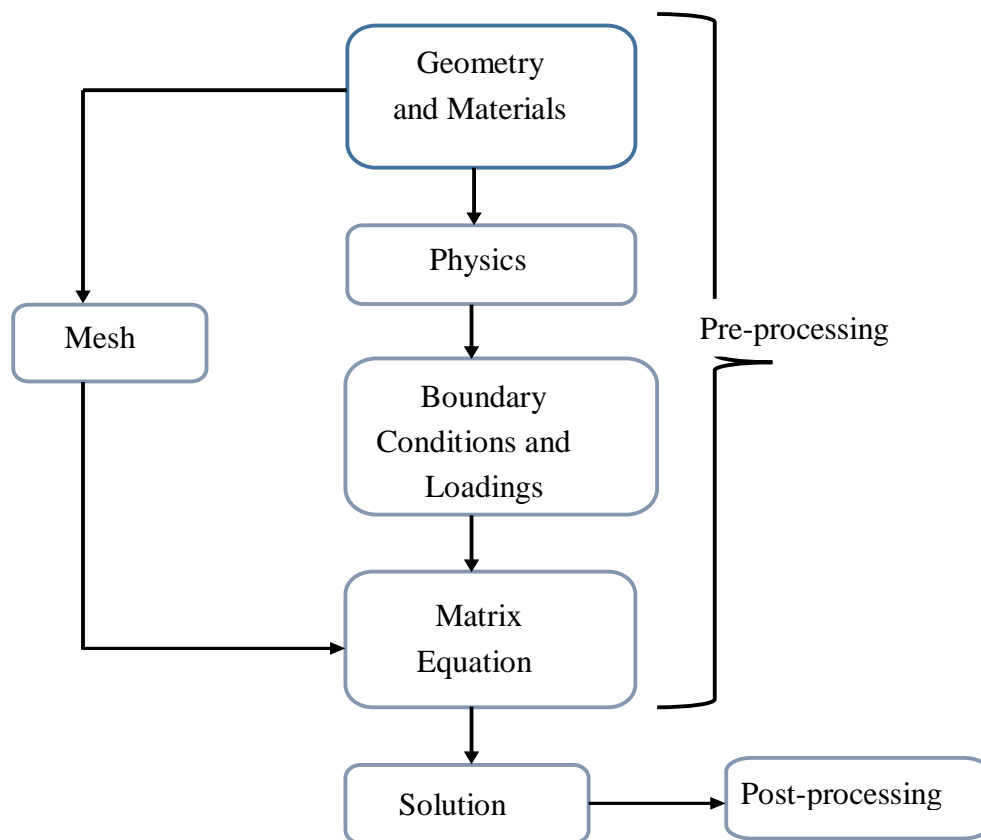


Figure 2.10: Basic steps to perform a finite element analysis in this research

The method can be divided into three elementary steps, namely pre-processing, solver and post-processing. The pre-processing steps enable the user to build the model. Since it contains all the information regarding the FEM application for interconnect study, it is convenient to divide it into smaller sub-steps. The first sub-step involves the creation of the interconnect geometry to represent the domain under study and assign the material properties to the domain. Then the physical environments of the problem under investigation are generated by assigning the underlying physics (or multi-physics), mathematical equations, and finite element formulation

to the model. After that, the application of appropriate loadings, boundary and initial conditions to the domain under study, as well as its discretization into finite elements, determines the matrix equation governing the model. This step is followed by solving the set of algebraic equations, which provides the physics related nodal solutions of the model. The numerical model equations are solved for different mesh types and element sizes. The most common elements are illustrated for the nodes (x and y in 2D and x , y , and z in 3D). Modern time-stepping algorithms automatically switch between explicit and implicit steps depending on the problem. A modern time-marching scheme has automatic control of the polynomial order and the step length for the time evolution of the numerical solution. Backwards differentiation formula (BDF) method is used in this study. The finite element method gives an approximate solution to the mathematical model equations. The difference between the solution to the numerical equations and the exact solution to the mathematical model equations is the error. In many cases, the error can be estimated before the numerical equations are solved (i.e., an a priori error estimate). A priori estimates are often used solely to predict the convergence order of the applied finite element method. After the solutions of the problems are determined, the post-processing step enables the user to evaluate the results of the finite element analysis by means of plotting and data exporting tools.

2.5 Meshing of the Physical Models

Physics controlled mesh is prepared using COMSOL Multiphysics Meshing. The element sizes for this meshing are different such as fine, extra fine, extremely fine, finer, coarse, coarser, extra coarse, extremely coarse, and normal. The number of mesh depends on different mesh types and element sizes. In 2D elements, triangular and rectangular are used and tetrahedral, Pyramidal, Prismatic and hexahedral are used for 3D elements. Extremely coarse is used in this study. Total number of mesh for 3D cases are around 35000-40000 whereas 1800-2300 for 2D cases. In Figure 2.11 and Figure 2.12, the computational domain are meshing with 336 edges and 185 vertexes where Figure 2.13 and Figure 2.14 has 381 edges and 193 vertexes. Figure 2.15-Figure 2.18 shows the mashing of the 2D view of the computational domain. Table 2.2 to Table 2.9 shows the details meshing for 2D and 3D cases.

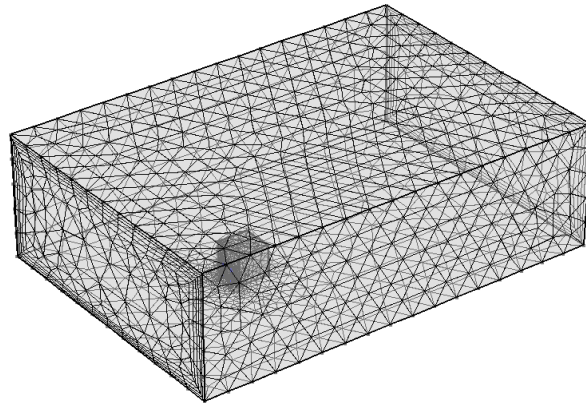


Figure 2.11: Meshing of windward wall with an opening (case 1)

Table 2.2: Meshing for case 1 in 3D

Element Type	Number of Element
Tetrahedral	22369
Pyramid	830
Prism	12996
Triangular	3676
Quadrilateral	374
Edge	336
Vertex	185
Total Element	36195

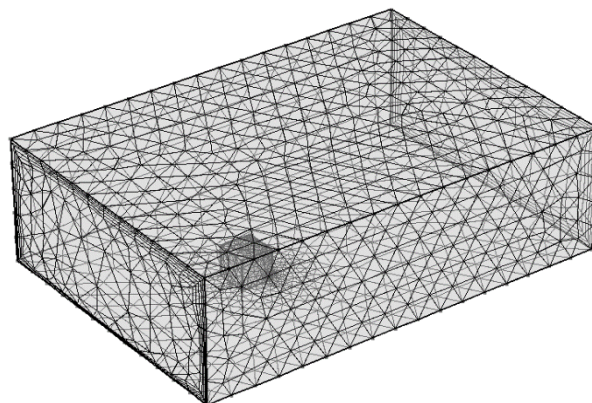


Figure 2.12: Meshing of leeward wall with an opening (case 2)

Table 2.3: Meshing for case 2 in 3D

Element Type	Number of Element
Tetrahedral	21948
Pyramid	822
Prism	12866
Triangular	3648
Quadrilateral	374
Edge	336
Vertex	185
Total Element	35636

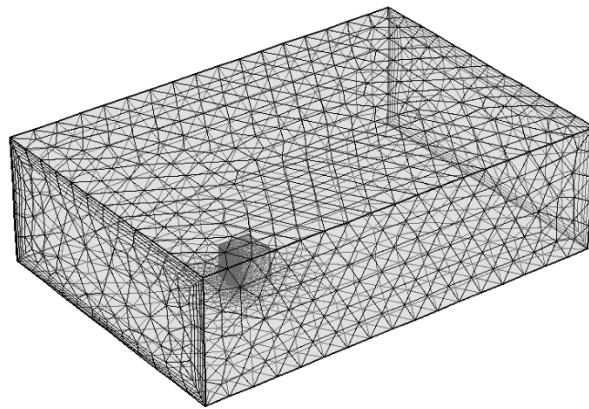


Figure 2.13: Meshing of windward wall of double openings (case 3)

Table 2.4: Meshing for case 3 in 3D

Element Type	Number of Element
Tetrahedral	25742
Pyramid	1038
Prism	12786
Triangular	3890
Quadrilateral	340
Edge	381
Vertex	193
Total Element	39566

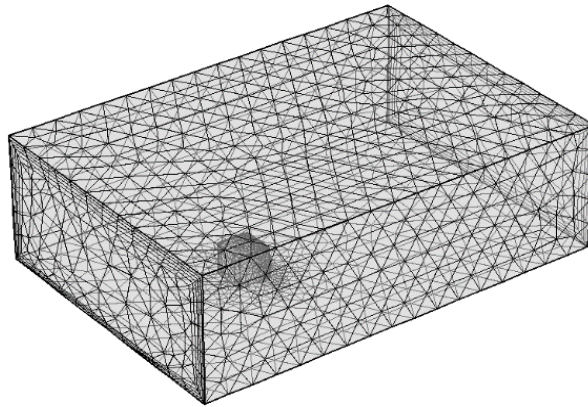


Figure 2.14: Meshing of leeward wall with double openings (case 4)

Table 2.5: Meshing for case 4 in 3D

Element Type	Number of Element
Tetrahedral	25715
Pyramid	1047
Prism	12675
Triangular	3870
Quadrilateral	340
Edge	381
Vertex	193
Total Element	39437

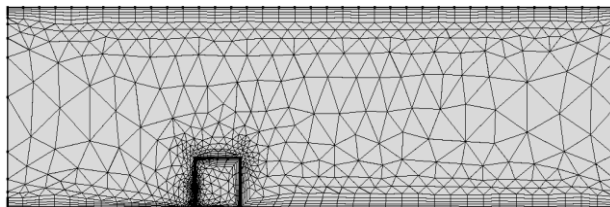


Figure 2.15(a) : Meshing of case 1 for 2D

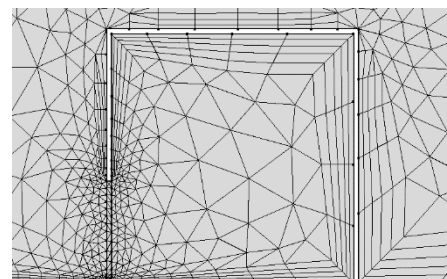


Figure 2.15(b) : Meshing of case 1 for 2D, close view

Table 2.6: Meshing for case 1 in 2D

Element Type	Number of Element
Triangular	1277
Quadrilateral	616
Edge	209
Vertex	14
Total Element	1893

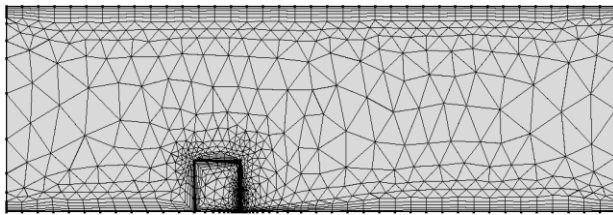


Figure 2.16(a) : Meshing of case 2 for 2D

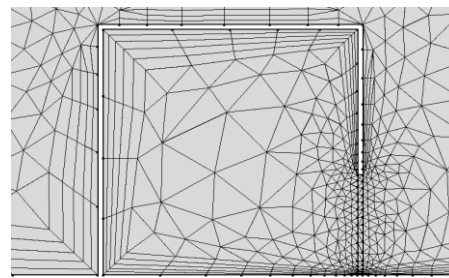


Figure 2.16(b) : Meshing of case 2 for 2D, close view

Table 2.7: Meshing for case 2 in 2D

Element Type	Number of Element
Triangular	1288
Quadrilateral	621
Edge	210
Vertex	14
Total Element	1909

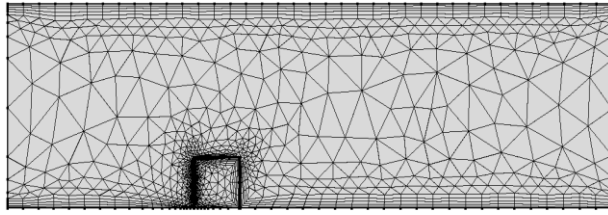


Figure 2.17(a) : Meshing of case 3 for 2D

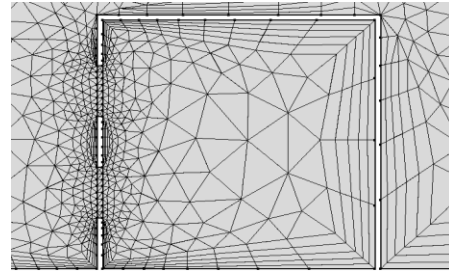


Figure 2.17(b) : Meshing of case 3 for 2D, close view

Table 2.8: Meshing for case 3 in 2D

Element Type	Number of Element
Triangular	1565
Quadrilateral	647
Edge	223
Vertex	20
Total Element	2212

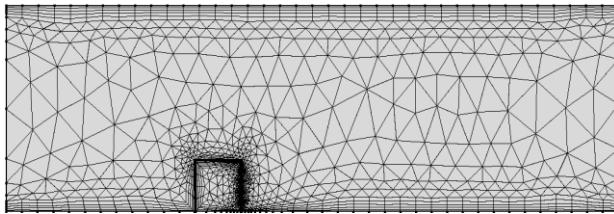


Figure 2.18(a) : Meshing of case 4 for 2D

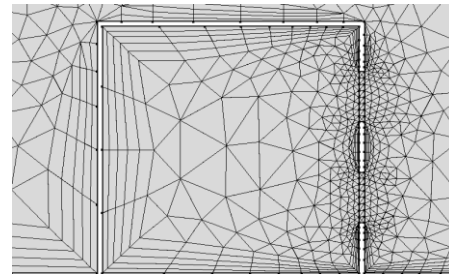


Figure 2.18(b) : Meshing of case 4 for 2D, close view

Table 2.9: Meshing for case 4 in 2D

Element Type	Number of Element
Triangular	1550
Quadrilateral	652
Edge	224
Vertex	20
Total Element	2202

2.6 Code Validation

Wind-driven single-sided ventilation was performed in the present study. In this validation study, CFD has been used to analyze single-sided ventilation by studying wind-driven windward flow through double opening. Single-sided ventilation was used to validate the CFD model [28]. For the CFD simulation, the building model was set up and placed within a larger computational domain. After setting up the CFD model according to the experimental setup, the simulation was performed. In Figure 2.19, three vertical lines in the middle section of the domain A, B, and C are identified. Location A and C have been chosen in order to describe the flow pattern close to the openings.

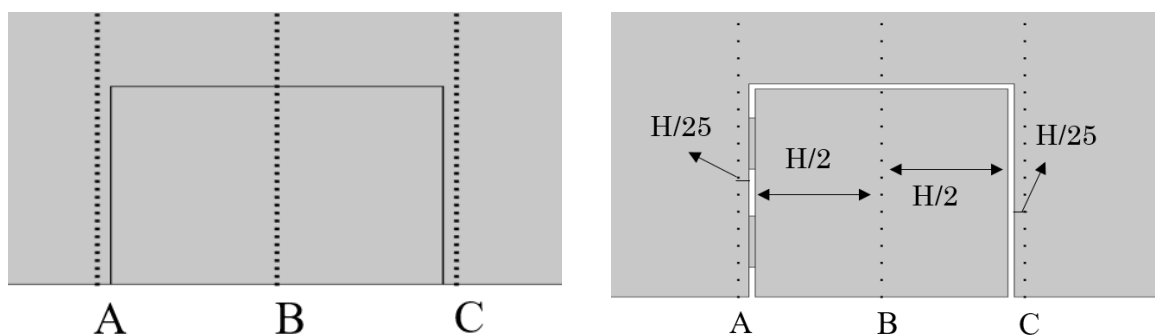
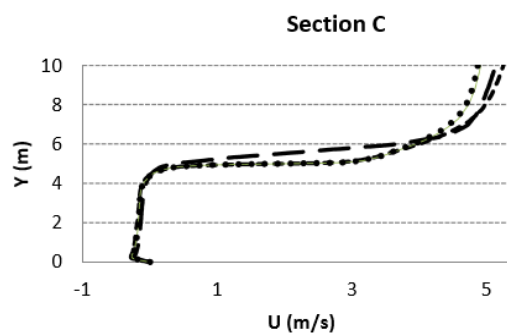
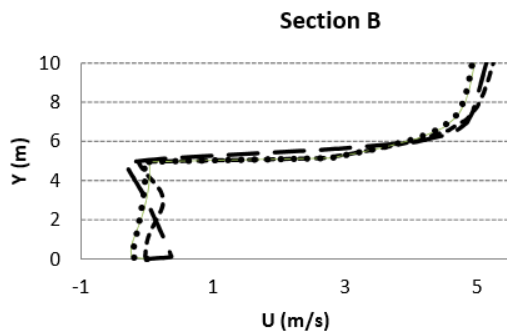
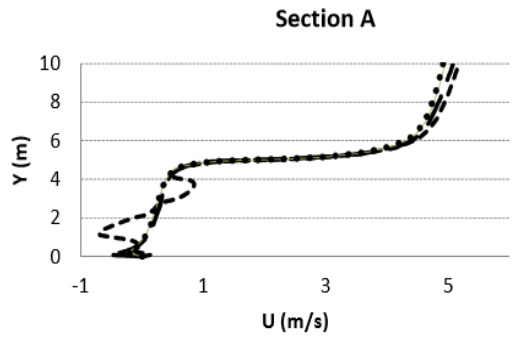


Figure 2.19: Location of the vertical lines

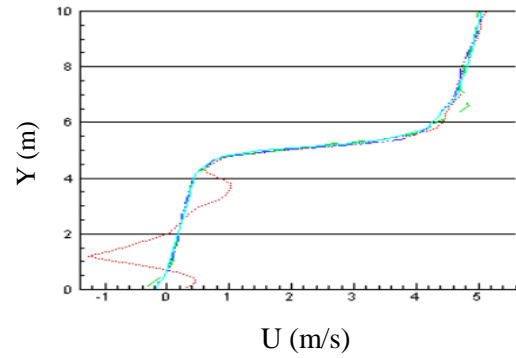
The velocity components have been determined, along streamwise and vertical direction, respectively. The third velocity component has been neglected as it is supposed to be zero, due to the symmetry of domain. Figure 2.20 shows the velocity field results for the model, in every section of the building. The plots of Figure 2.20 shows the vertical distribution of x -direction velocity U for ventilation patterns evaluated. From this validation case, it is clear that the agreement between present results and results obtained in Idris & Huynh [28] for the interaction between outdoor and indoor flow in single-sided ventilation is very good.

Results obtained in [28]

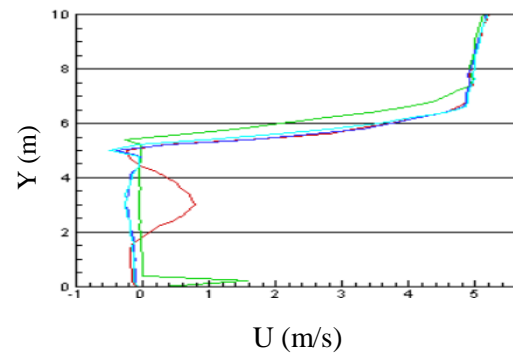


Results obtained in this research

Section A



Section B



Section C

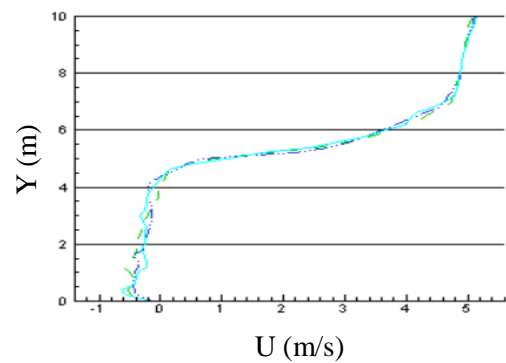


Figure 2.20: Code validation of the model

2.7 Conclusion

Natural ventilation is a critical strategy in the move towards energy-efficient building design. Single-sided ventilation is a significant type of natural ventilation, especially since single-sided building forms are so prevalent, especially in Dhaka city. This chapter has compiled four cases on single-sided natural ventilation in the field of building technology to determine the airflow available in Dhaka city. Research in the area of thermal comfort and indoor air quality will also be necessary to analyze the full potential of single-sided ventilation. This background information is significant in taking steps towards the improvement of natural ventilation design in Dhaka city. CFD modeling is a necessary tool in natural ventilation design. It enables designers to analyze different designs and to evaluate the abilities of these designs before the actual implementation of them. However, since CFD has the capabilities of being a powerful tool in this respect, it is also necessary to ensure that it is applied accurately. As natural ventilation is characterized by unpredictable and complicated airflow patterns, which is a challenge to the field of CFD modeling, but code validation shows that the performance of CFD has been very good and promising overall in velocity distribution. Therefore, the CFD tool has been used for natural ventilation studies.

Natural Ventilation without Solar Radiation Effect

From the previous chapter, it is clear that CFD is a powerful tool and can provide great potential for the future design of naturally ventilated buildings. Based on the validation of single-sided ventilation for the indoor and outdoor environment, the case for computational modeling of single-sided natural ventilation is strongly supported. In chapter 2, the single-sided wind-driven natural ventilation with opening/s on the windward wall and the leeward wall has been considered. In this chapter, all the results from the research are described for all cases without the solar radiation effect. Firstly, airflow inside and around the building are discussed. Finally, the ventilation rate is calculated.

3.1 Introduction

Fresh air plays a vital role in our lives. The term “indoor air quality” (IAQ) usually mentions the amount and type of pollutants present in the air. So, it is very substantial that the air around us should be fresh enough for the human body. Tham [48] stated that the indoor environment is dynamic and affected by several parameters, such as materials, HVAC systems, and the presence of human beings. All these parameters bring impurities into the air and make the air polluted. These parameters are parts of the indoor environment that cannot be neglected and, therefore, a more holistic approach is needed to efficiently remove the impurities from indoor air. In addition, Jones [49] presented a large number of emission sources that can lead to indoor air pollution, and these can cause significant effects on health. Moreover, Sundell [50] mentioned that indoor air was believed to be a major environmental factor in the past, but then other factors, such as outdoor air quality, energy consumption, and sustainable buildings, became dominant. It is true that a major environmental concern today regards global warming due to outdoor air pollution, but indoor air quality cannot be beyond this concern. There are well-defined ASHRAE standards which give information about the tolerable number of pollutants in the air. It also essentially refers to the air quality within and around buildings, which relates to the health and comfort of building occupants.

3.2 Results and Discussion

The present investigation focuses on the application of three-dimensional RANS modeling on wind-driven natural ventilation of single/double opening/s at the windward wall and the

leeward walls of the single-sided building. This section provides the information about the airflow rate and flow pattern provide, which are free from the conservation of energy due to the absence of solar radiation effect. The size of the domain is an important factor, especially for modeling airflow in buildings, because the realistic representation of ambient and external airflow are essential. It is necessary to consider a small computational domain with less number of grids to minimize the computational time. Airflow is mandatory for all three-dimensional models. It must be ensured that the airflow is free from all kinds of hindrances in the outer domain for all cases.

3.2.1 Velocity Distribution

In this study, four physical models have been used in the context of the weather of Dhaka city to examine the wind profiles inside and outsides of the buildings through single/double opening/s. To compare with other results, three vertical lines from A to C are considered, shown in Figure 3.1. Among these lines, the single line B is situated inside the building and the other two lines A and C which are outside, but close to the building, in which to show the behavior of the inside and outside velocity of the flow respectively along these lines. The velocity components have been determined, along streamwise and vertical direction, respectively. The third velocity component has been neglected as it is supposed to be zero, due to the symmetry of the domain.

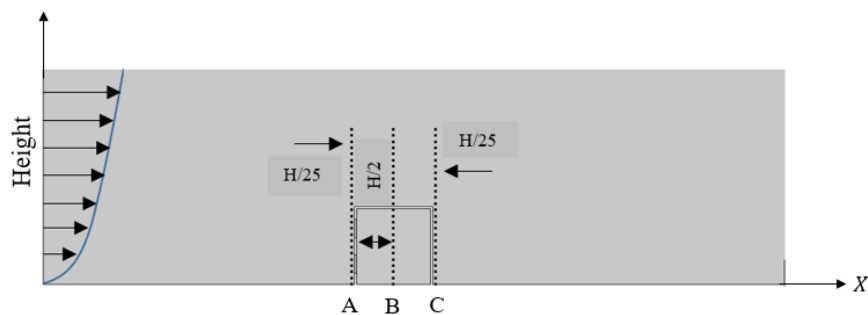


Figure 3.1: Location of velocity measurements

Since measurement line A, is on the opposite side of the opening/s for leeward cases, so the velocity profiles are approximately the same for case 2 and case 4 but an important line for case 1 and case 3. Conversely, the velocity profiles are approximately the same for case 1 and case 3 because measurement line C is on the opposite side of the opening/s for windward cases, so it is in favor of case 2 and case 4. The velocities of air are changed from time to time. The plots of Figure 3.2-3.10 show the streamwise velocity U for single-sided windward opening

(case 1) calculated for 0.5, 1, 1.5, 2, 2.5, 3, 5, 10, and 15 seconds. In these cases, it is observed that, the velocities are changed from time to time. After a few seconds, the changes are going to come down, which is approximately 3 seconds at that time-dependent results bear a physical resemblance to steady. Similarly, Figure 3.12-3.20 show the streamwise velocity U for single sided leeward opening (case 2), Figure 3.22-3.30 show the streamwise velocity U for single sided windward double openings (case 3) and Figure 3.32-3.40 show the streamwise velocity U for single sided leeward double openings (case 4). Meteorological wind speeds are varying from 2-4 m/s in Dhaka city.

In measurement line A, the velocity of air are fluctuating from 0 to 0.2 m/s for all cases at time $t = 0.5$ second. But at time $t = 1$ second, the ups and downs of streamwise velocity for the case 3 is much more than other cases, and the variation is from 0 to 0.4 m/s for the double windward openings. Also, the behavior of case 3 is from 0 to 0.5 m/s when other cases are from 0 to 0.2 m/s at time $t = 2$ second.

In measurement line B, the velocities of air are approximately the same for all cases at time $t = 0.5$ second. Air velocities fluctuate when time is increasing. At time $t = 1$ second, the fluctuation of streamwise velocity for the double leeward openings is greater than other cases, and the fluctuation is from 0 to 0.3 m/s for case 4. But at time $t = 2$ second, the behavior of air velocity for case 3 is much higher than the case 4. At time $t = 2$ second, the fluctuation of air velocity is from 0 to 0.4 m/s for case 3 when other cases are from 0 to 0.2 m/s. At time $t = 3$ second, the ups and downs of streamwise velocity for case 3 are from 0 to 0.4 m/s when other cases are from 0 to 0.1 m/s.

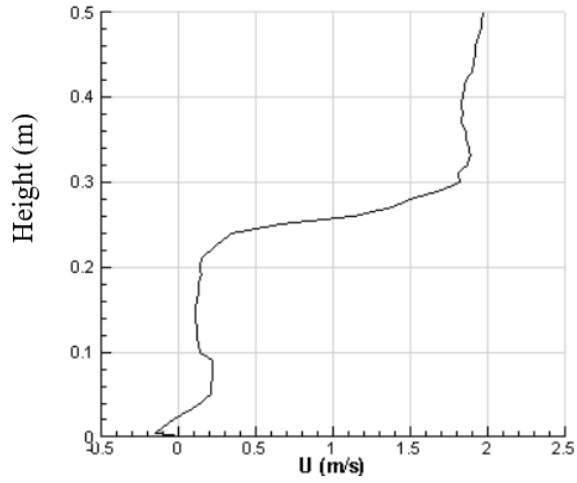
In measurement line C, the air velocity is fluctuating so much for double leeward openings, and the variation is from 0 to 0.5 m/s at time $t = 0.5$ second. But at time $t = 1$ second, the ups and downs of streamwise velocity for the double leeward openings are from 0 to 0.4 m/s. Moreover, the behavior of case 2 and case 4 are from 0 to 0.3 m/s when other cases are from 0 to 0.2 m/s at time $t = 2$ second and $t = 3$ second.

In the windward single opening (Case 1), the maximum air enters into the upper side of the opening and comes out through the lower side of that opening, but for the leeward single opening (case 2), the maximum air enters into the lower side of the opening and comes out through the upper side of that opening. Also, in the windward double openings (Case 3), the maximum air enters into the upper opening and comes out through the lower opening, but for the leeward double openings (Case 4), the maximum air enters into the building through the lower opening and comes out through the upper opening.

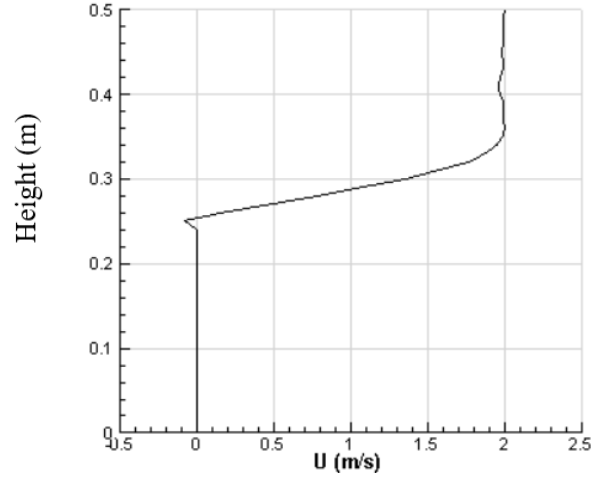
Since, after 3 seconds the changes are not worth watching so the vertical velocity is calculated for 3rd second. Figure 3.11, Figure 3.21, Figure 3.31 and Figure 3.41 are the vertical velocity V for case 1, case 2, case 3 and case 4 respectively at 3rd second. Section basis comparison of streamwise velocity and vertical velocity for 3rd second are shown in Figure 3.42 and Figure 3.43 respectively. In computational domain, the behavior of streamwise velocity distribution for all cases are shown in Figure 3.44. The difference is evident in the regions close to horizontal surfaces. Figure 3.45 shows the velocity distribution for all cases in xy -plane at time $t = 15$ second. In this analysis, the flow pattern inside the building as well as computational domain for all cases are considered. To show the flow pattern, air flow distribution and stream lines are essential. Figure 3.46-3.47 show the air flow distribution for all cases in computational domain and cubic building respectively at 15th second. Figure 3.48-3.49 show the stream lines for all cases in computational domain and cubic building respectively at 15th second.

Above the roof of the building (height > 0.25), the velocity components U and V for all cases are similar in every section, but in the cubic building, flow directions and velocity components have some disagreements in few sections. To choose the location of the opening/s and description of the velocity profile inside the building and near to the openings are main purpose of this study.

Section A



Section B



Section C

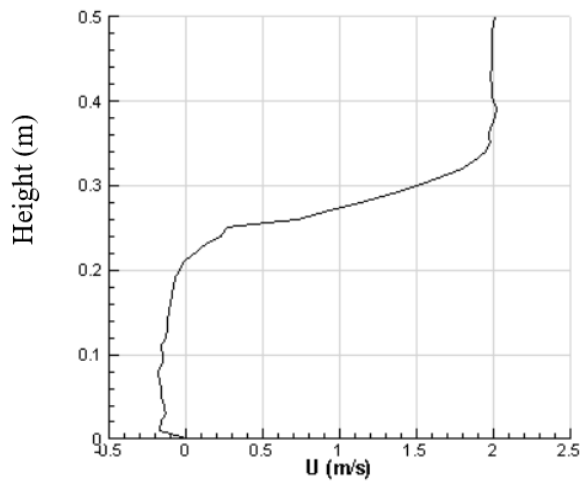
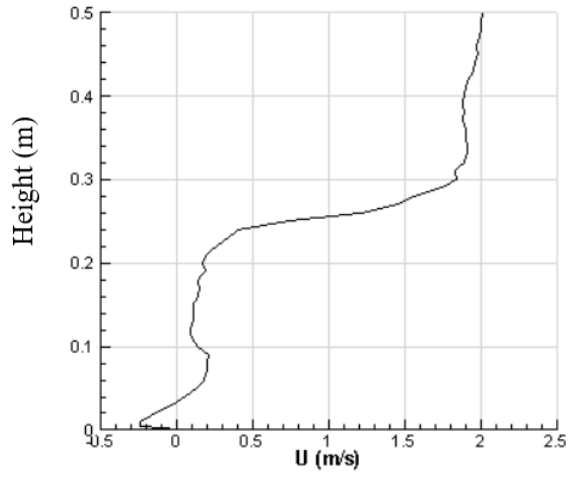
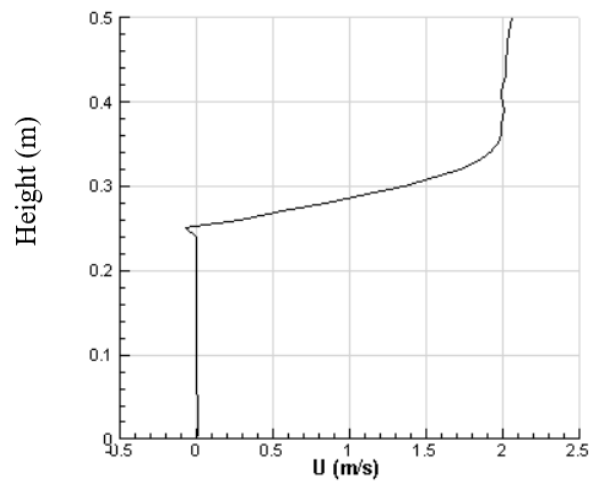


Figure 3.2: Velocity distribution at $t = 0.5$ s for single-sided ventilation with an opening on the windward wall (Case 1)

Section A



Section B



Section C

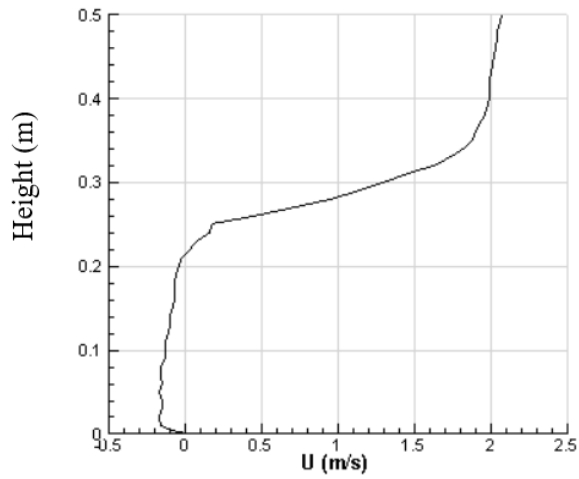
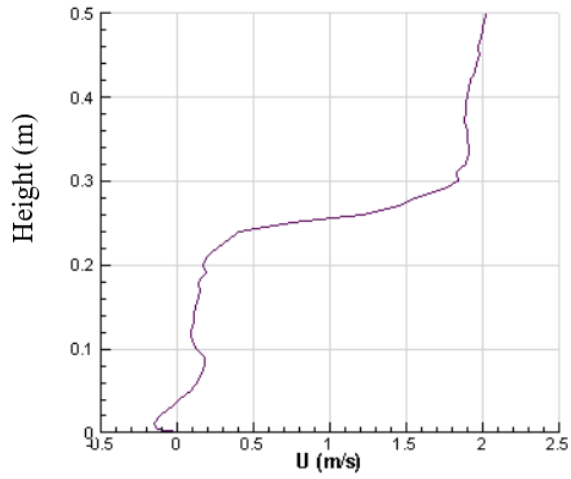
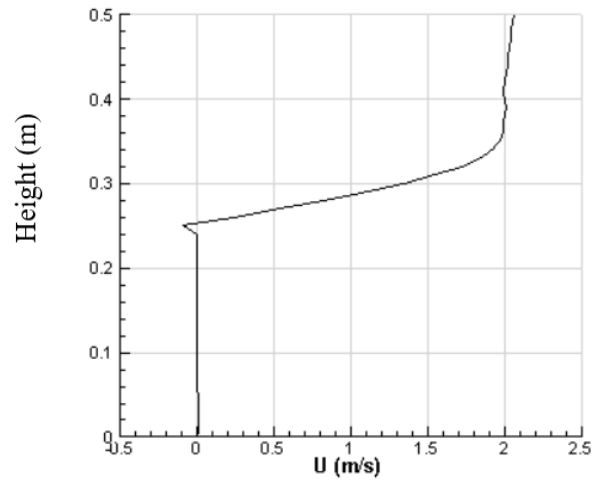


Figure 3.3: Velocity distribution at $t = 1$ s for single-sided ventilation with an opening on the windward wall (Case 1)

Section A



Section B



Section C

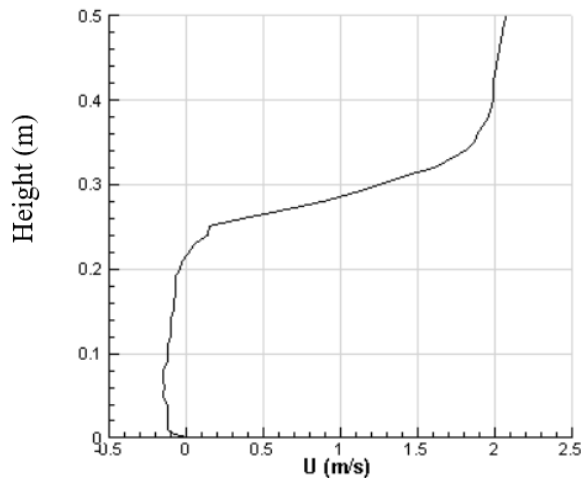
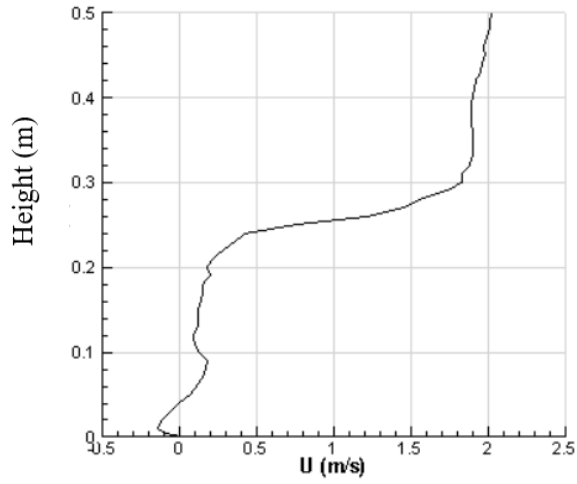
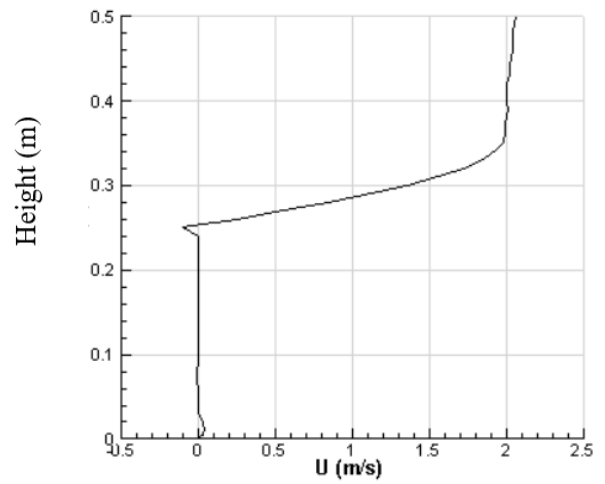


Figure 3.4: Velocity distribution at $t = 1.5$ s for single-sided ventilation with an opening on the windward wall (Case 1)

Section A



Section B



Section C

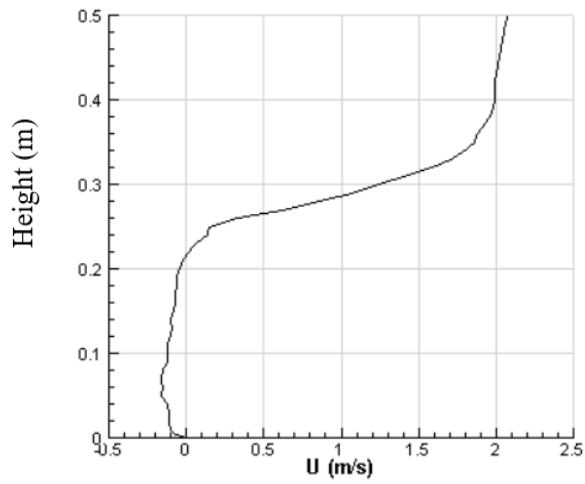
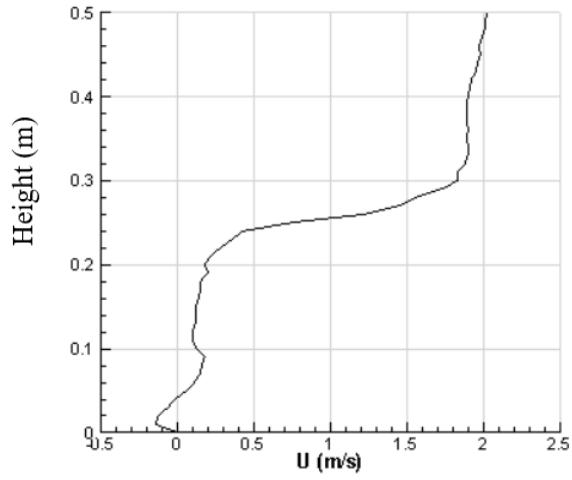
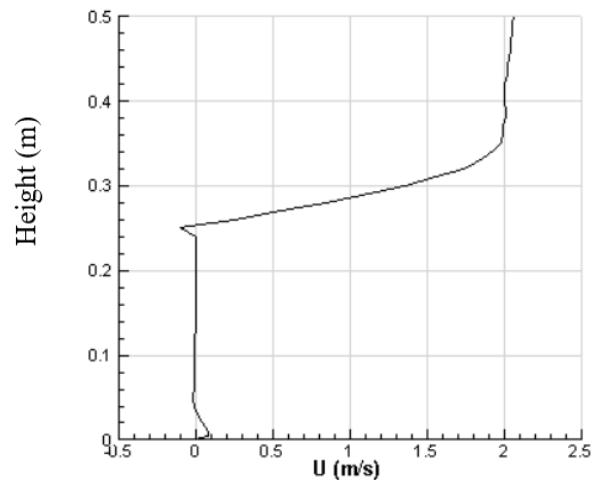


Figure 3.5: Velocity distribution at $t = 2$ s for single-sided ventilation with an opening on the windward wall (Case 1)

Section A



Section B



Section C

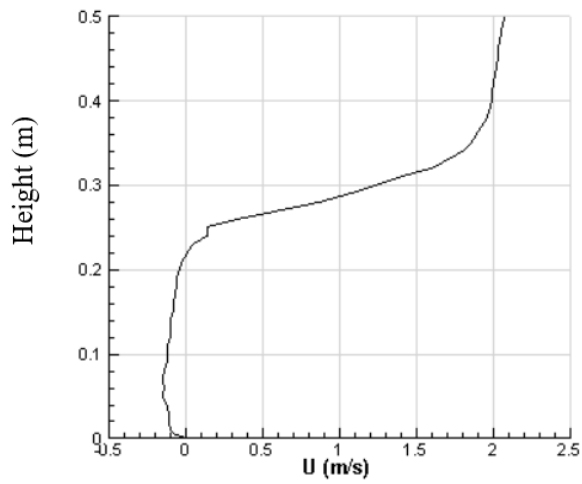
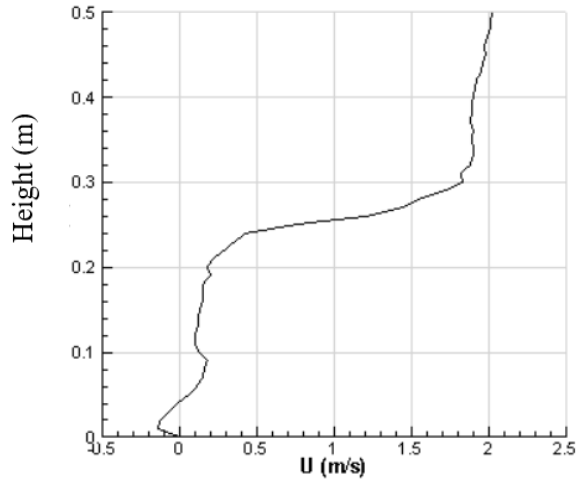
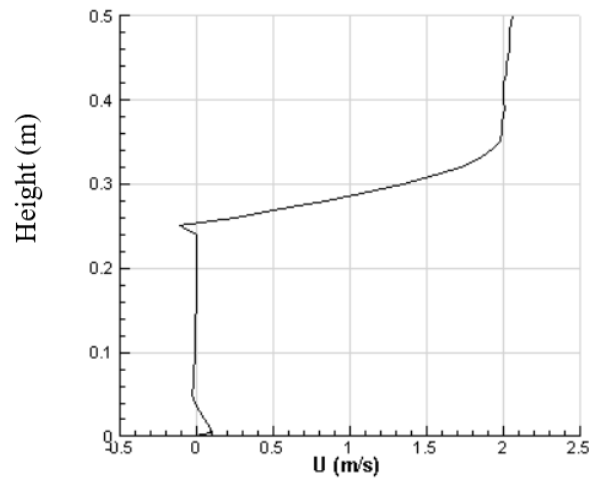


Figure 3.6: Velocity distribution at $t = 2.5$ s for single-sided ventilation with an opening on the windward wall (Case 1)

Section A



Section B



Section C

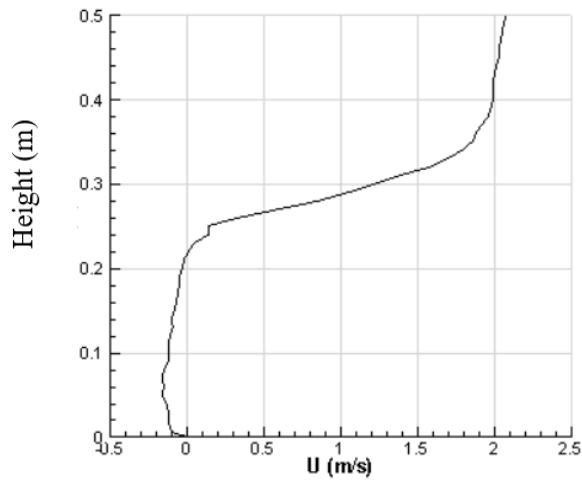
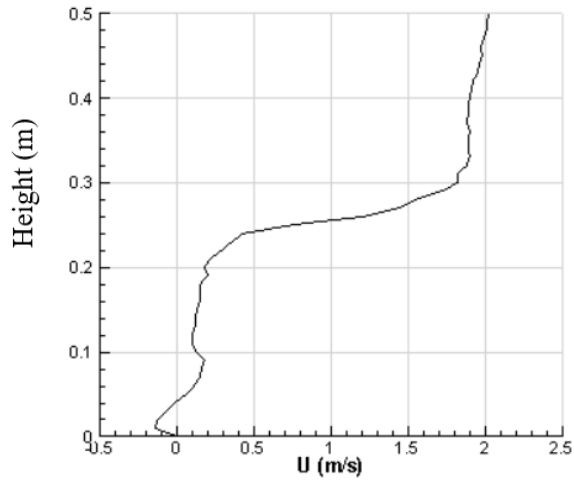
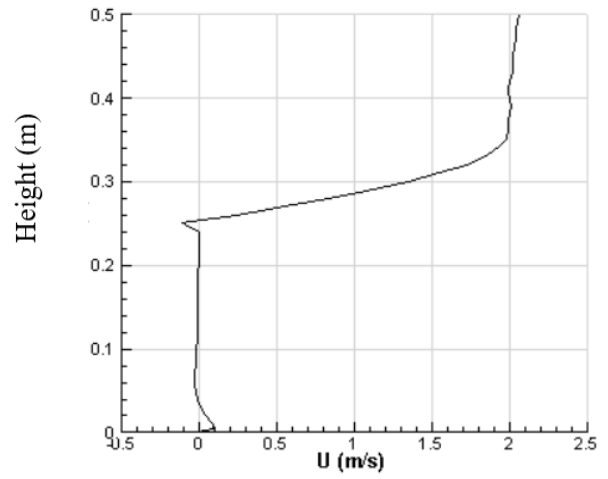


Figure 3.7: Velocity distribution at $t = 3$ s for single-sided ventilation with an opening on the windward wall (Case 1)

Section A



Section B



Section C

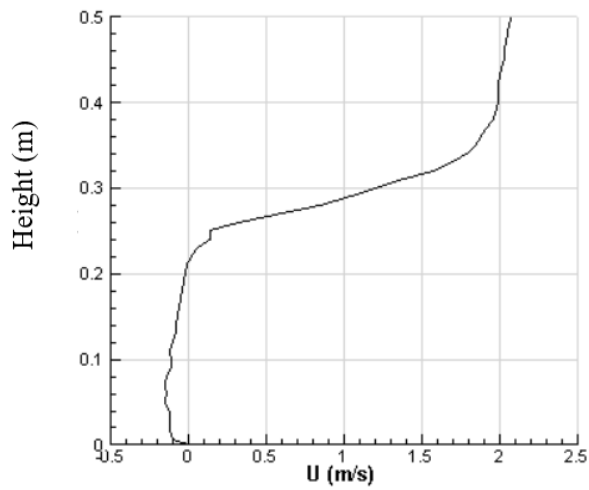


Figure 3.8: Velocity distribution at $t = 5$ s for single-sided ventilation with an opening on the windward wall (Case 1)

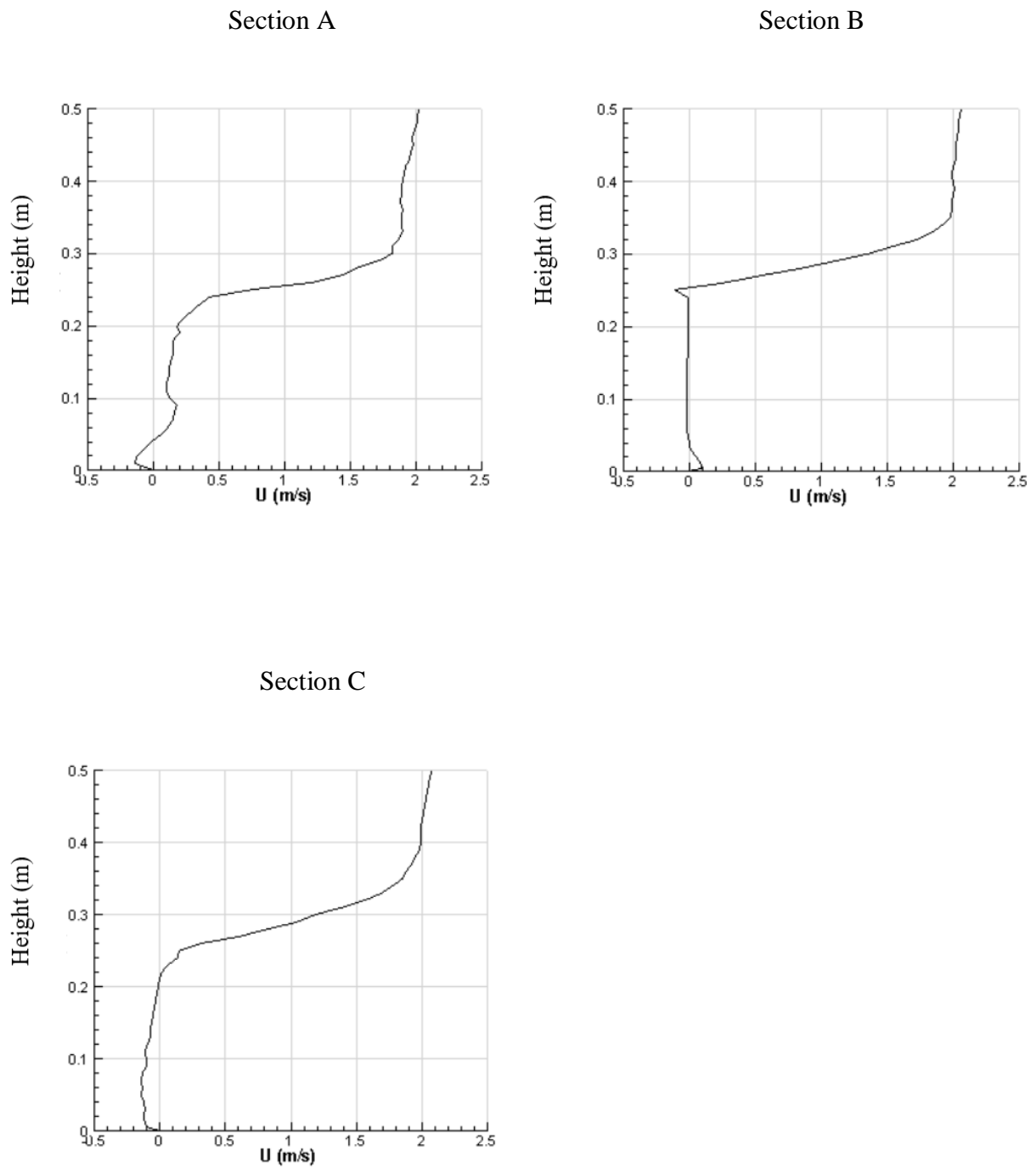


Figure 3.9: Velocity distribution at $t = 10$ s for single-sided ventilation with an opening on the windward wall (Case 1)

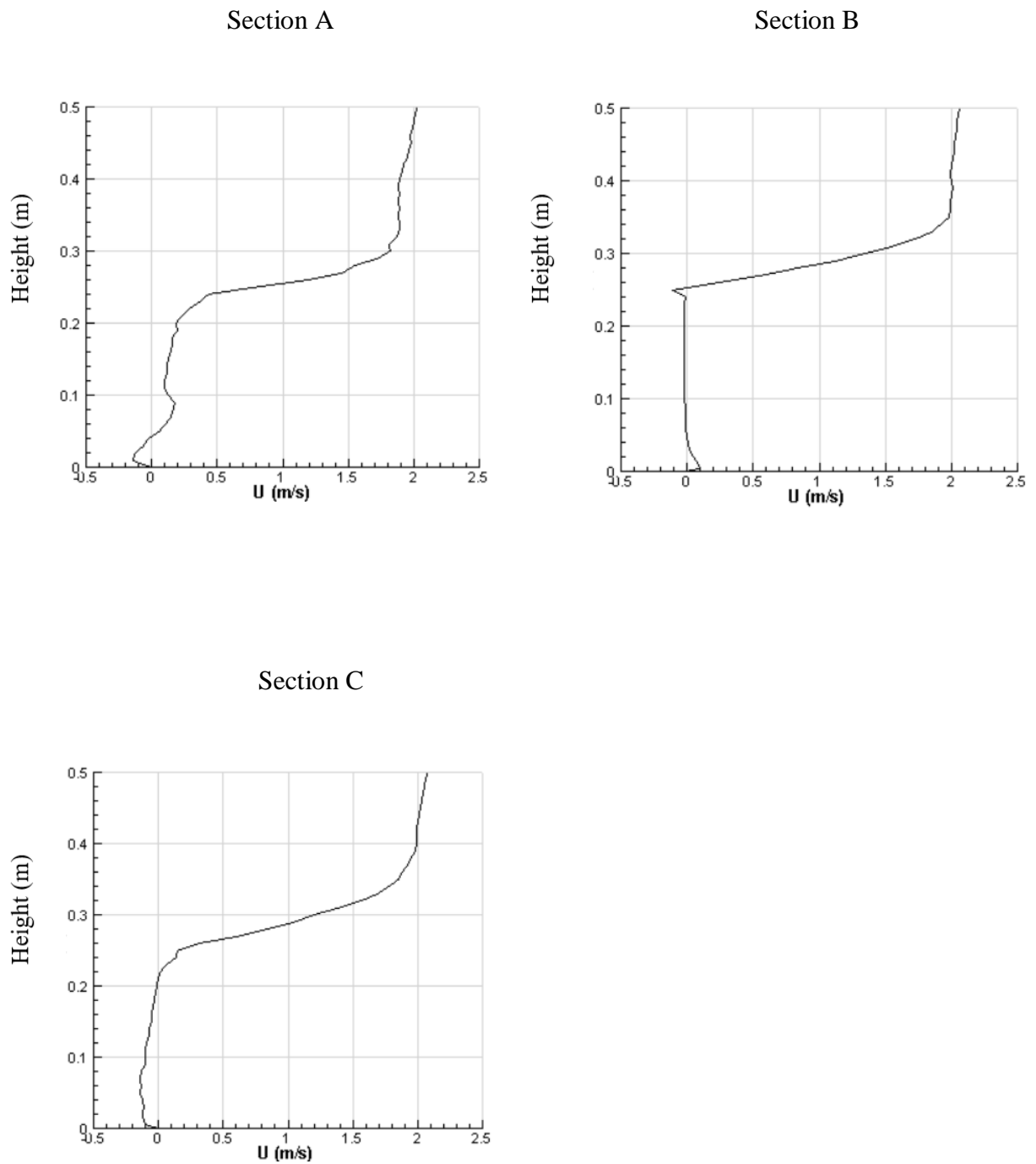


Figure 3.10: Velocity distribution at $t = 15$ s for single-sided ventilation with an opening on the windward wall (Case 1)

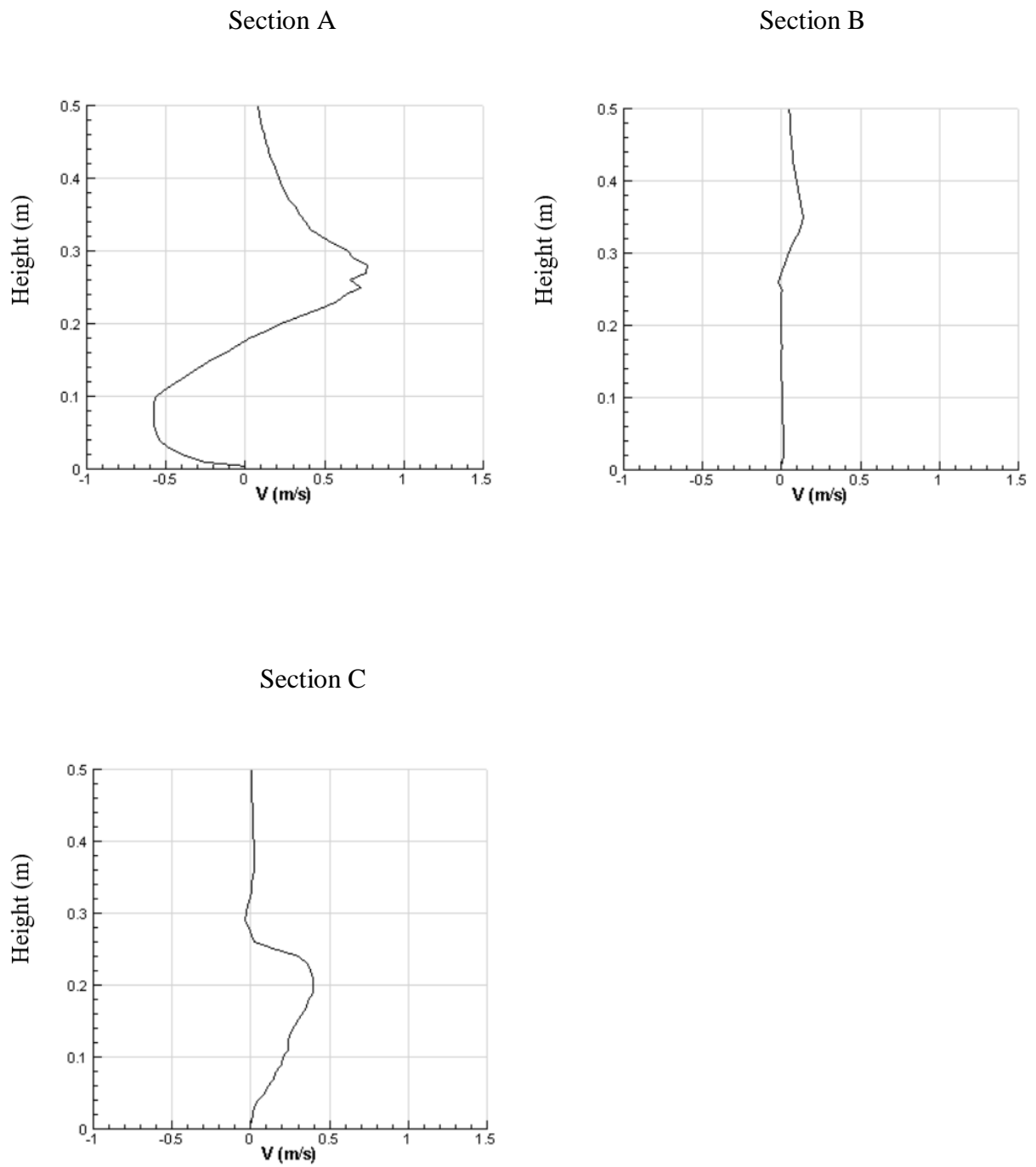


Figure 3.11: Velocity distribution along vertical direction at $t = 3$ s for single-sided ventilation with an opening on the windward wall (Case 1)

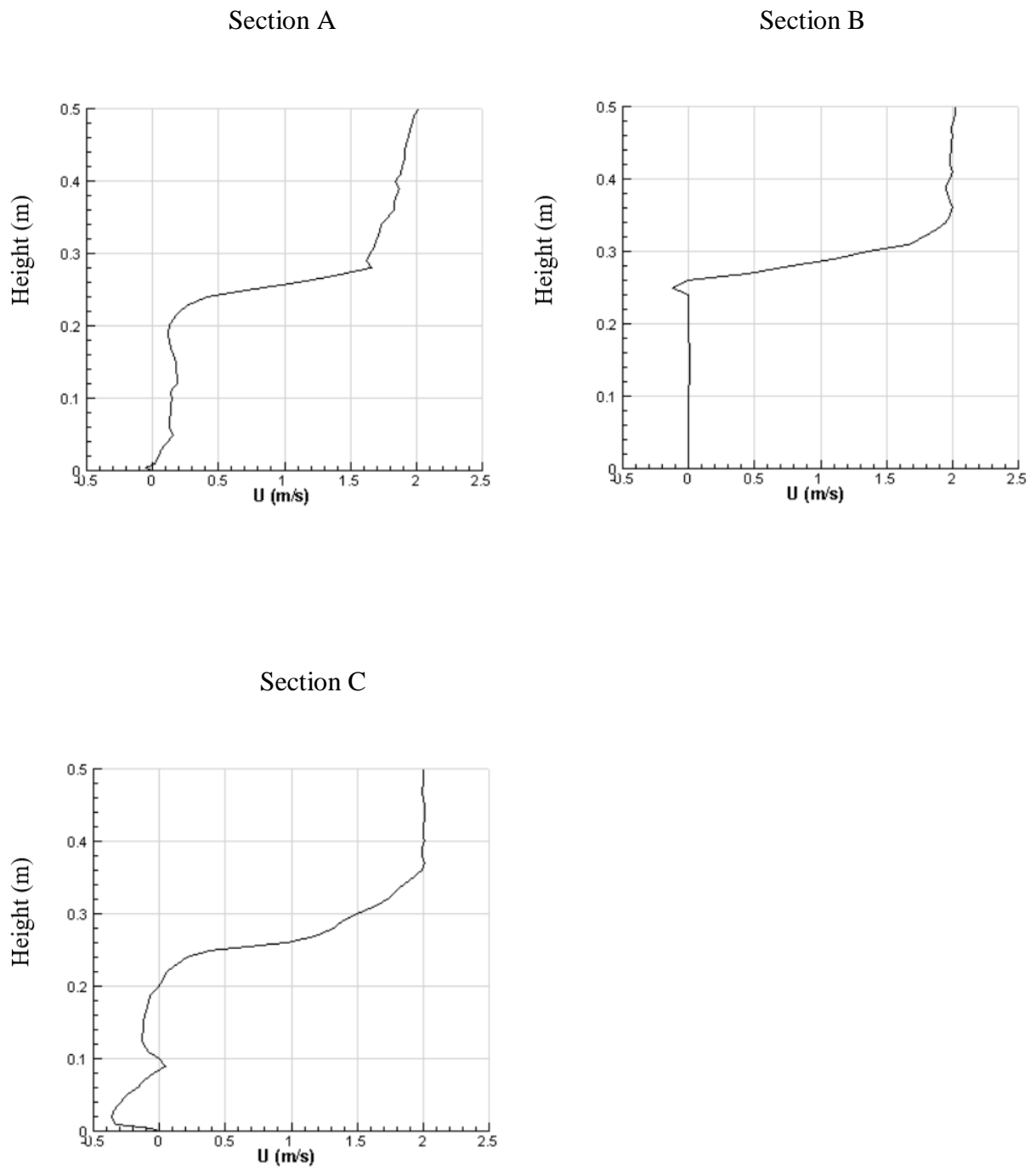


Figure 3.12: Velocity distribution at $t = 0.5$ s for single-sided ventilation with an opening on the leeward wall (Case 2)

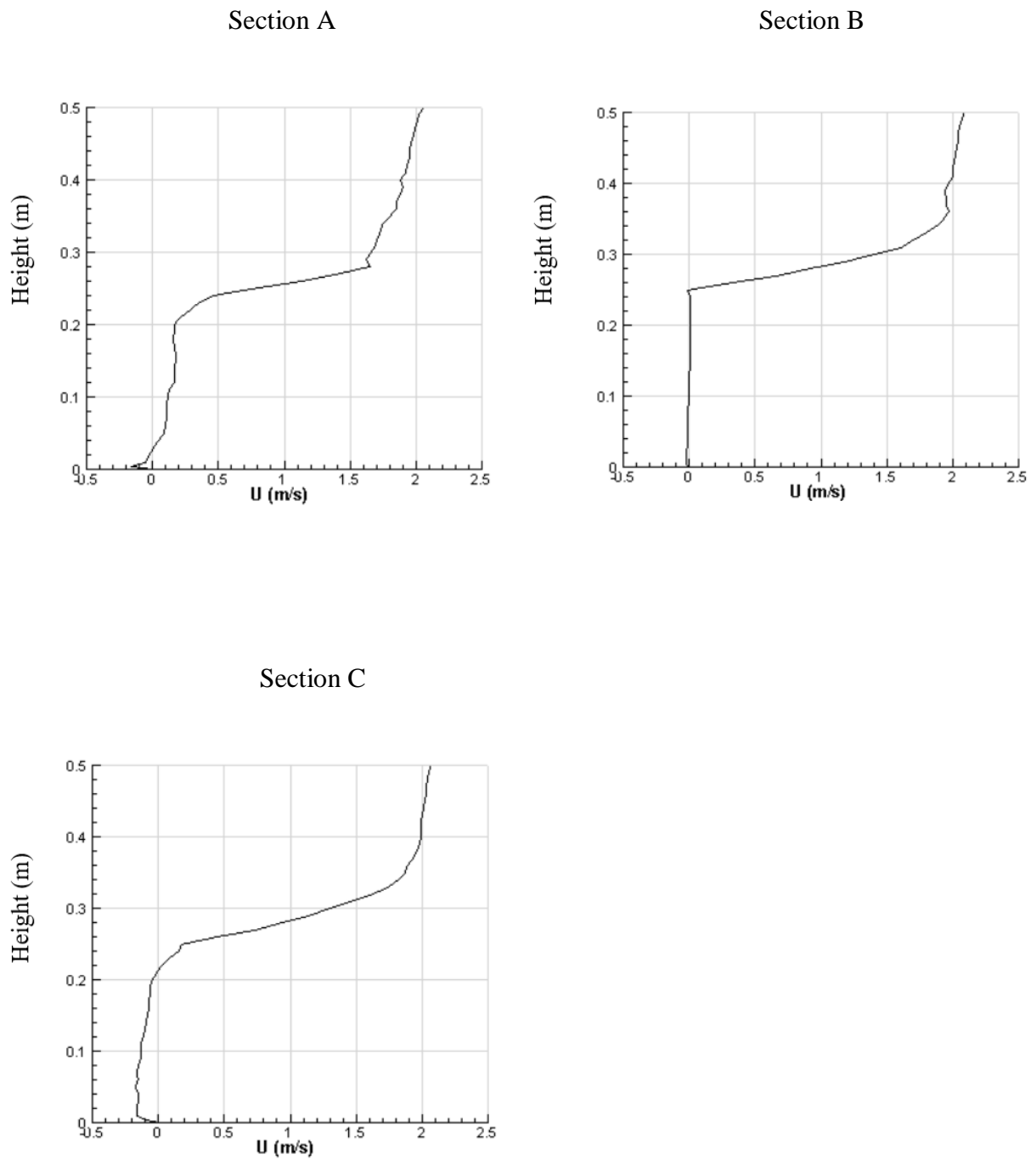
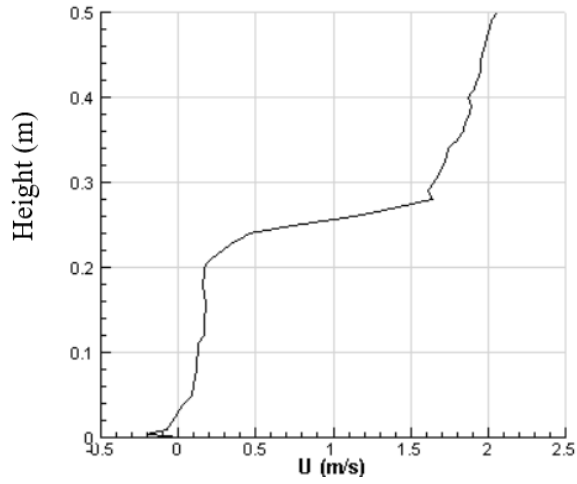
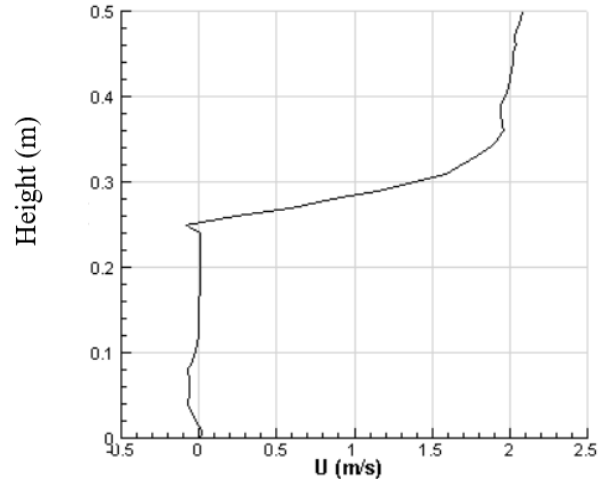


Figure 3.13: Velocity distribution at $t = 1$ s for single-sided ventilation with an opening on the leeward wall (Case 2)

Section A



Section B



Section C

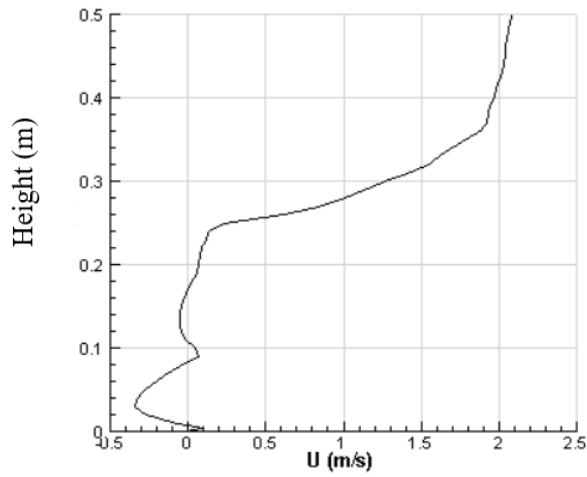


Figure 3.14: Velocity distribution at $t = 1.5$ s for single-sided ventilation with an opening on the leeward wall (Case 2)

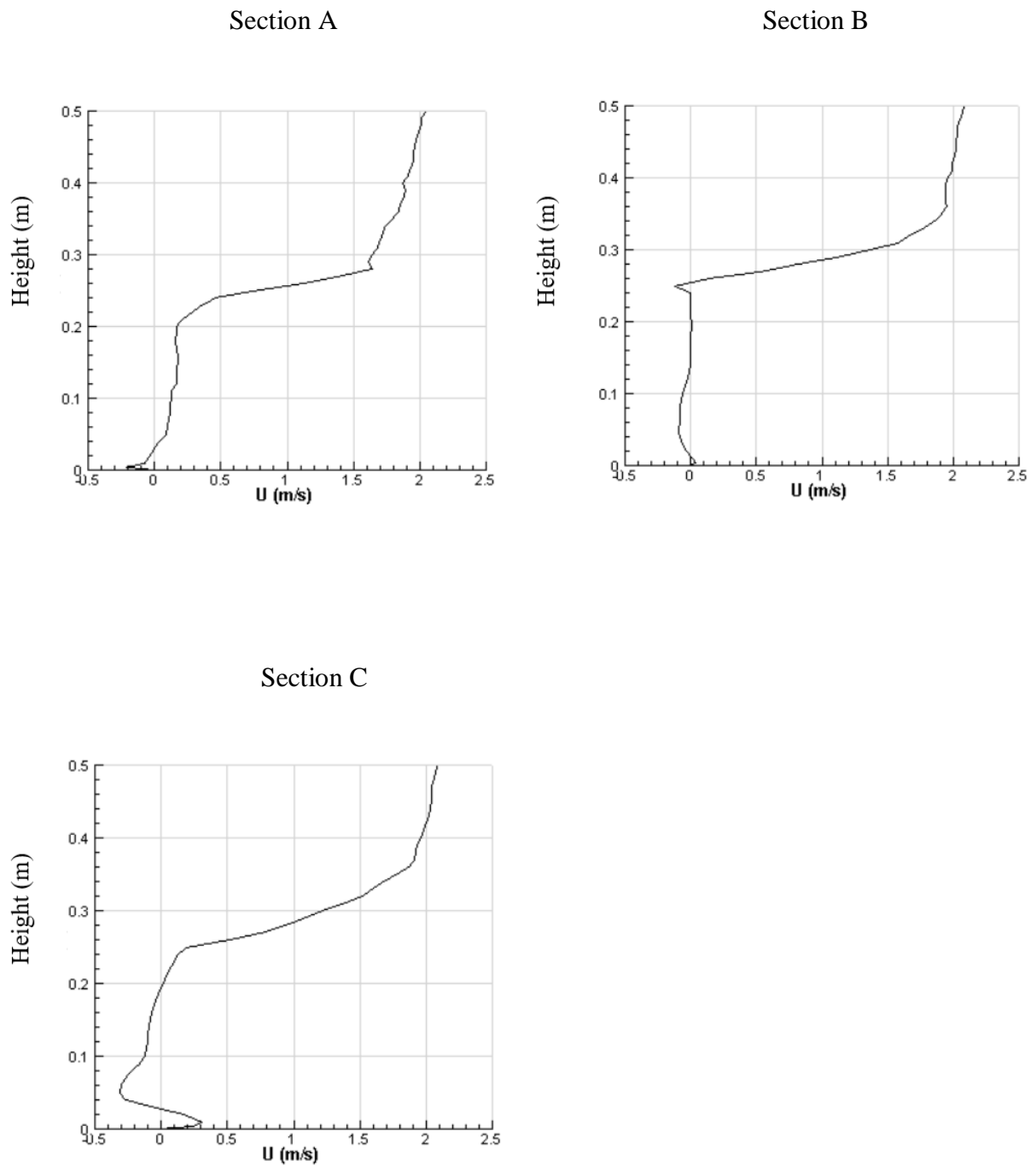


Figure 3.15: Velocity distribution at $t = 2$ s for single-sided ventilation with an opening on the leeward wall (Case 2)

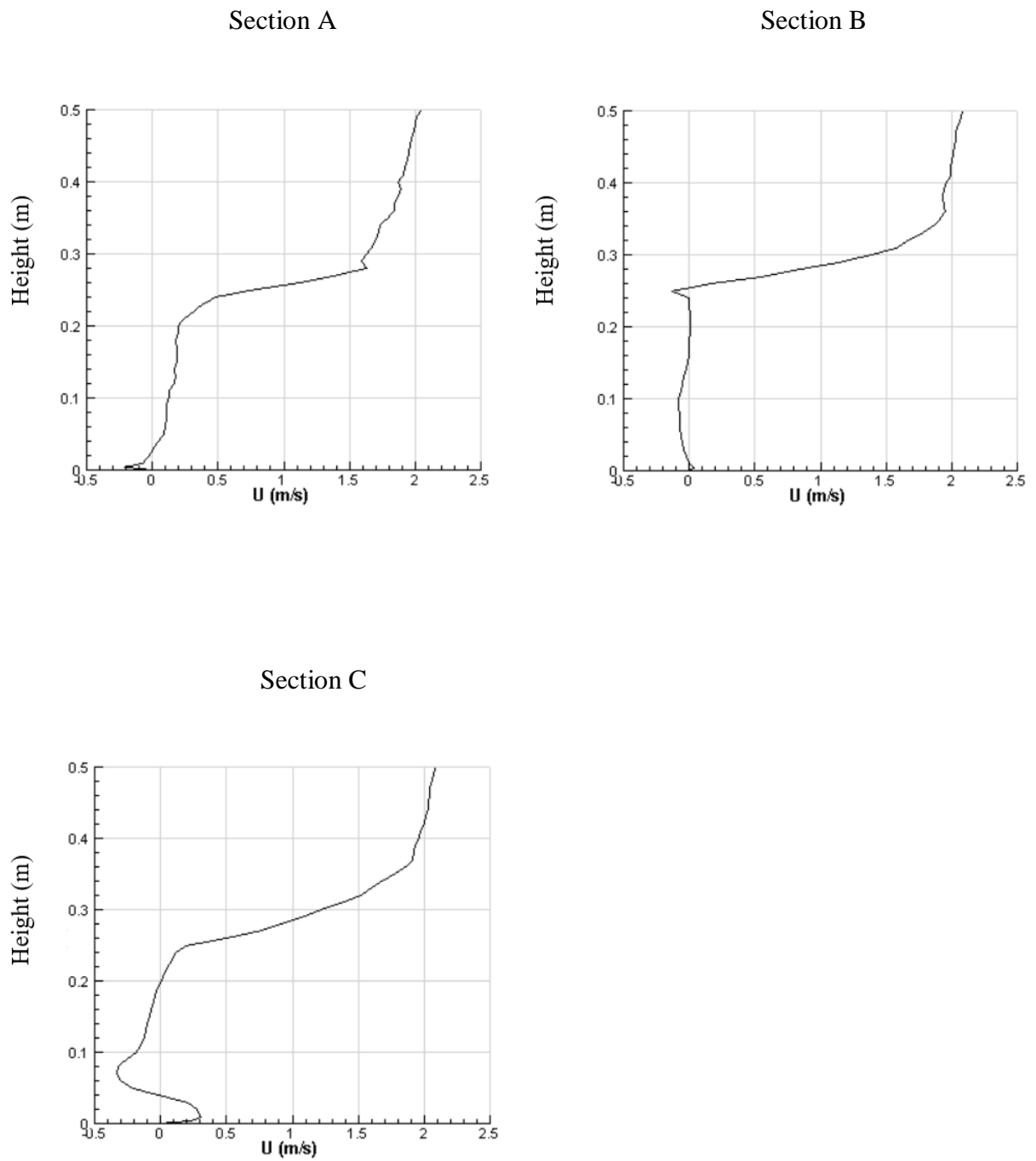


Figure 3.16: Velocity distribution at $t = 2.5$ s for single-sided ventilation with an opening on the leeward wall (Case 2)

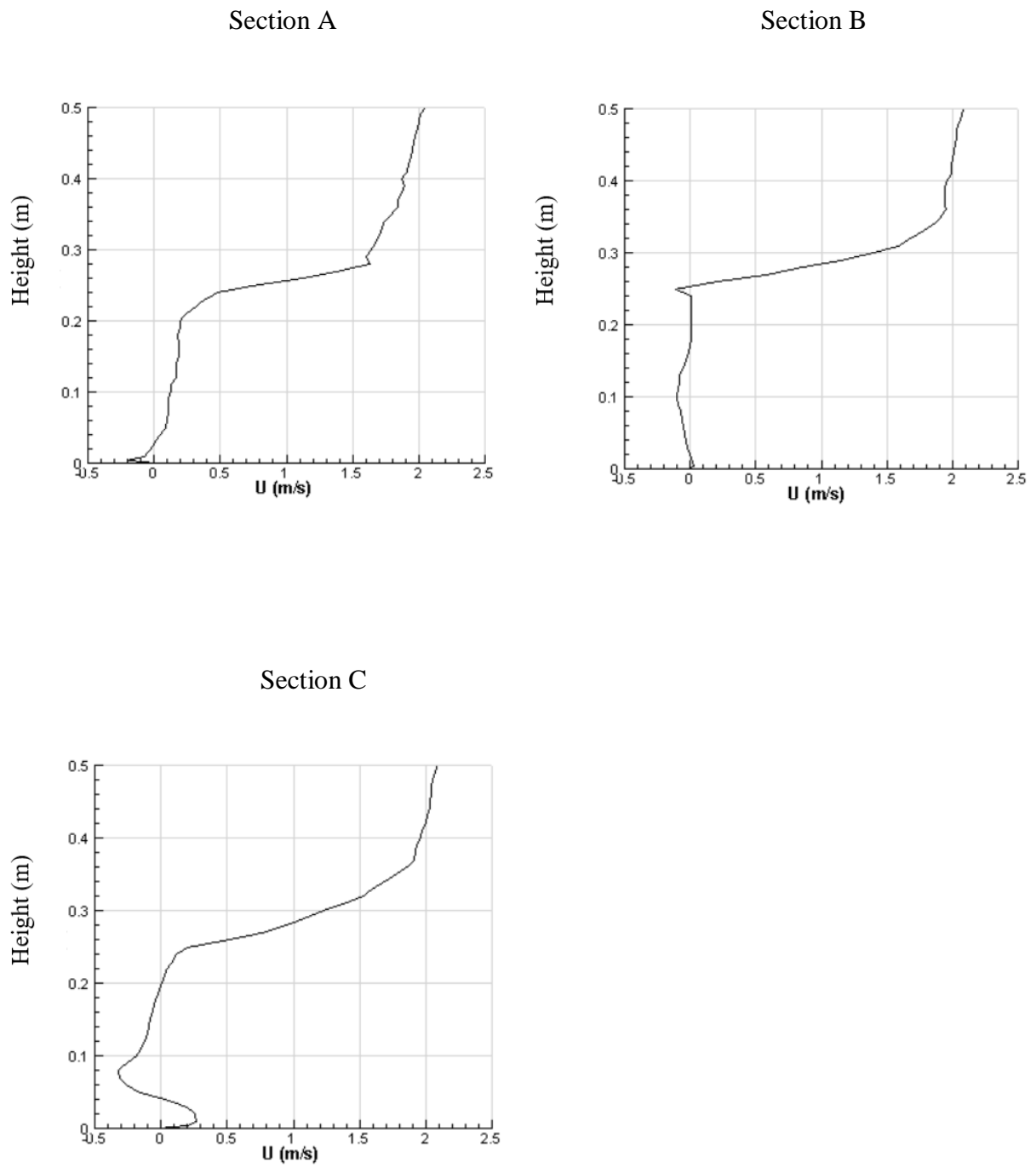


Figure 3.17: Velocity distribution at $t = 3$ s for single-sided ventilation with an opening on the leeward wall (Case 2)

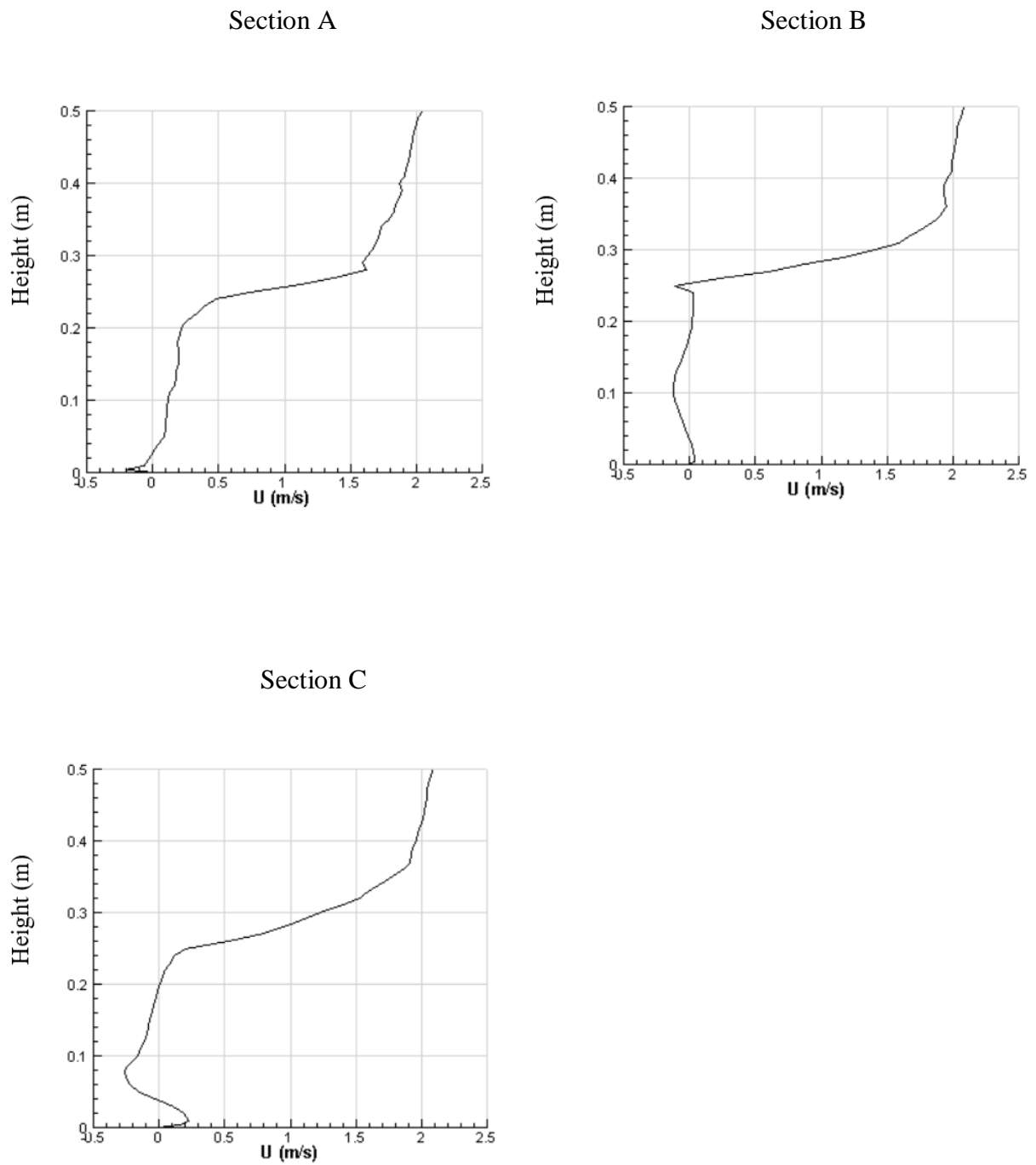
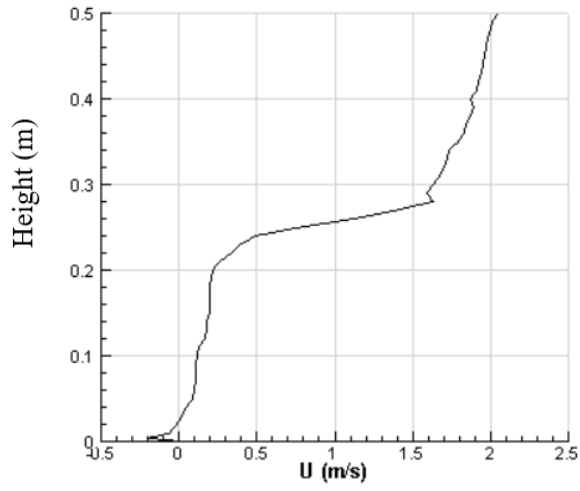
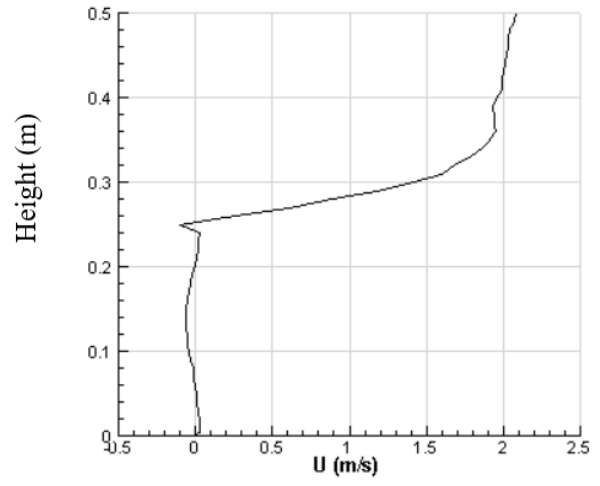


Figure 3.18: Velocity distribution at $t = 5$ s for single-sided ventilation with an opening on the leeward wall (Case 2)

Section A



Section B



Section C

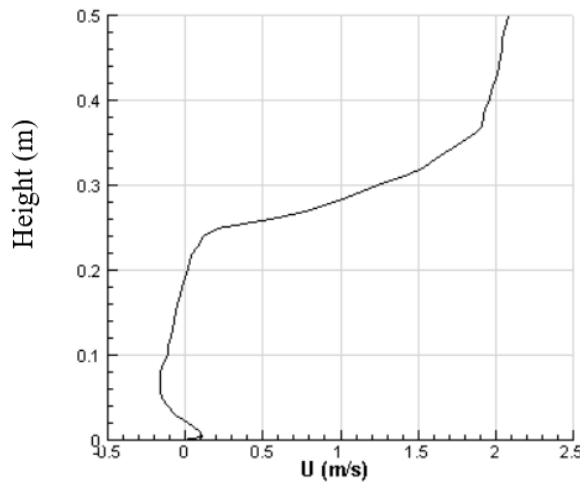
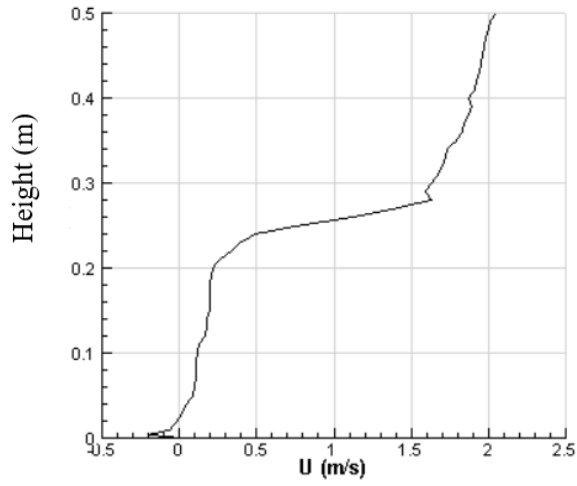
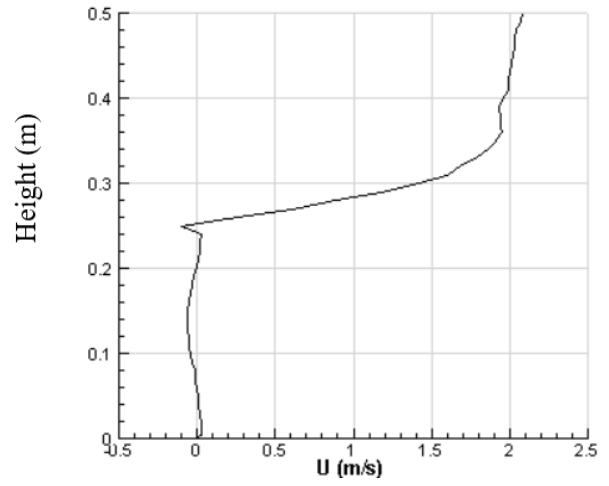


Figure 3.19: Velocity distribution at $t = 10$ s for single-sided ventilation with an opening on the leeward wall (Case 2)

Section A



Section B



Section C

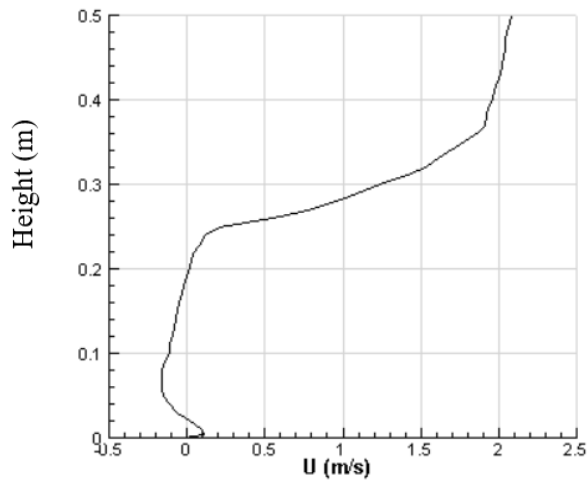


Figure 3.20: Velocity distribution at $t = 15$ s for single-sided ventilation with an opening on the leeward wall (Case 2)

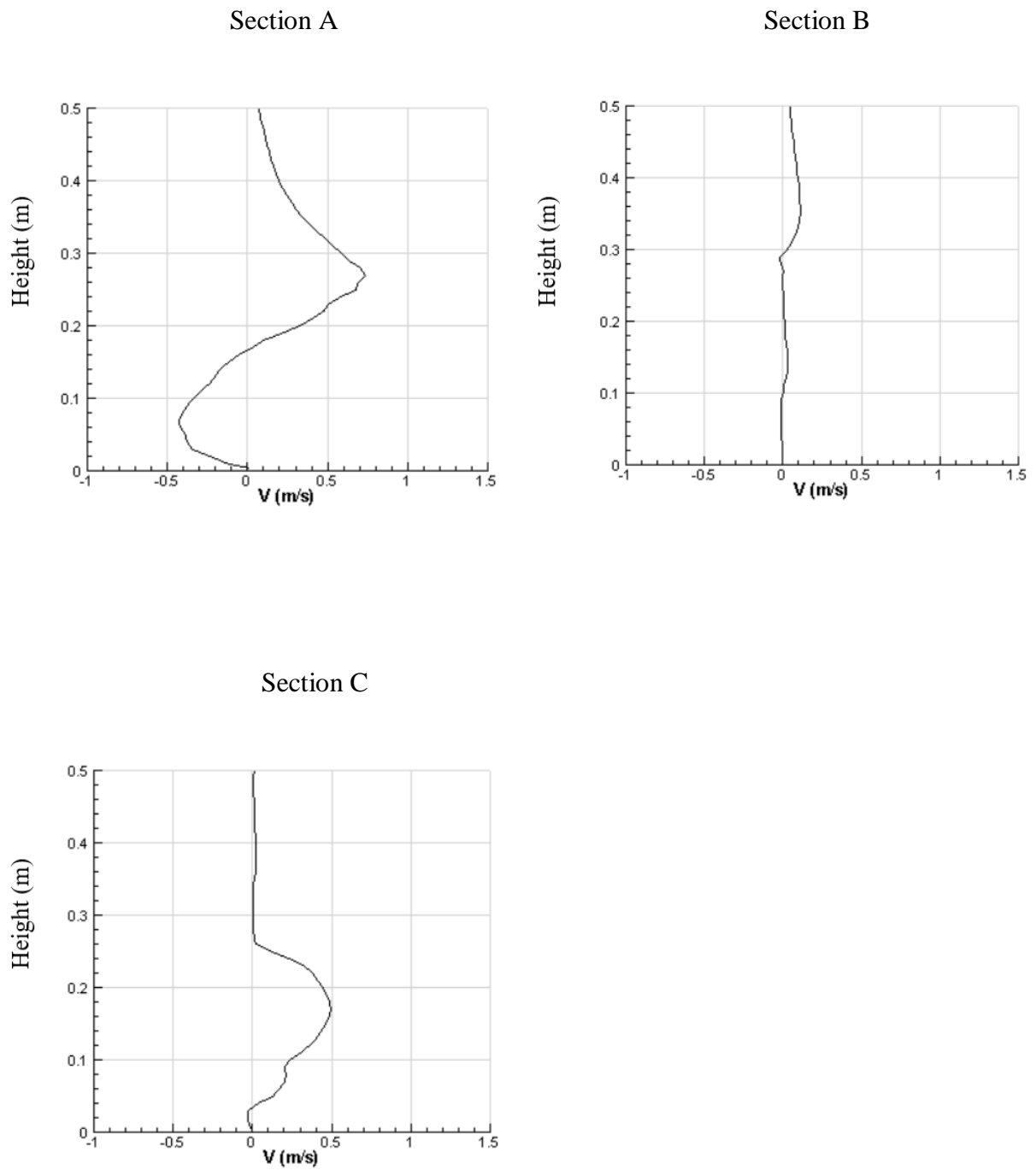


Figure 3.21: Velocity distribution along vertical direction at $t = 3$ s for single-sided ventilation with an opening on the leeward wall (Case 2)

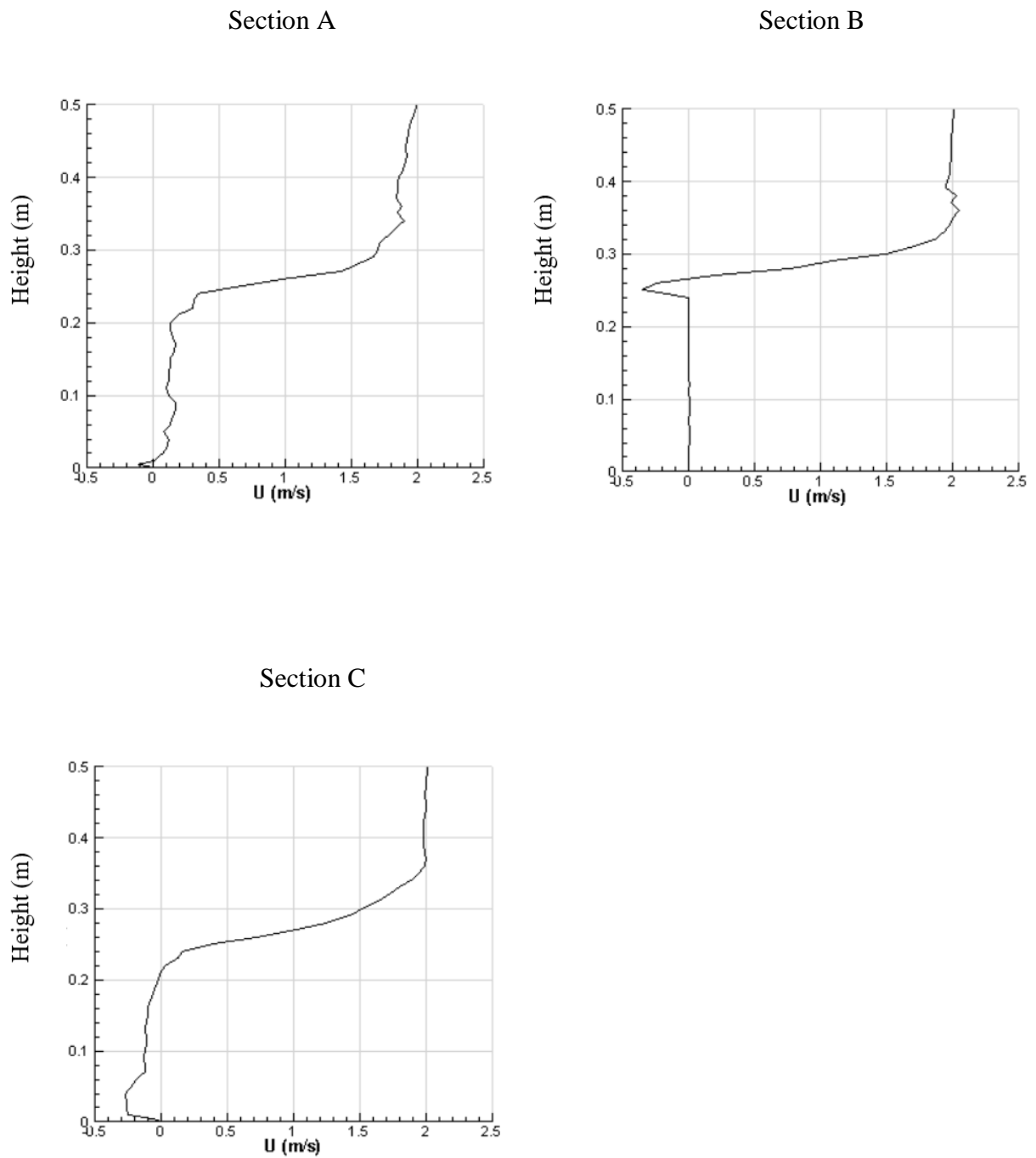
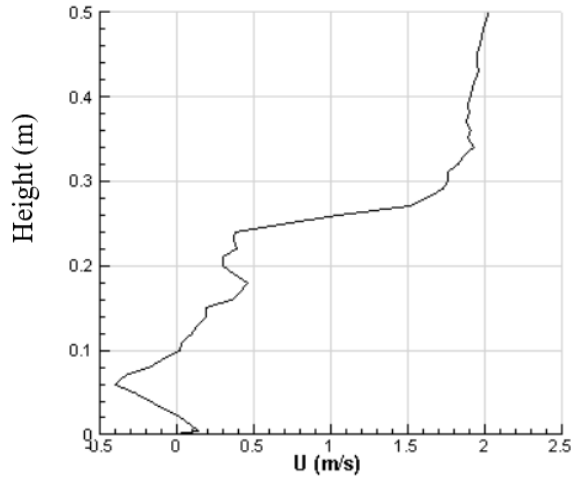
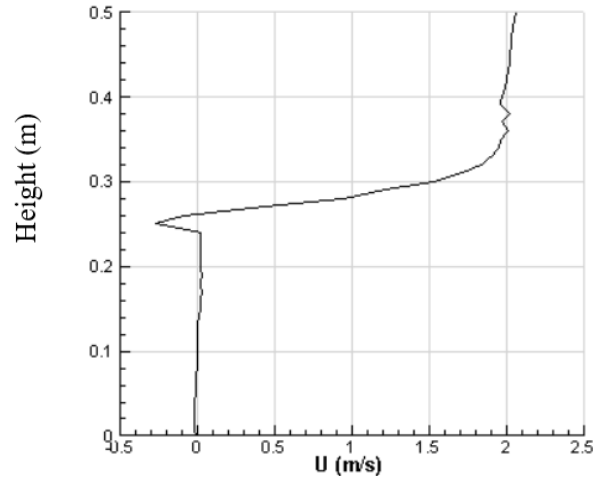


Figure 3.22: Velocity distribution at $t = 0.5$ s for single-sided ventilation with double openings on the windward wall (Case 3)

Section A



Section B



Section C

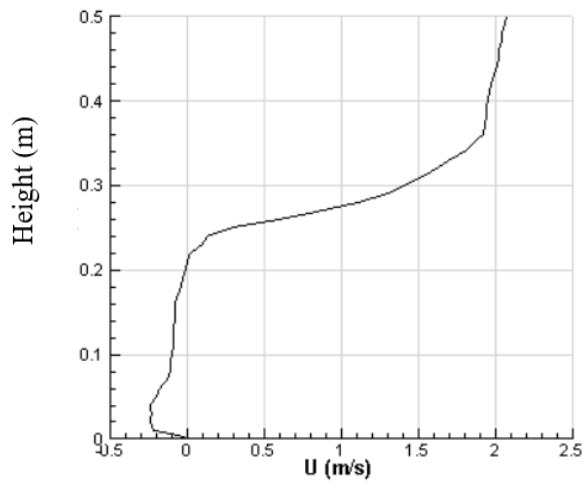


Figure 3.23: Velocity distribution at $t = 1$ s for single-sided ventilation with double openings on the windward wall (Case 3)

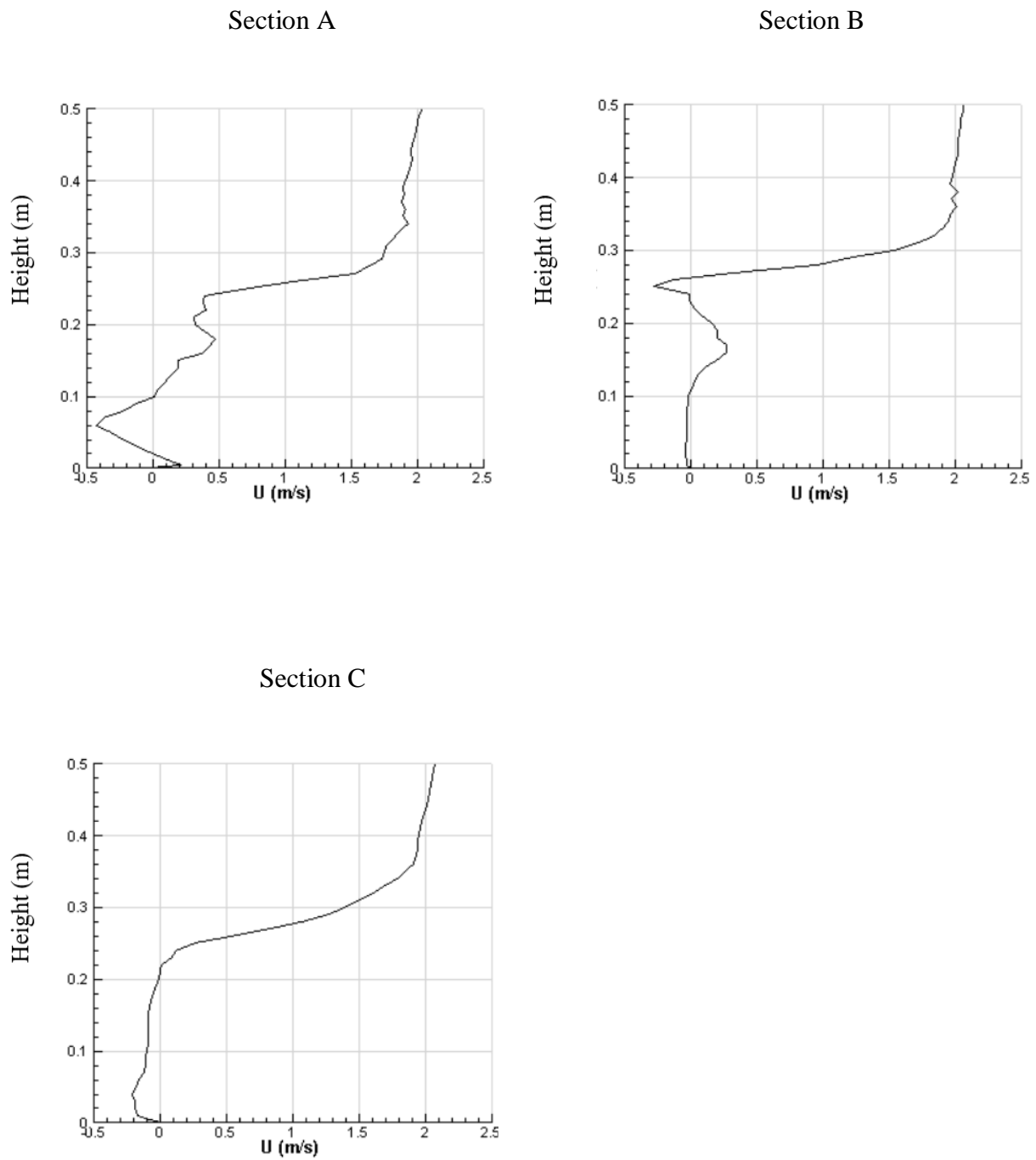


Figure 3.24: Velocity distribution at $t = 1.5$ s for single-sided ventilation with double openings on the windward wall (Case 3)

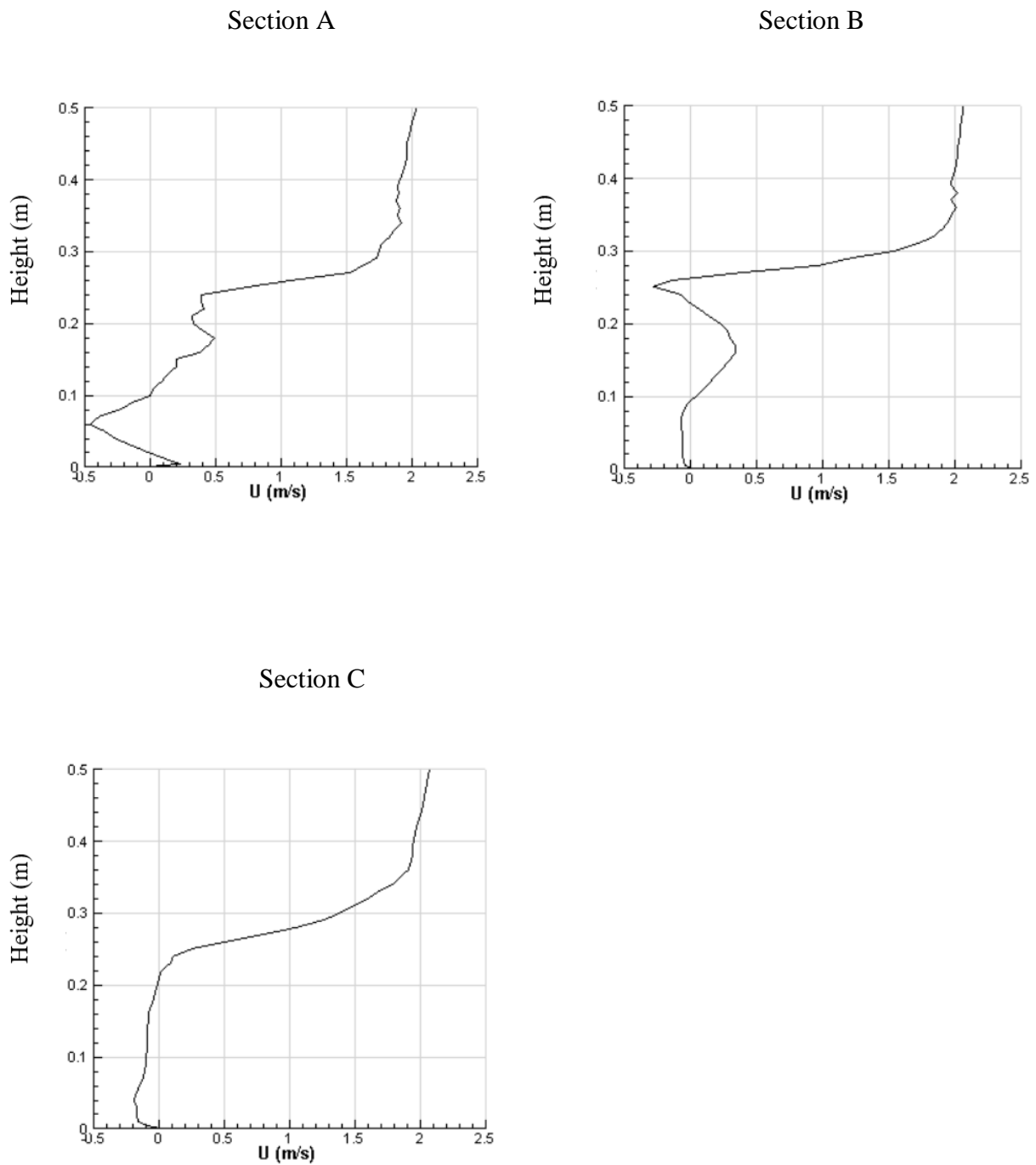


Figure 3.25: Velocity distribution at $t = 2$ s for single-sided ventilation with double openings on the windward wall (Case 3)

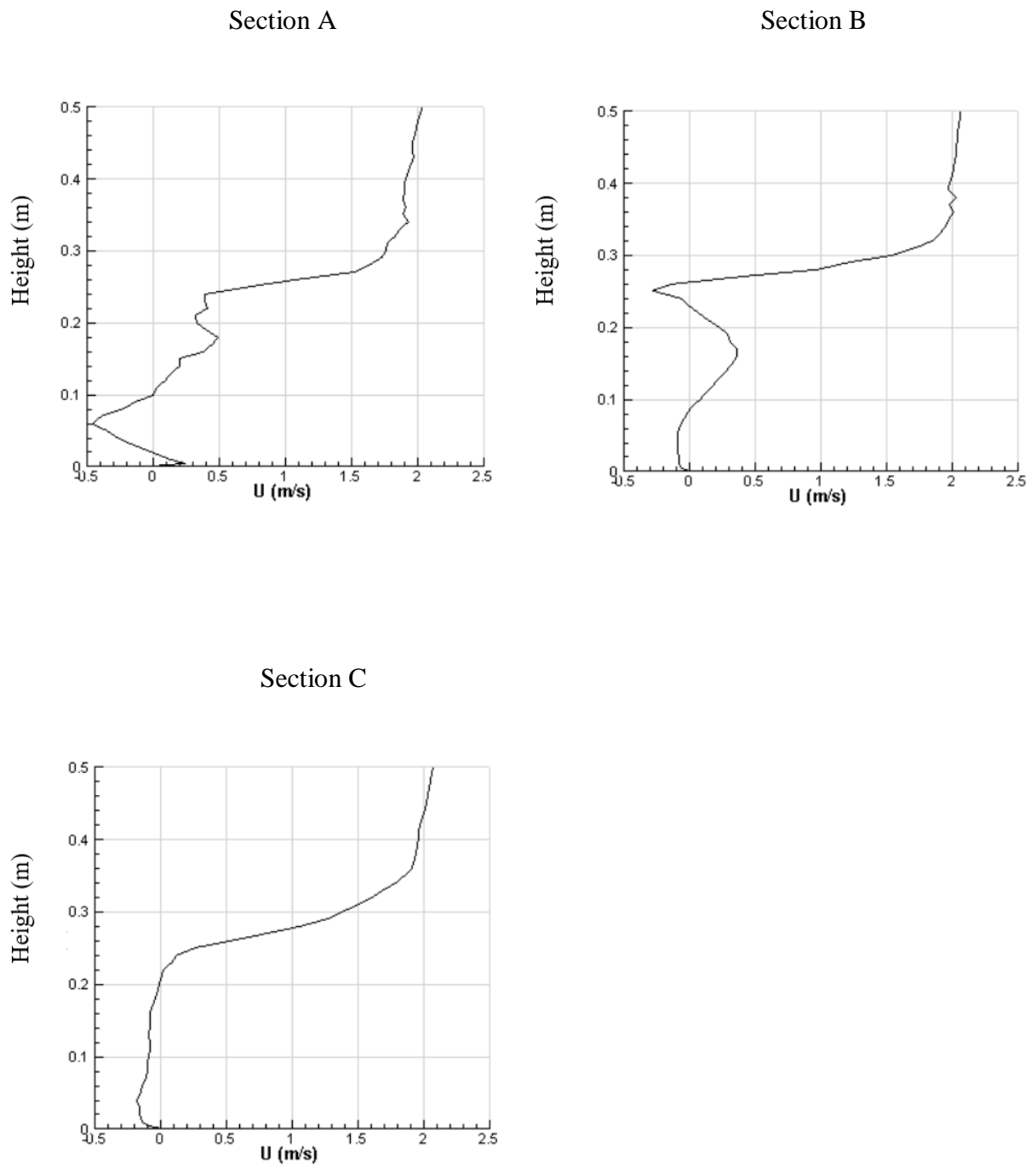


Figure 3.26: Velocity distribution at $t = 2.5$ s for single-sided ventilation with double openings on the windward wall (Case 3)

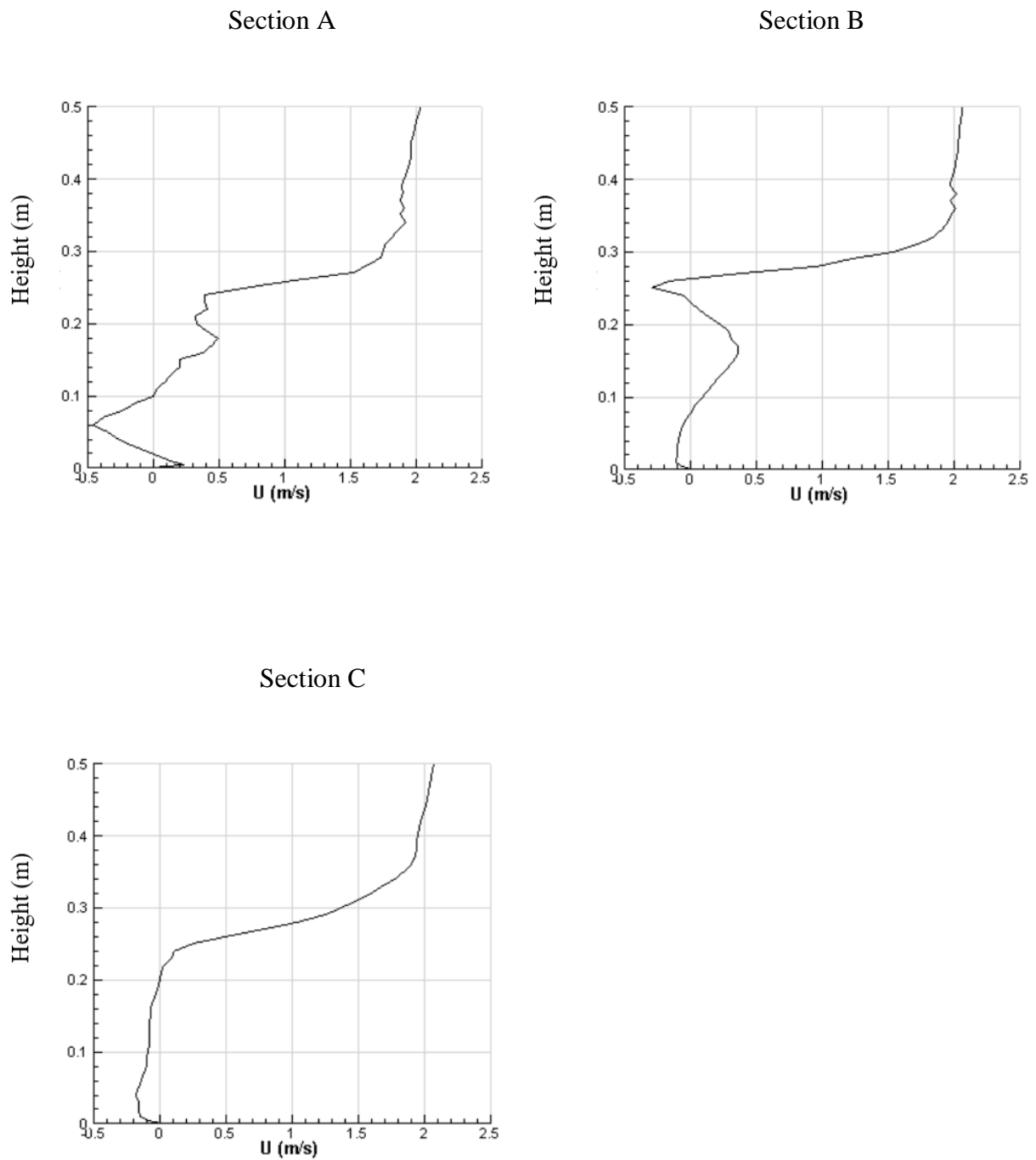


Figure 3.27: Velocity distribution at $t = 3$ s for single-sided ventilation with double openings on the windward wall (Case 3)

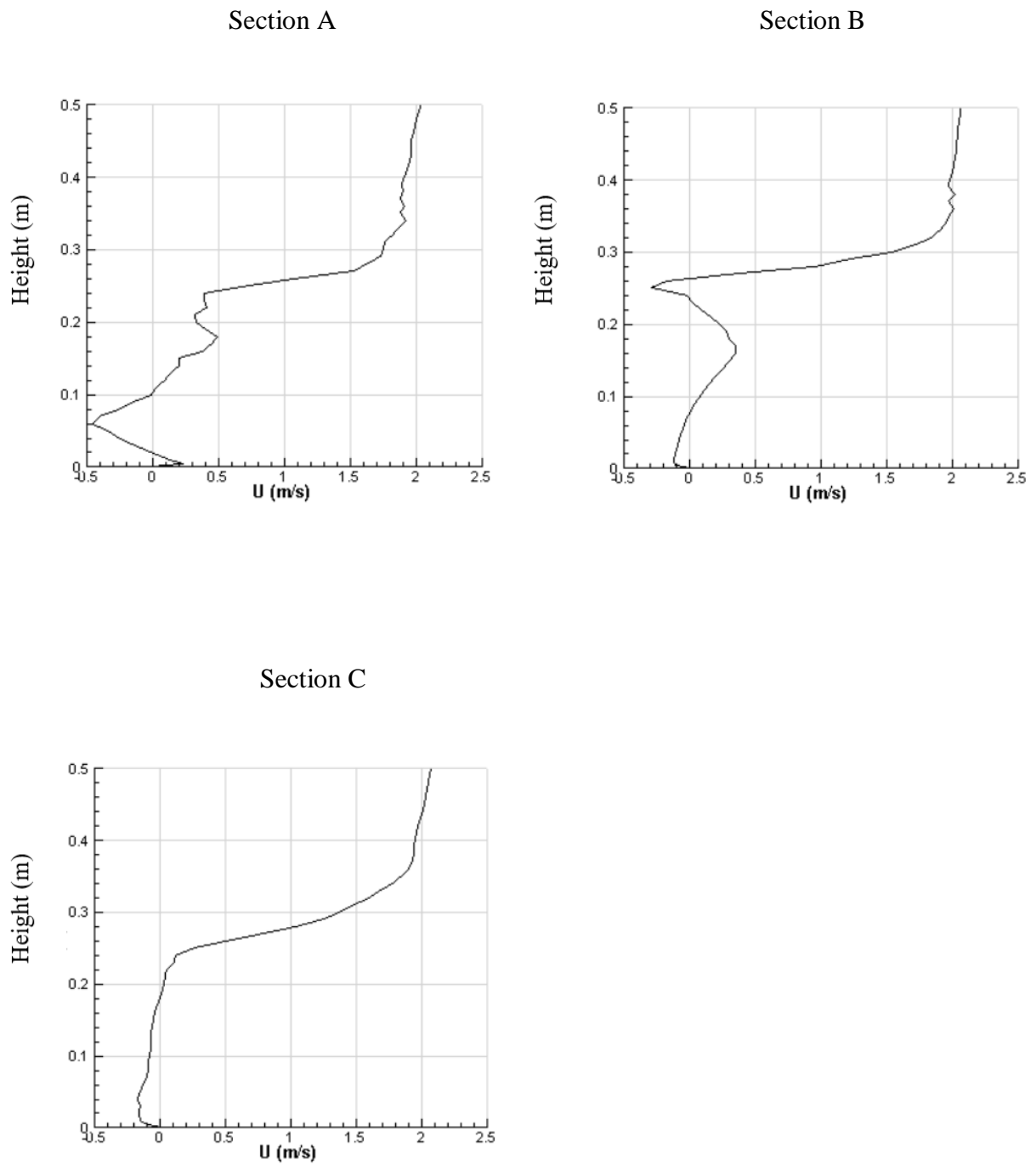


Figure 3.28: Velocity distribution at $t = 5$ s for single-sided ventilation with double openings on the windward wall (Case 3)

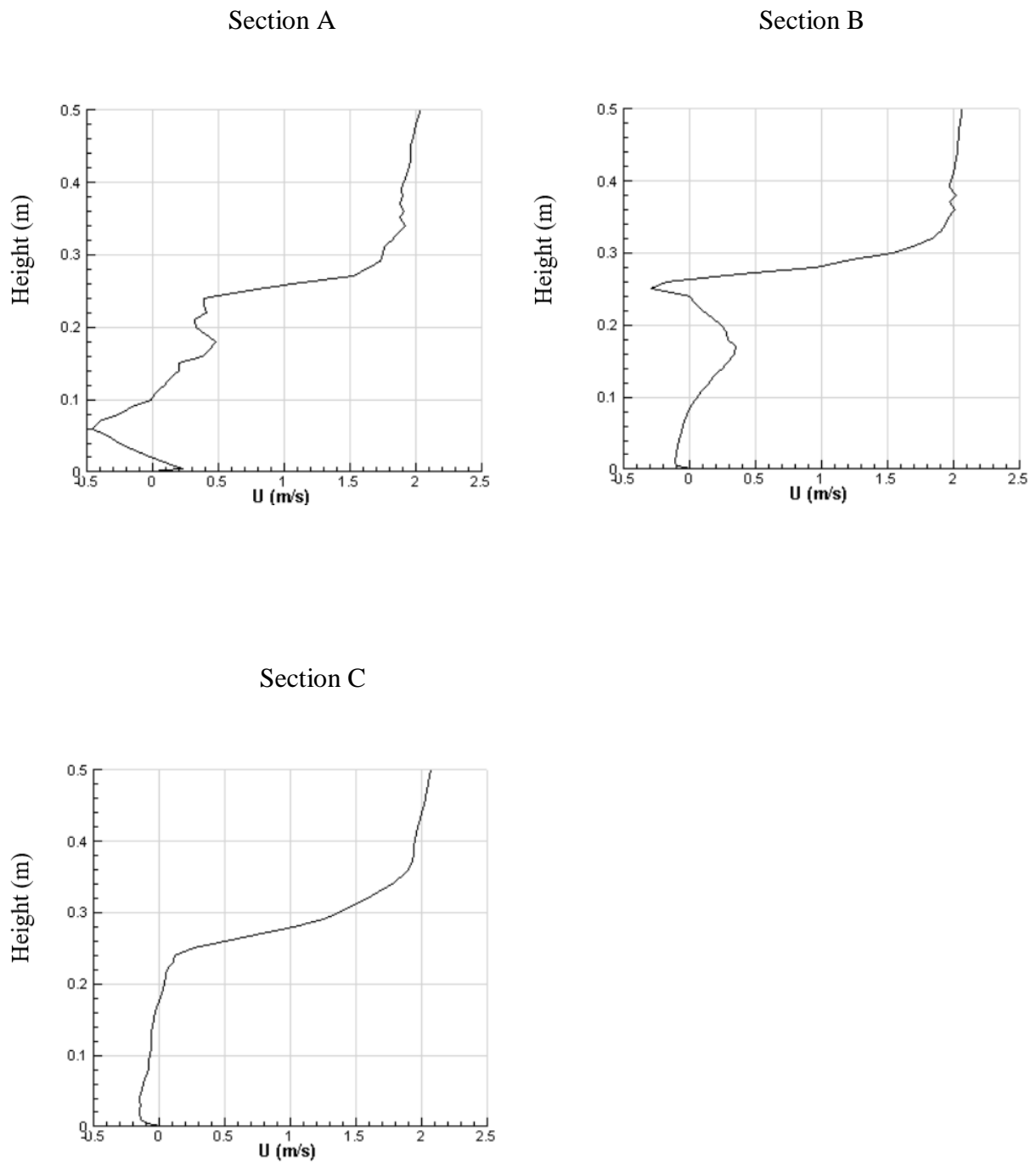


Figure 3.29: Velocity distribution at $t = 10$ s for single-sided ventilation with double openings on the windward wall (Case 3)

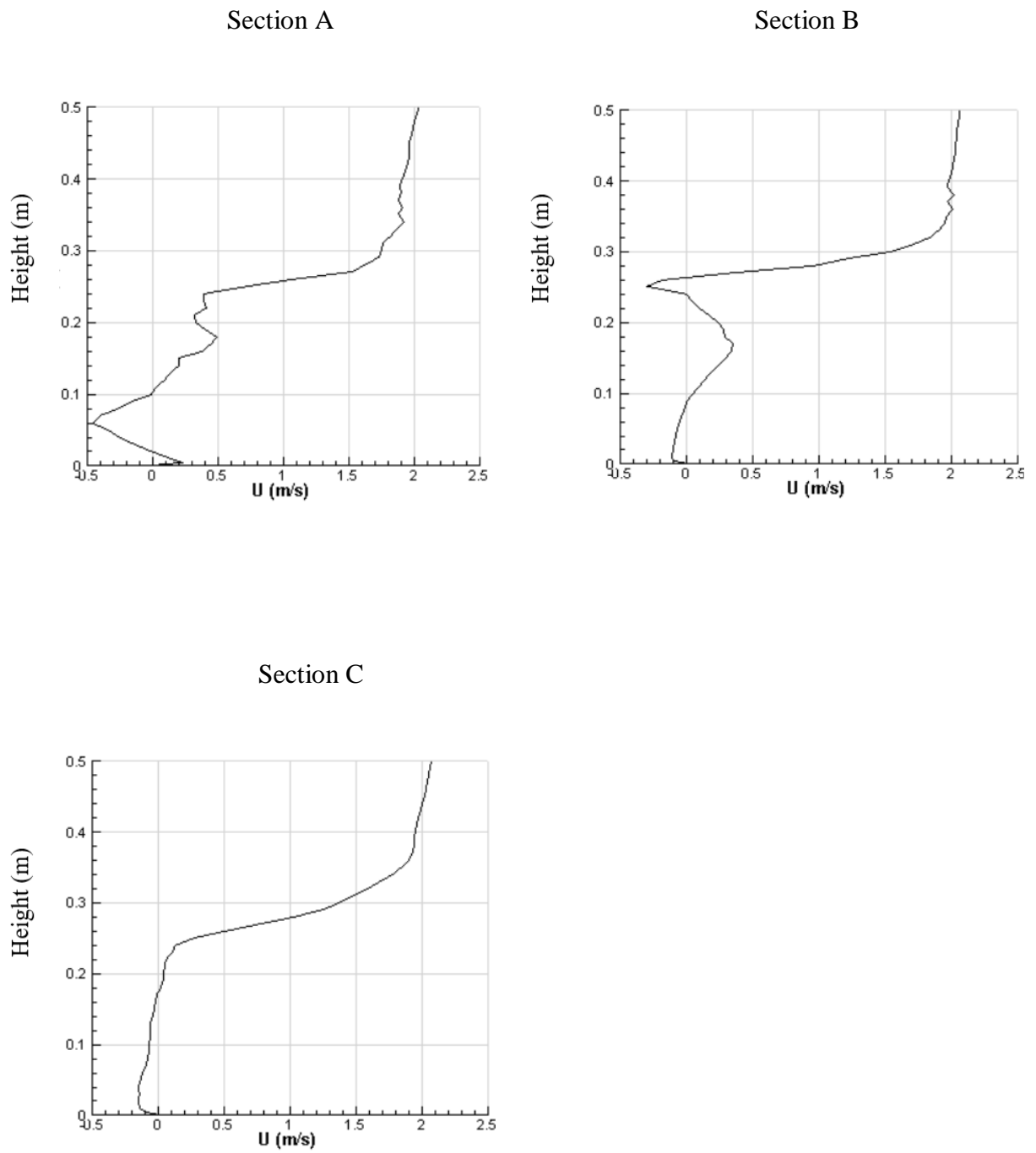


Figure 3.30: Velocity distribution at $t = 15$ s for single-sided ventilation with double openings on the windward wall (Case 3)

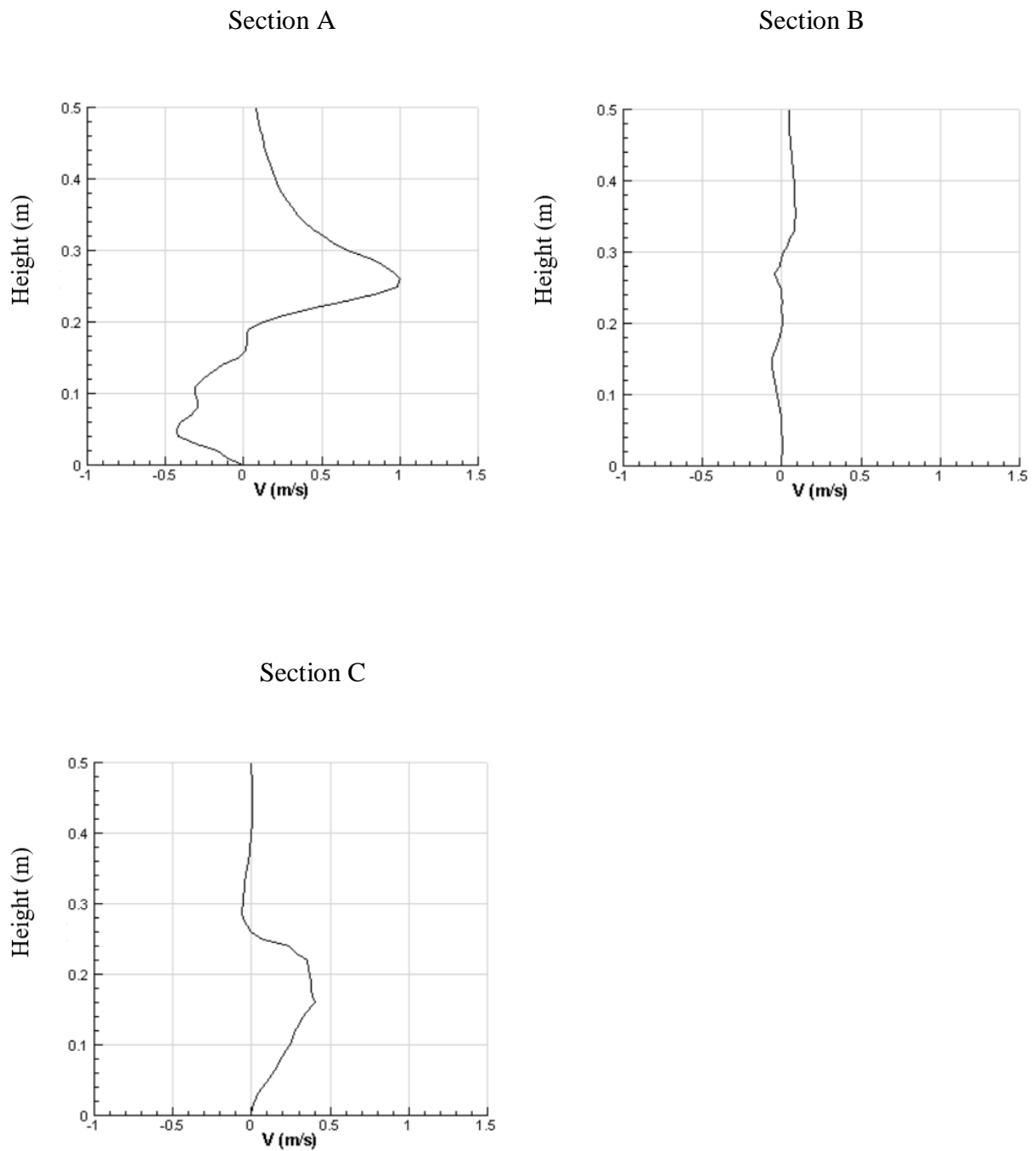


Figure 3.31: Velocity distribution along vertical direction at $t = 3$ s for single-sided ventilation with double openings on the windward wall (Case 3)

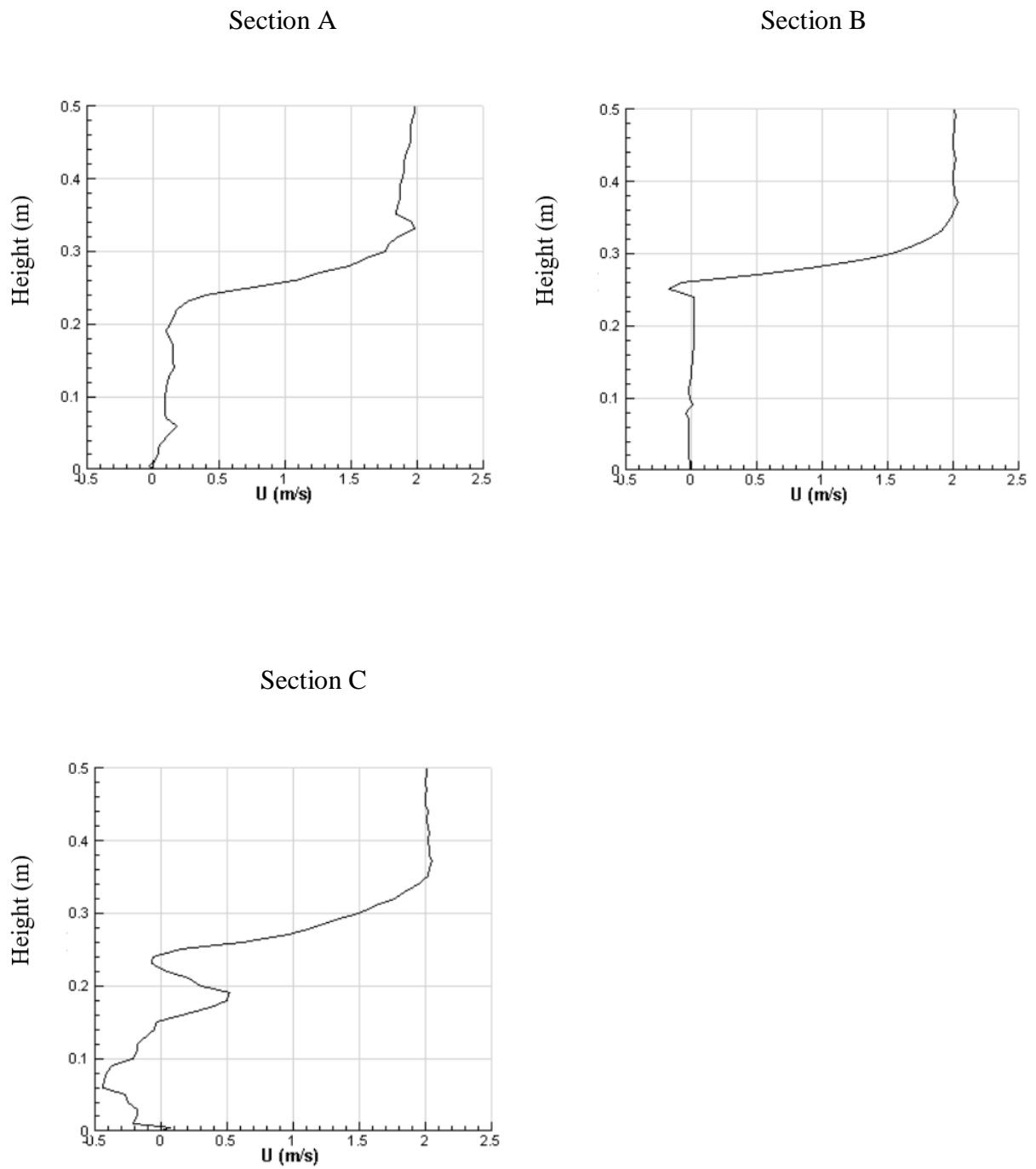


Figure 3.32: Velocity distribution at $t = 0.5$ s for single-sided ventilation with double openings on the leeward wall (Case 4)

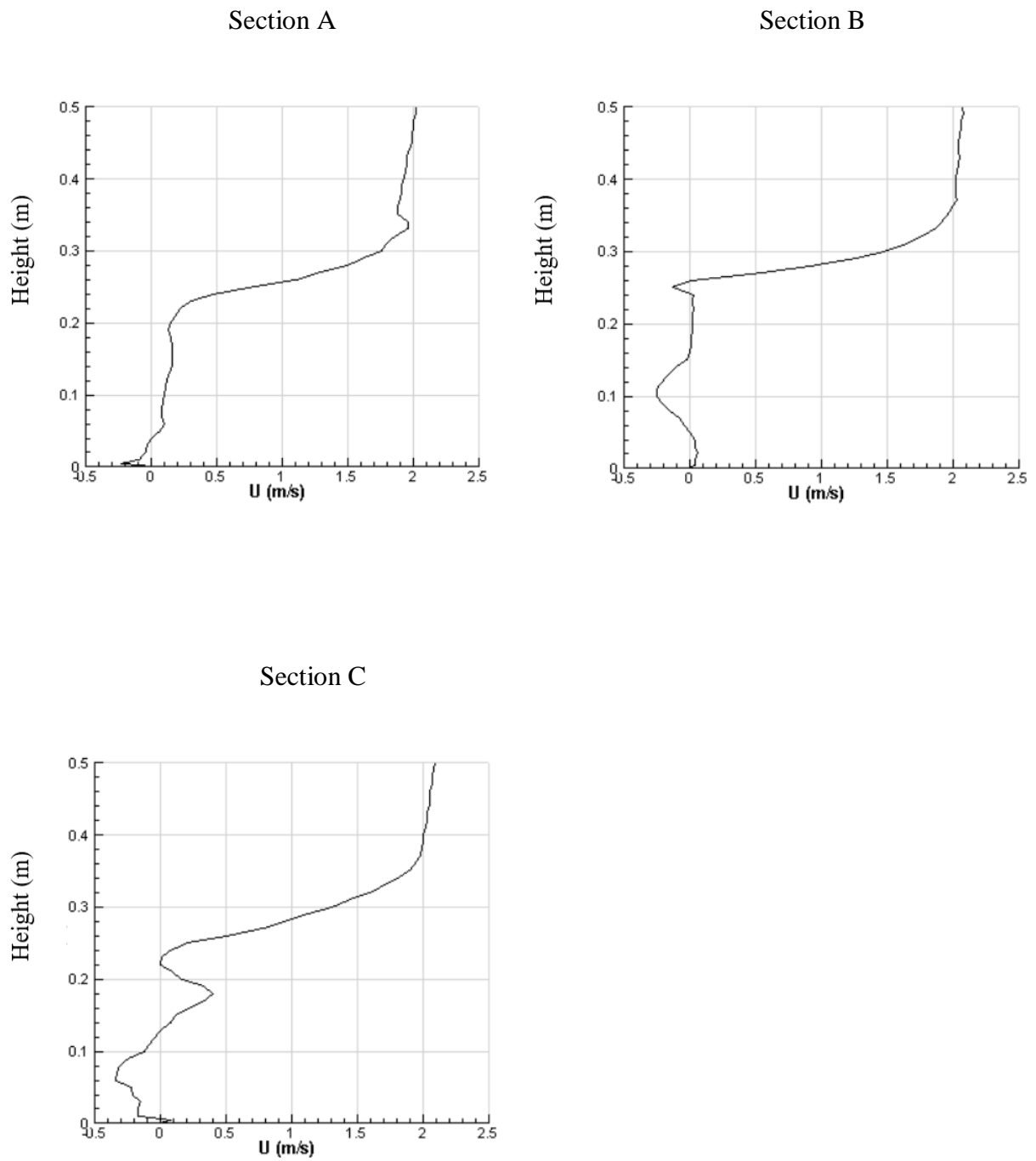


Figure 3.33: Velocity distribution at $t = 1$ s for single-sided ventilation with double openings on the leeward wall (Case 4)

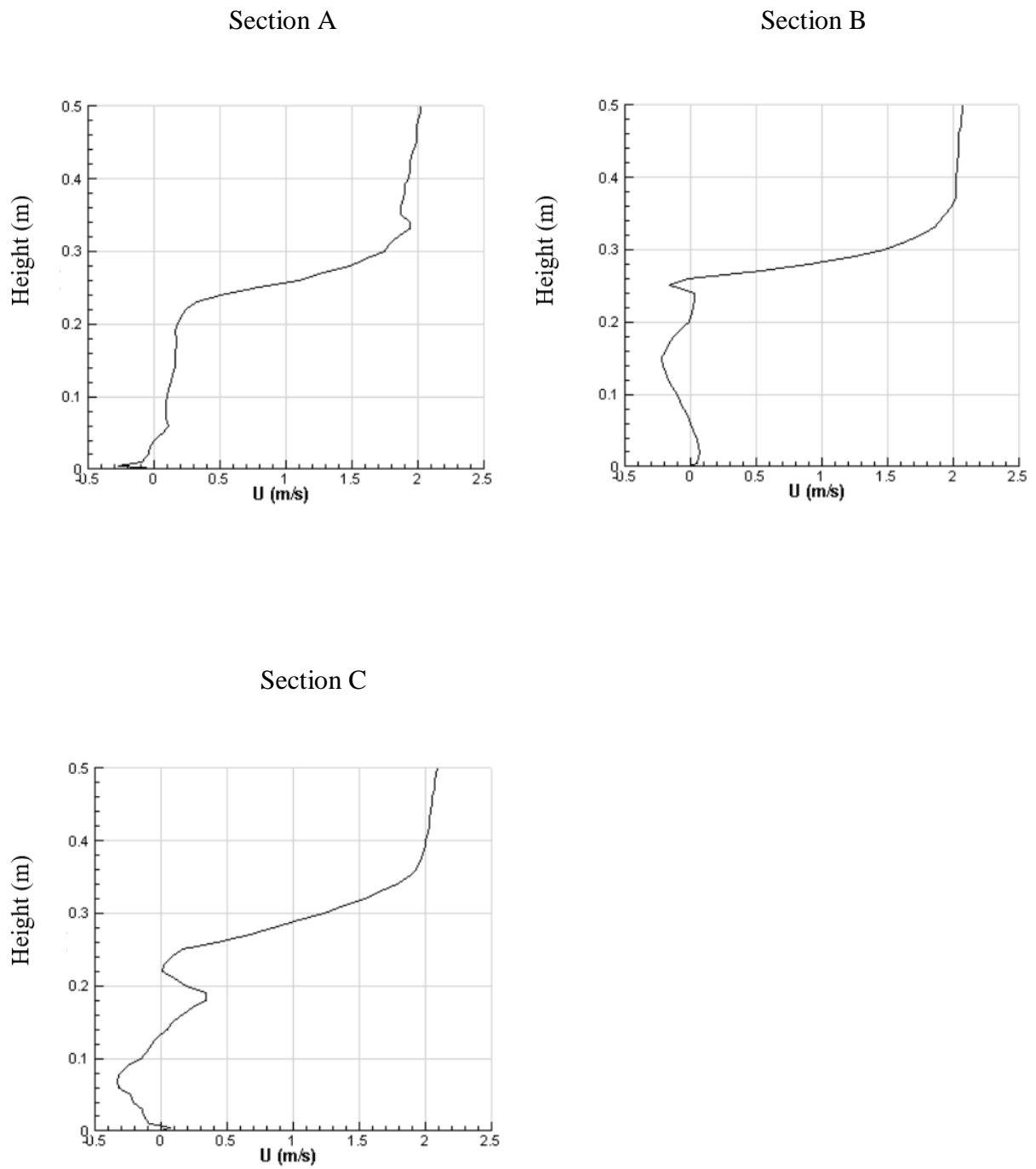


Figure 3.34: Velocity distribution at $t = 1.5$ s for single-sided ventilation with double openings on the leeward wall (Case 4)

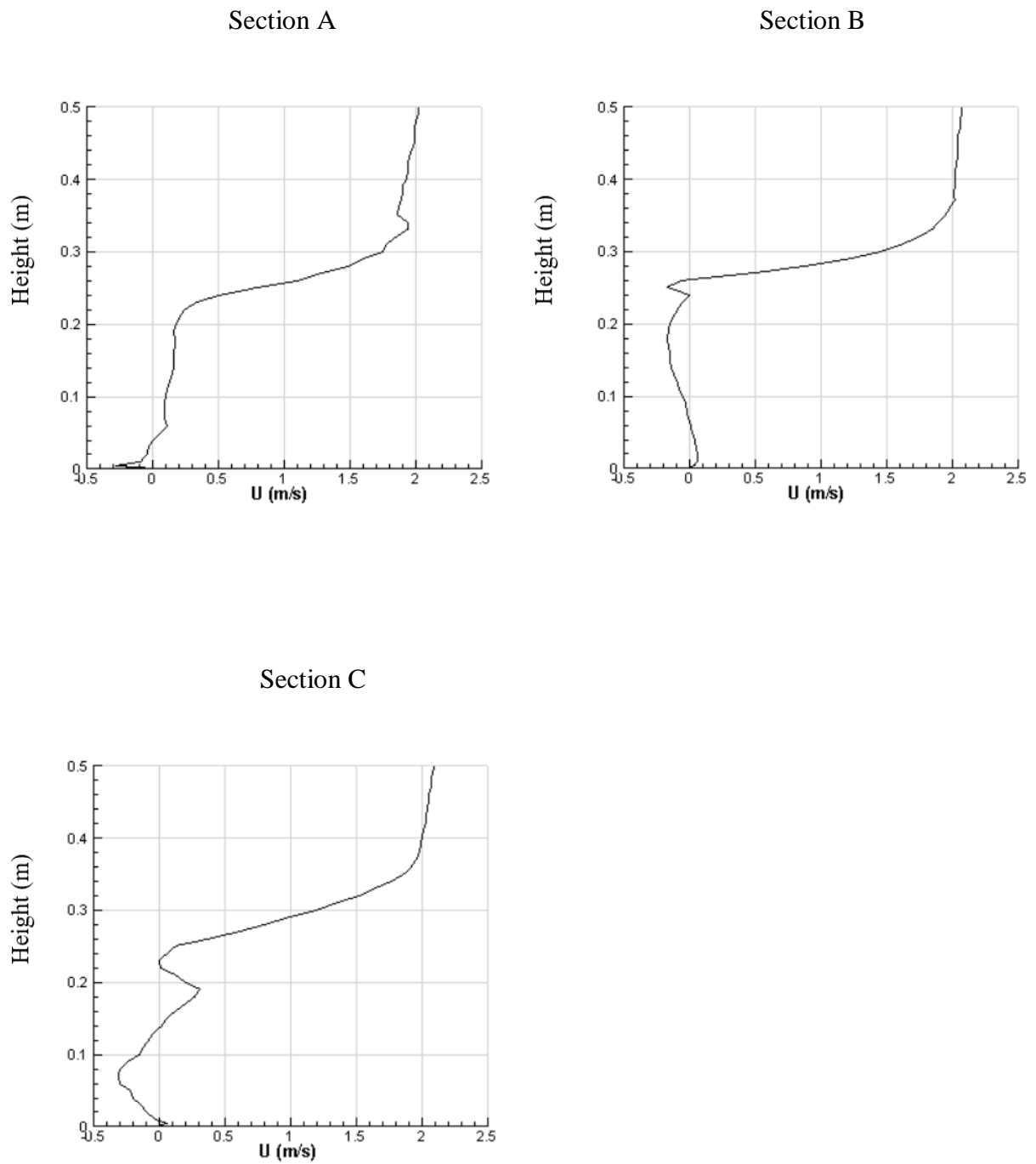


Figure 3.35: Velocity distribution at $t = 2$ s for single-sided ventilation with double openings on the leeward wall (Case 4)

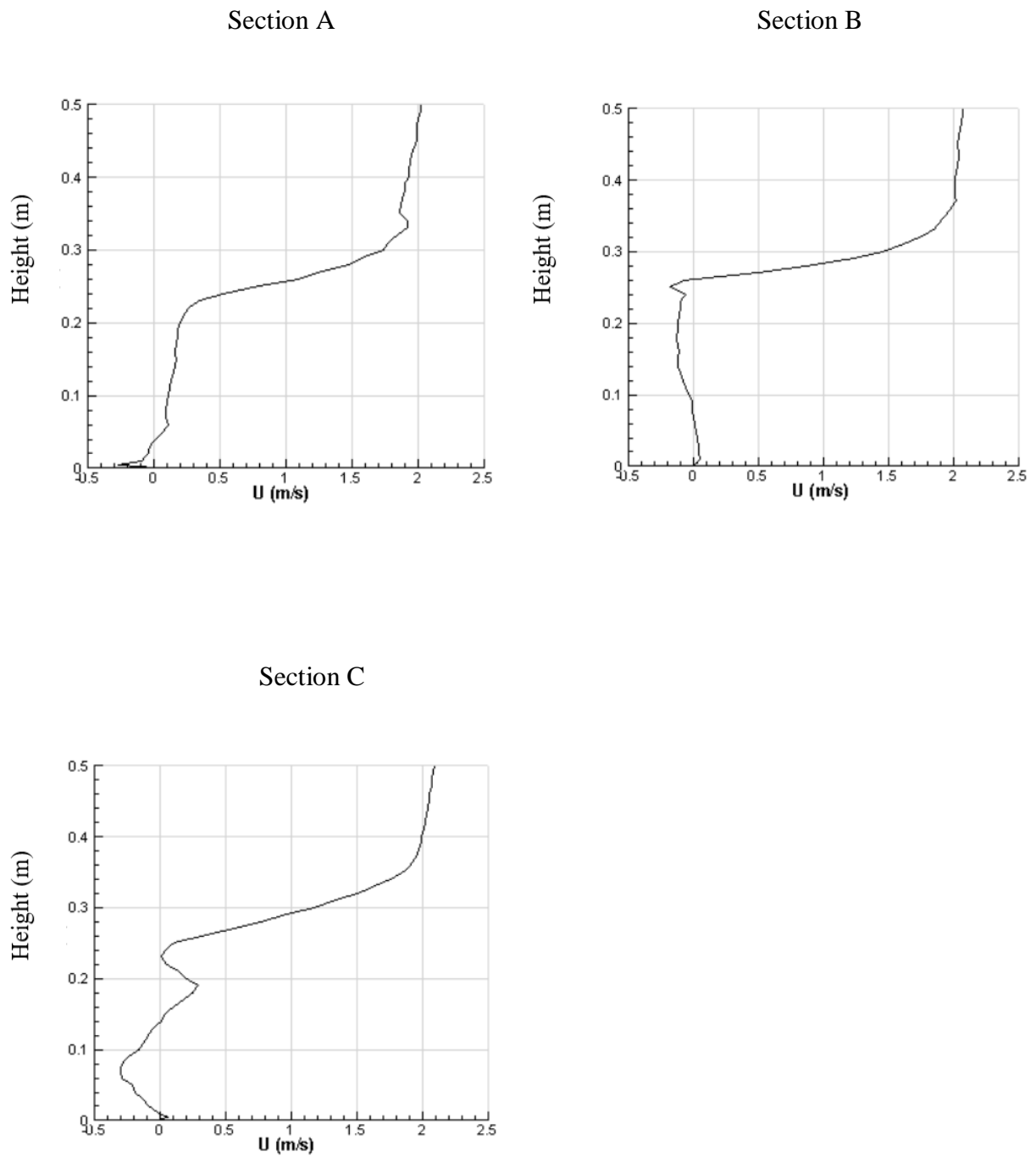


Figure 3.36: Velocity distribution at $t = 2.5$ s for single-sided ventilation with double openings on the leeward wall (Case 4)

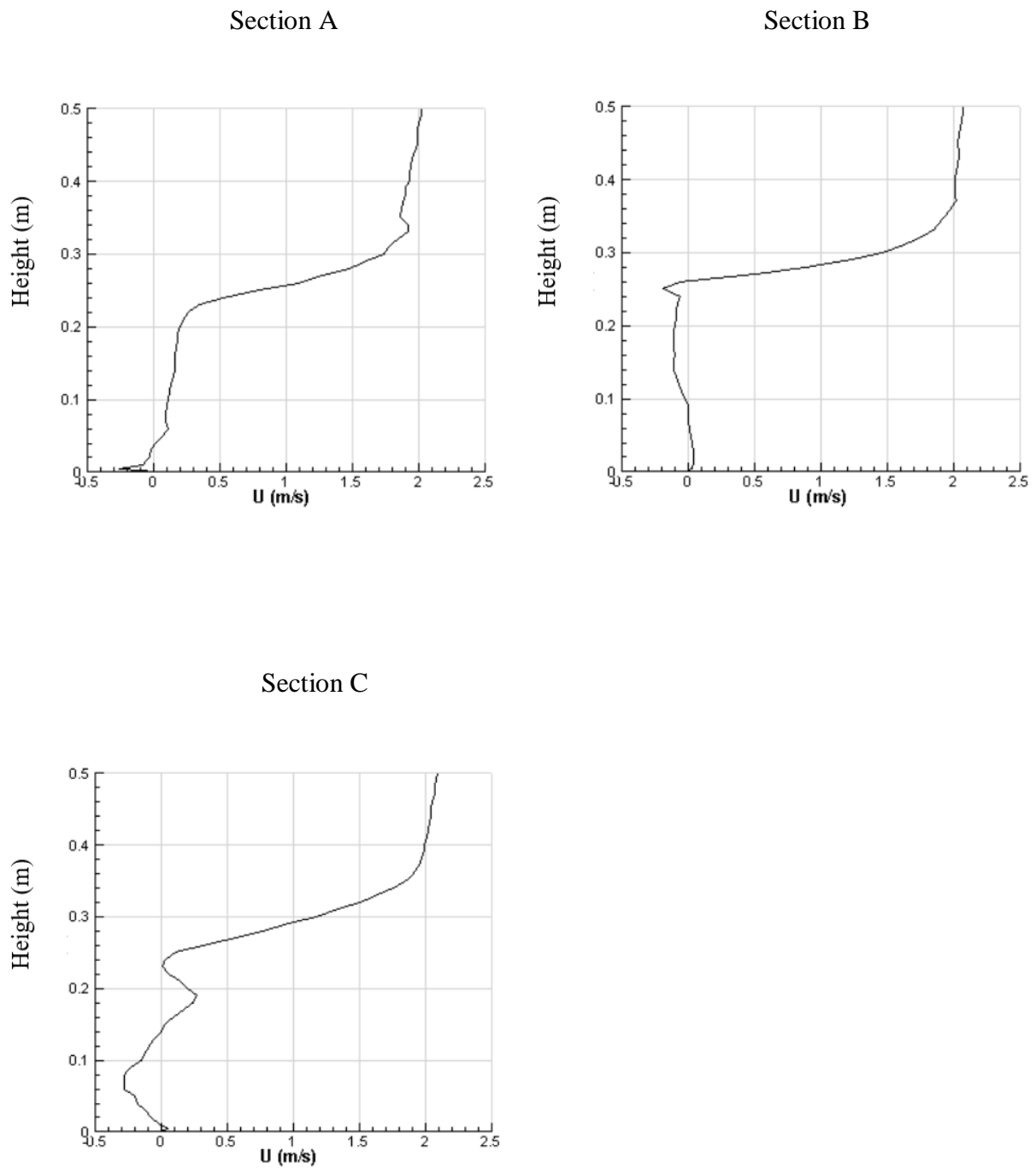


Figure 3.37: Velocity distribution at $t = 3$ s for single-sided ventilation with double openings on the leeward wall (Case 4)

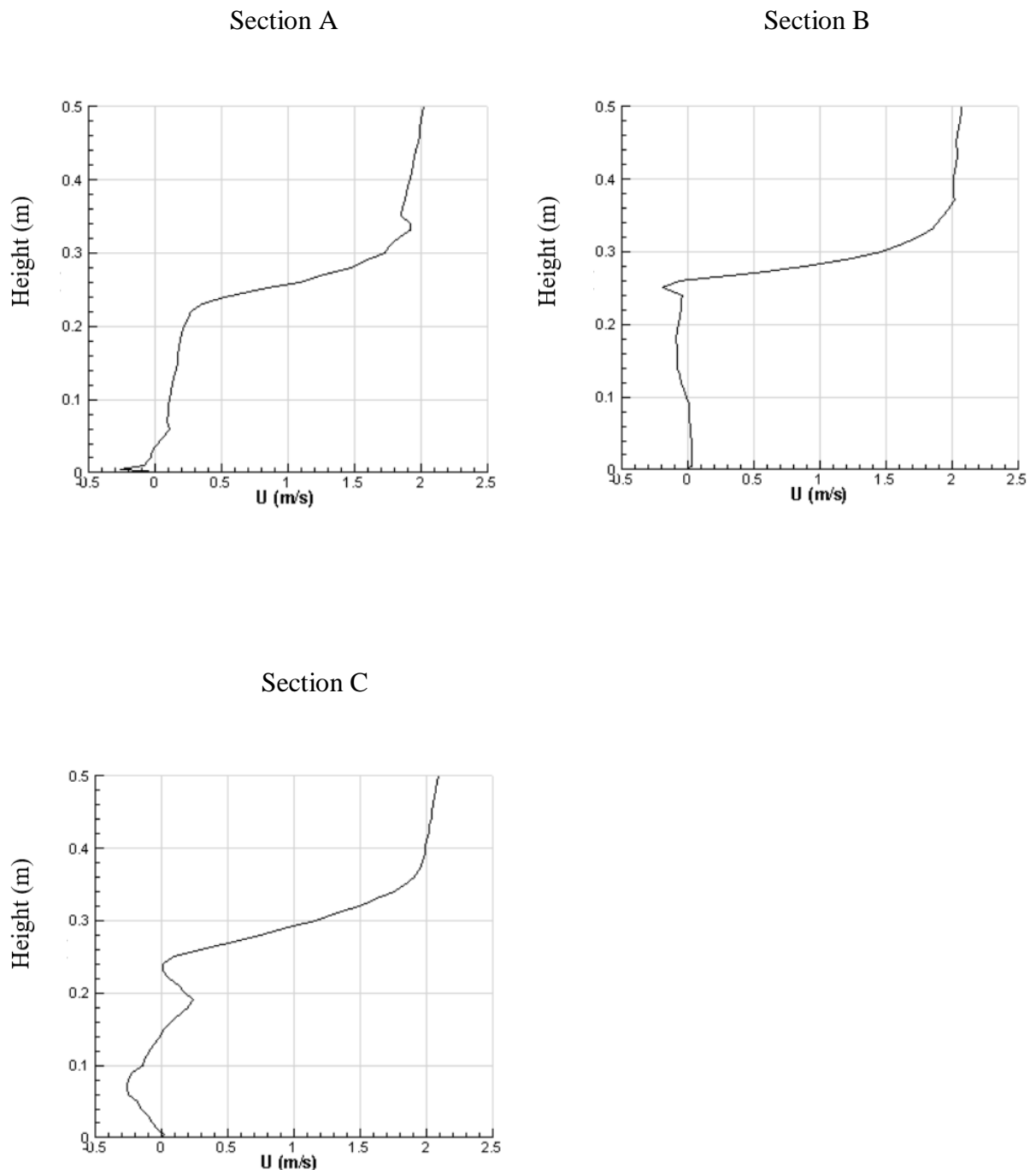


Figure 3.38: Velocity distribution at $t = 5$ s for single-sided ventilation with double openings on the leeward wall (Case 4)

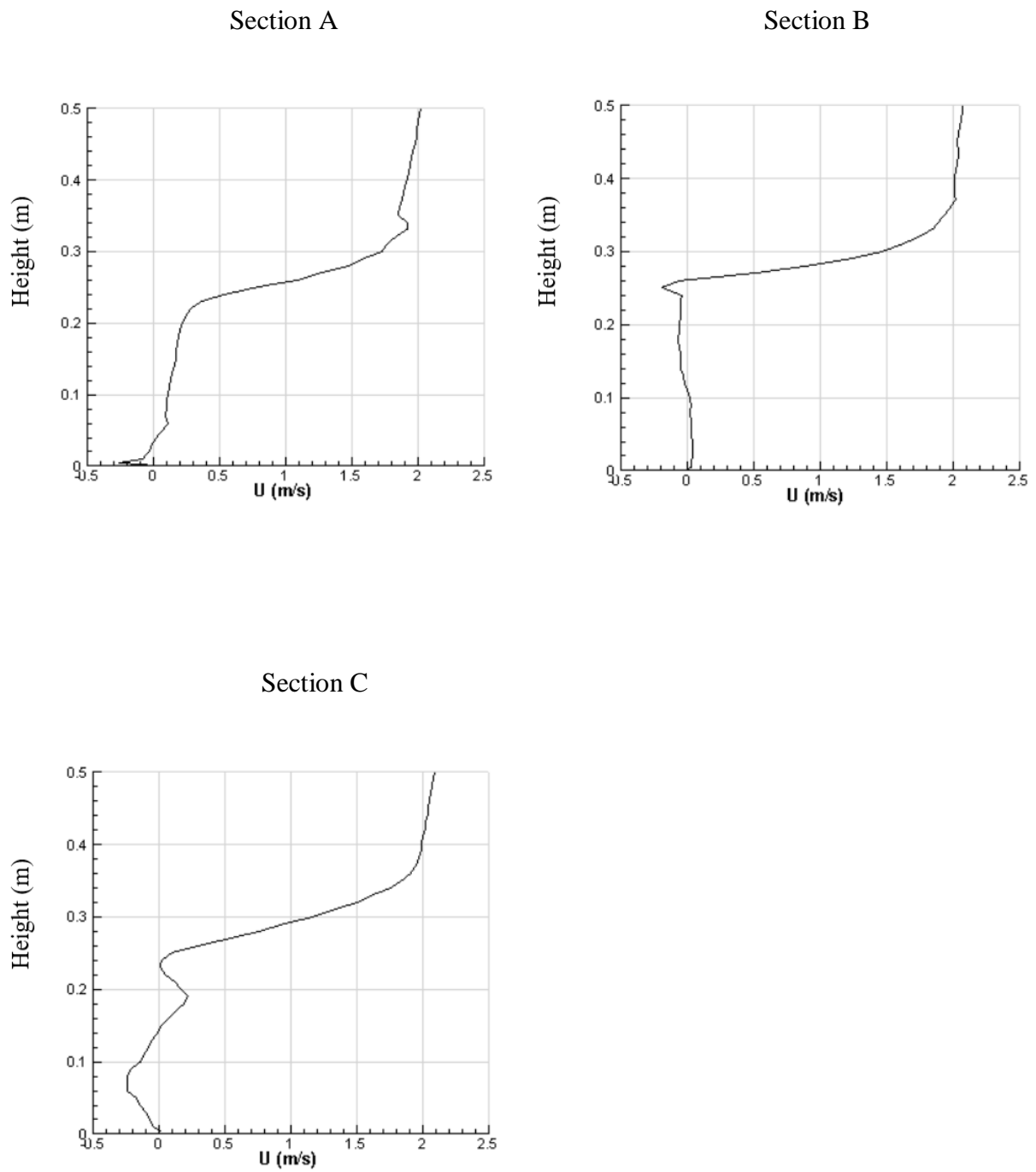


Figure 3.39: Velocity distribution at $t = 10$ s for single-sided ventilation with double openings on the leeward wall (Case 4)

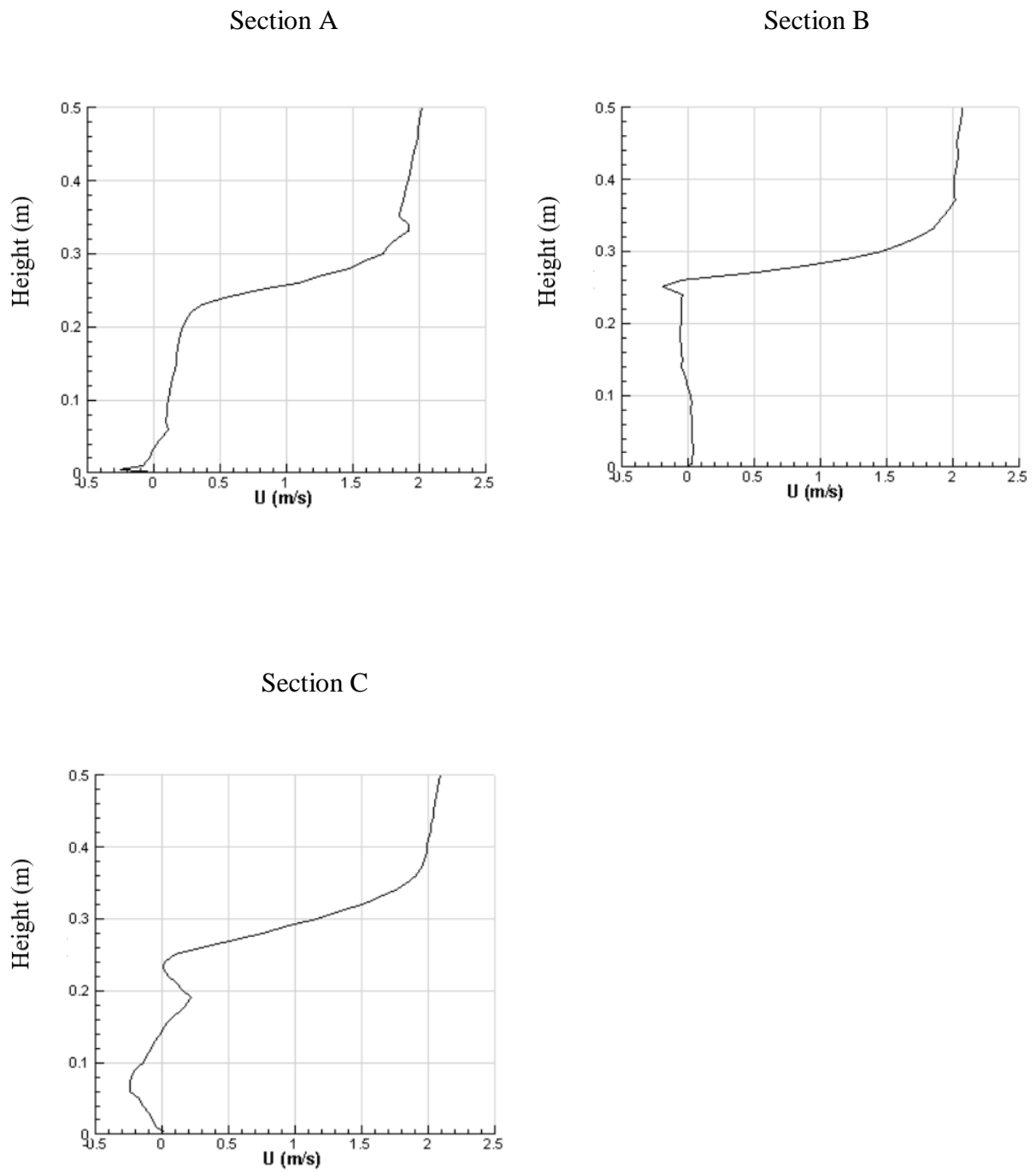


Figure 3.40: Velocity distribution at $t = 15$ s for single-sided ventilation with double openings on the leeward wall (Case 4)

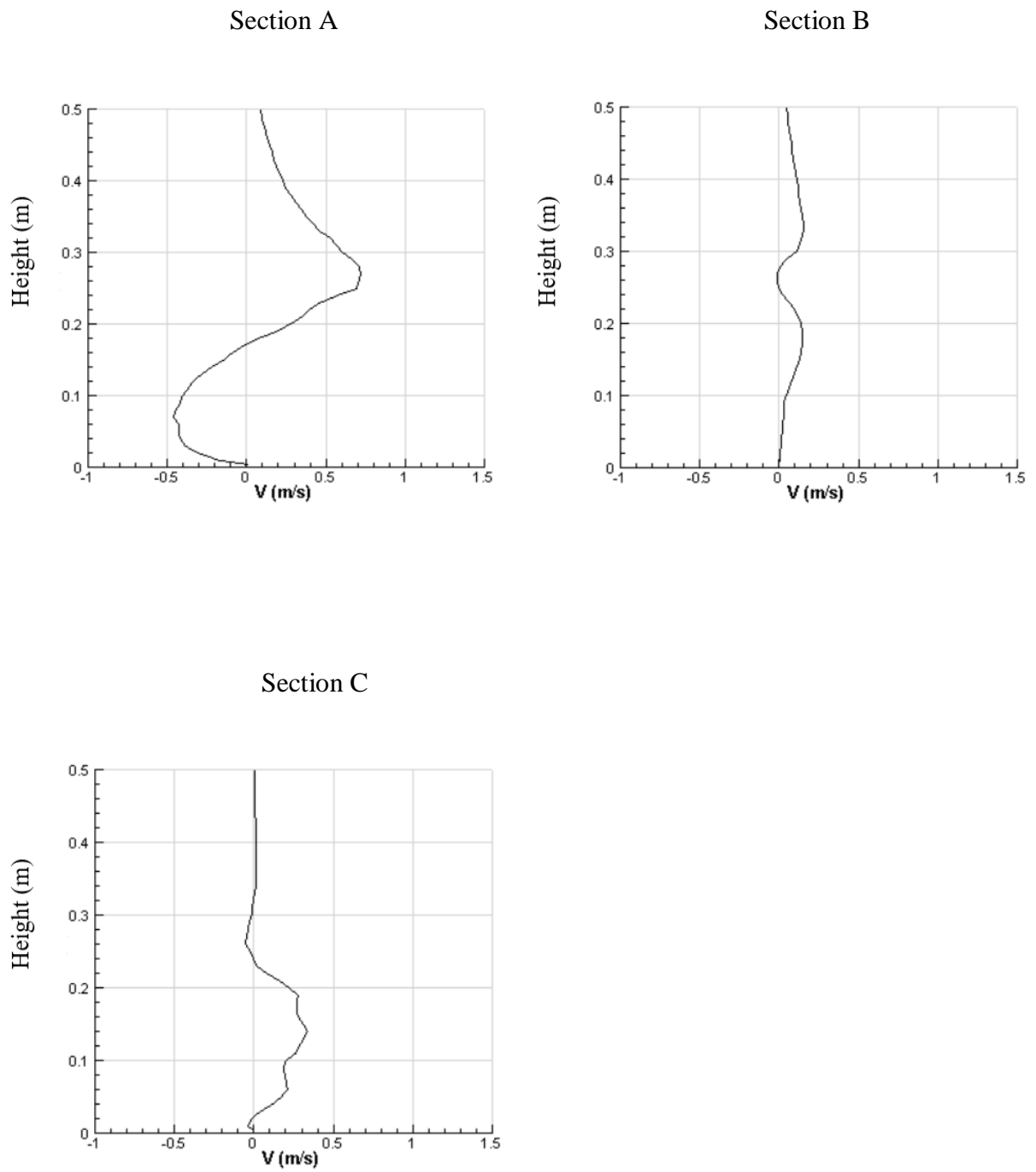


Figure 3.41: Velocity distribution along vertical direction at $t = 3$ s for single-sided ventilation with double openings on the leeward wall (Case 4)

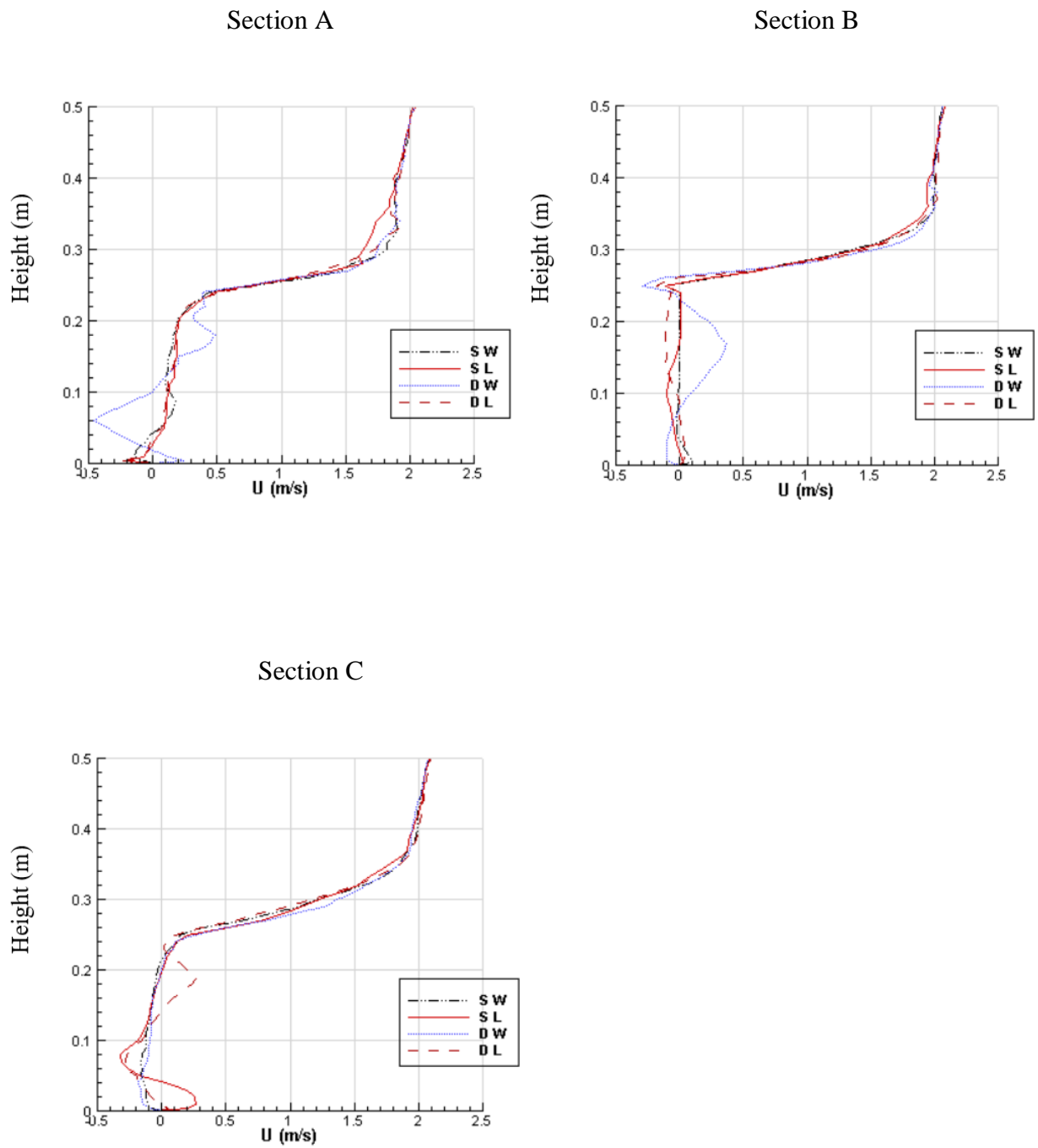


Figure 3.42: Velocity distribution for all cases (case 1: S W, Case 2: S L, Case 3: D W, case 4: D L) at $t = 3$ s

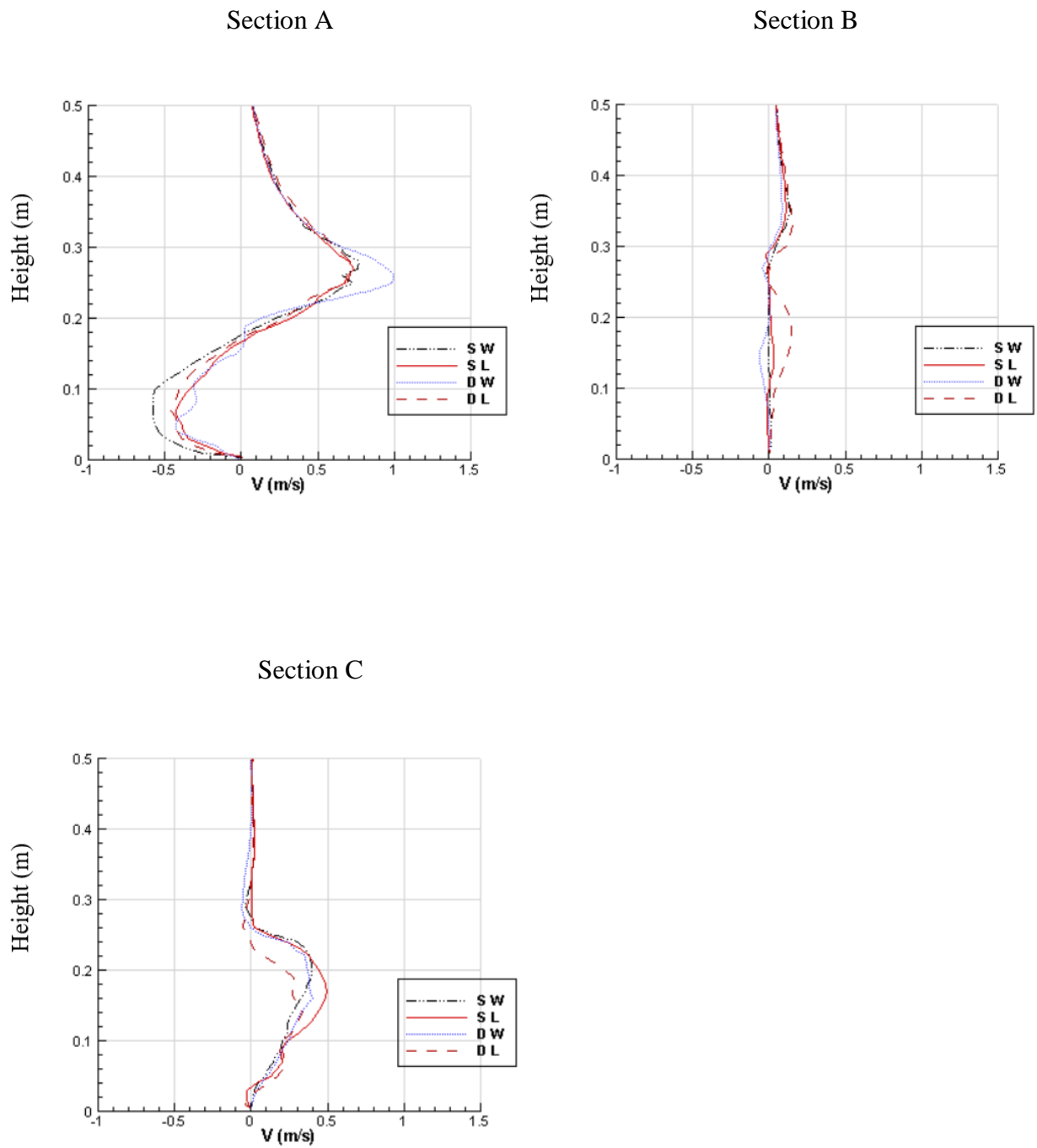


Figure 3.43: Velocity distribution along vertical direction for all cases (case 1: S W, Case 2: S L, Case 3: D W, Case 4: D L) at $t = 3$ s

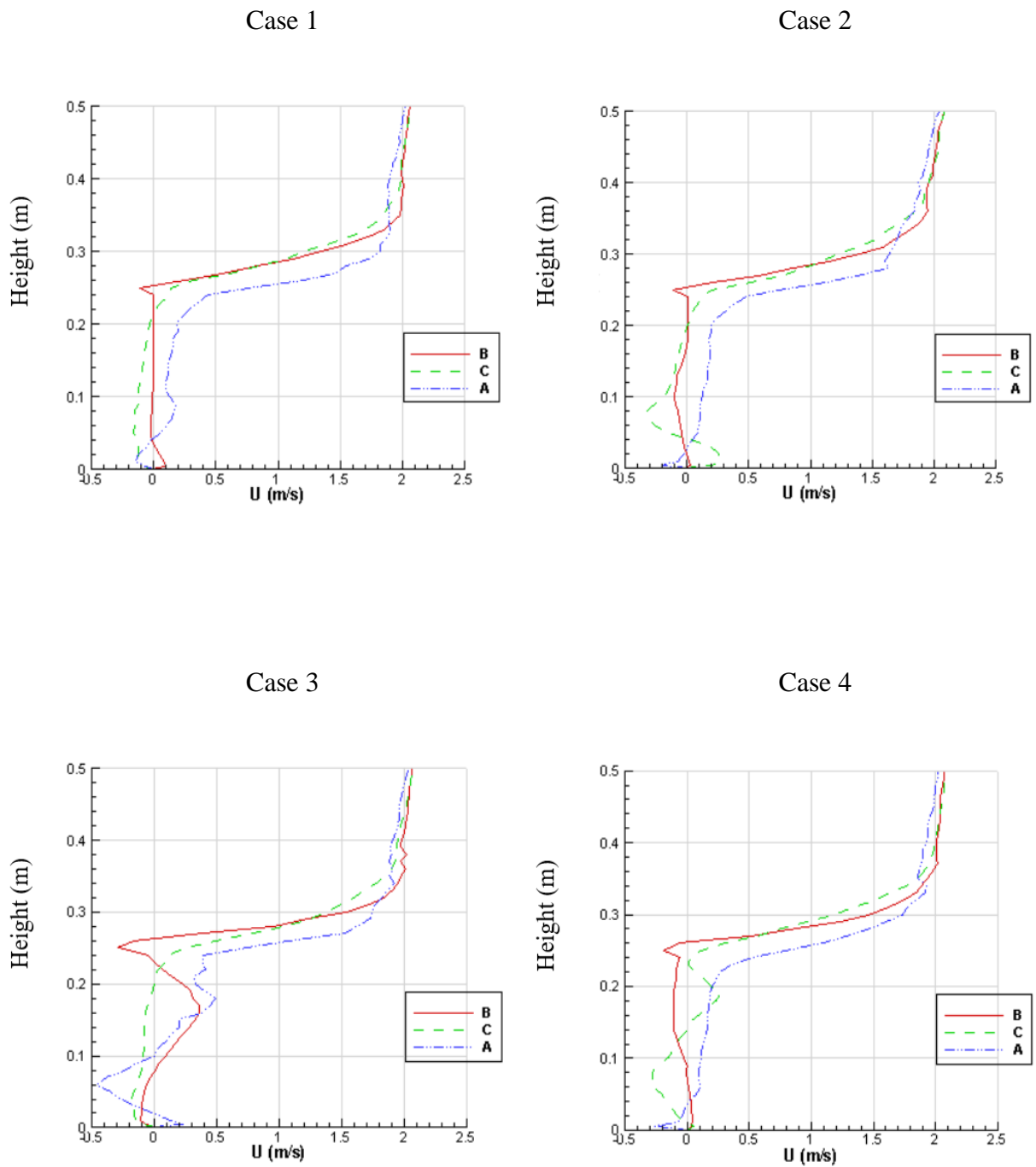
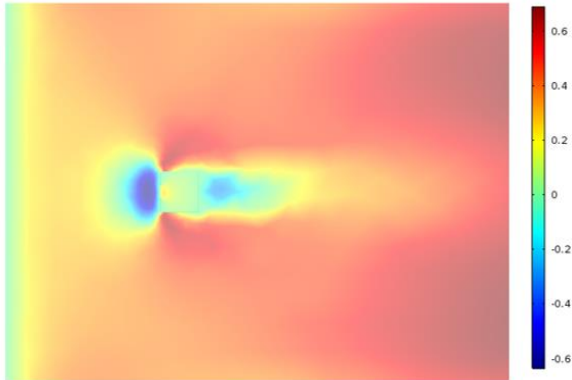
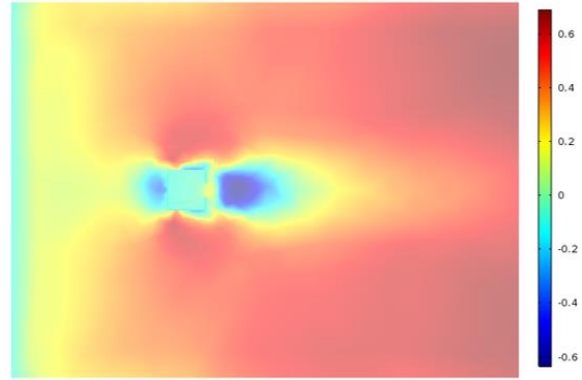


Figure 3.44: Velocity distribution for all cases in computational domain (Dash dot dot line: Section A, Solid line: Section B, Dashed line: Section C) at $t = 3 s$

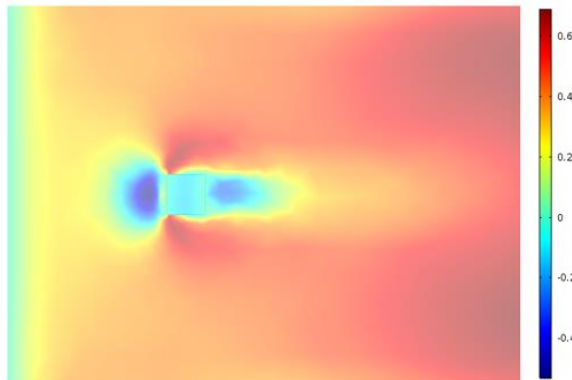
Case 1



Case 2



Case 3



Case 4

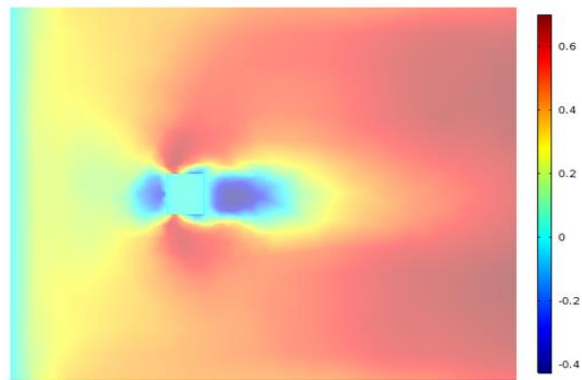


Figure 3.45: Velocity distribution for all cases in xy -plane at $t = 15$ s

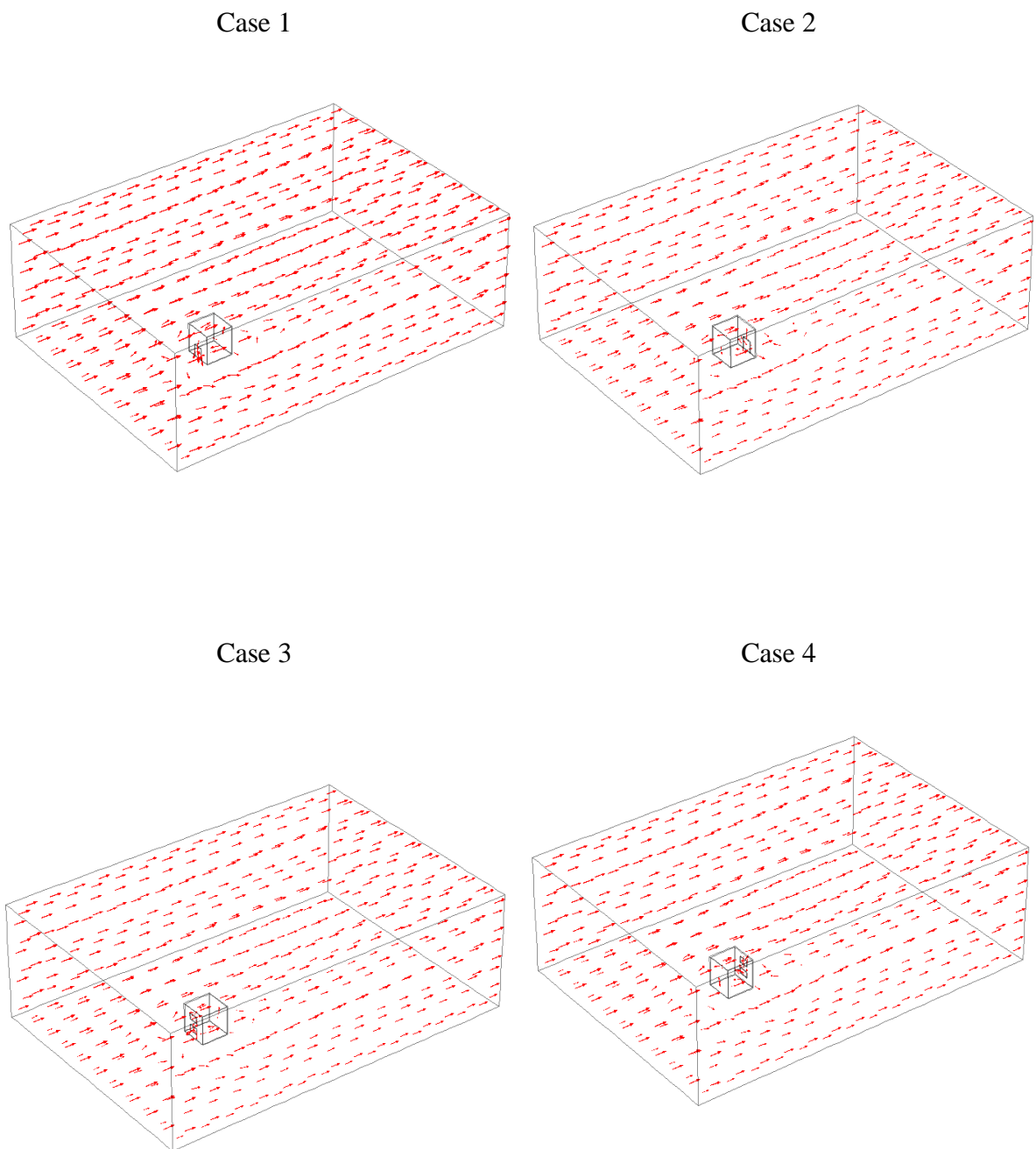
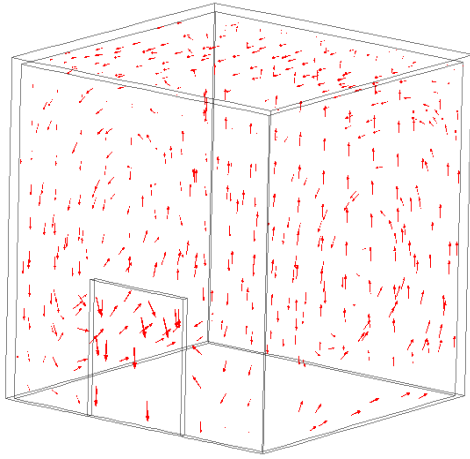
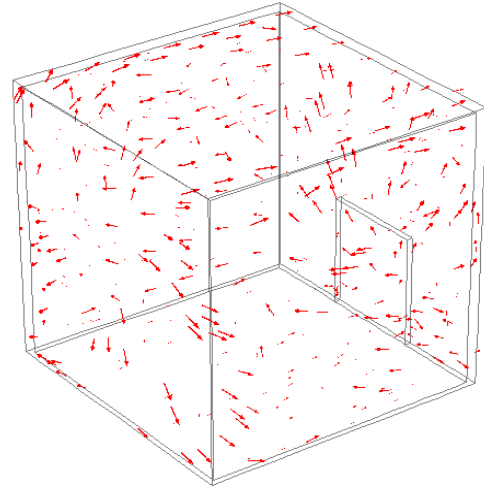


Figure 3.46: Air flow distribution in computational domain for all cases at $t = 15$ s

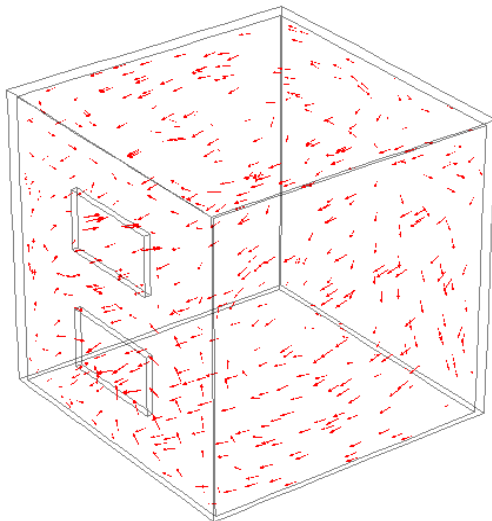
Case 1



Case 2



Case 3



Case 4

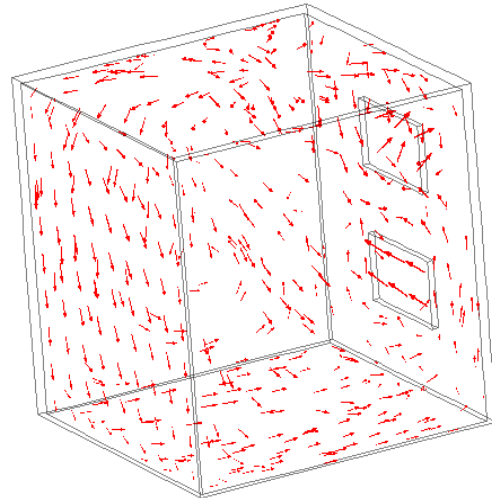


Figure 3.47: Air flow distribution in cubic building for all cases at $t = 15$ s

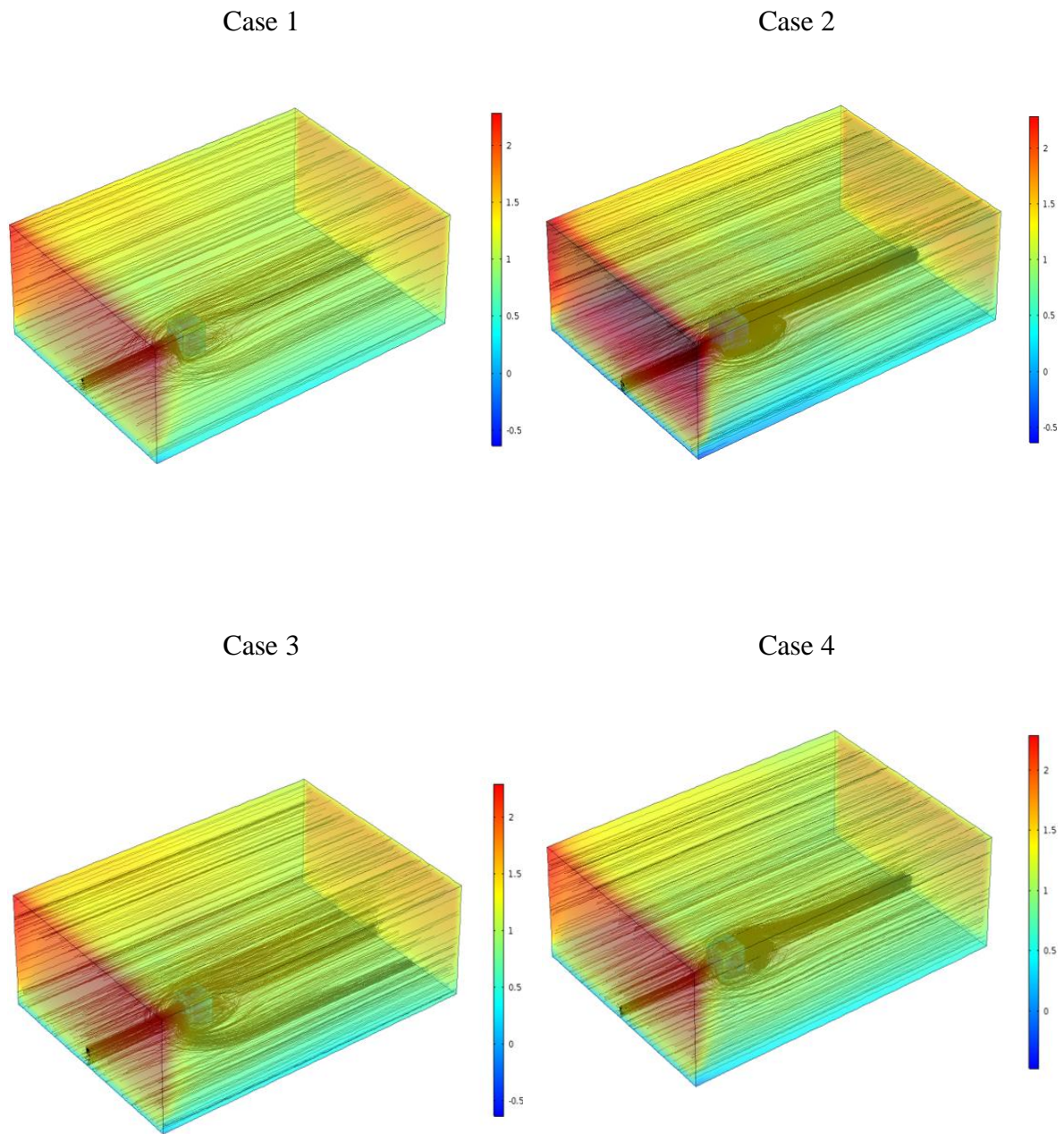


Figure 3.48: Velocity stream lines in computational domain for all cases at $t = 15$ s

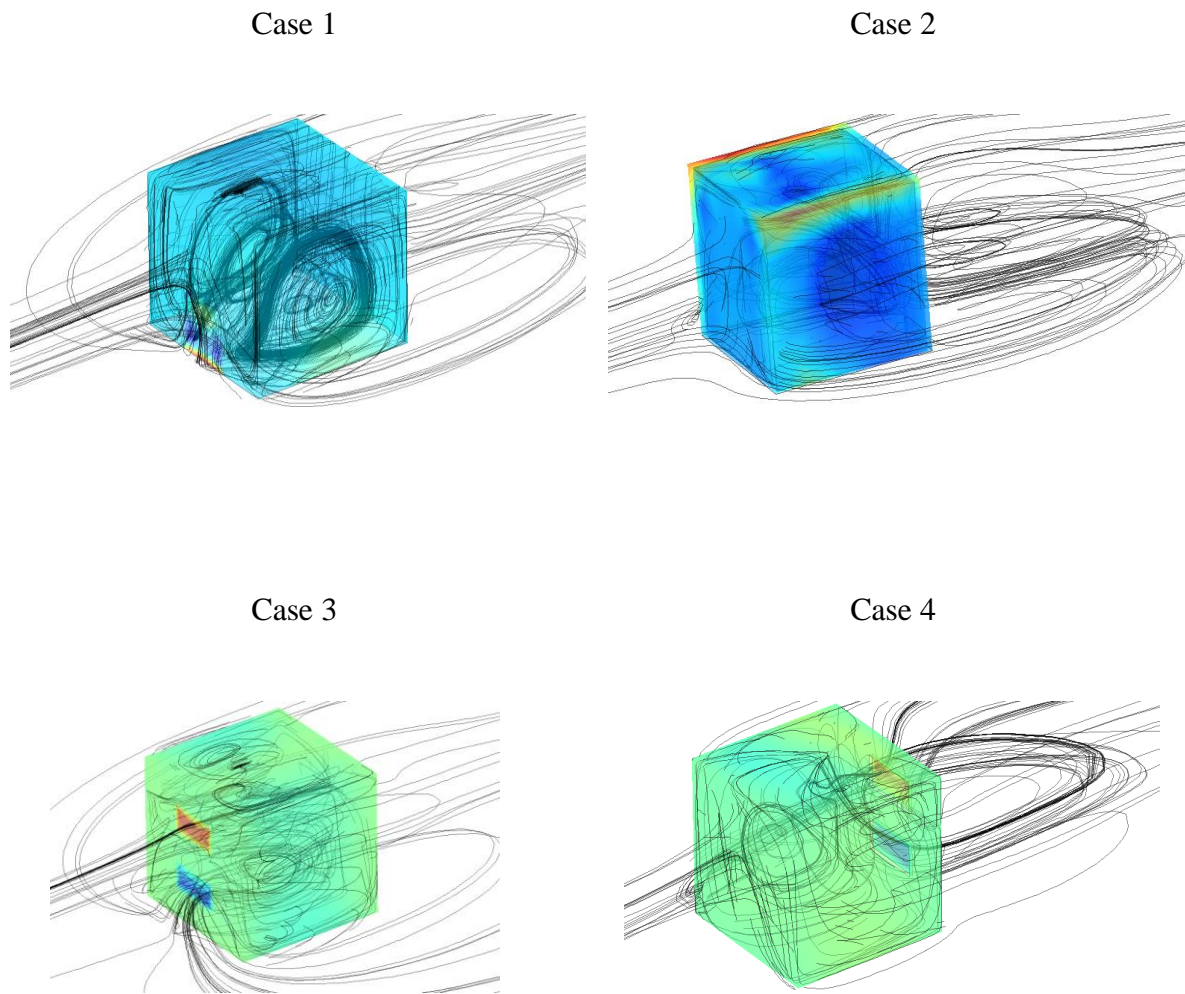


Figure 3.49: Velocity stream lines in cubic building for all cases at $t = 15$ s

3.2.2 Pressure

To model different windy conditions, pressure difference ΔP between the outer wall and the wall to the corridor are constant 0 and 1. Figure 3.50 shows the values of the pressure in xy - plane of the computational domain and all figures are approximately the same here.

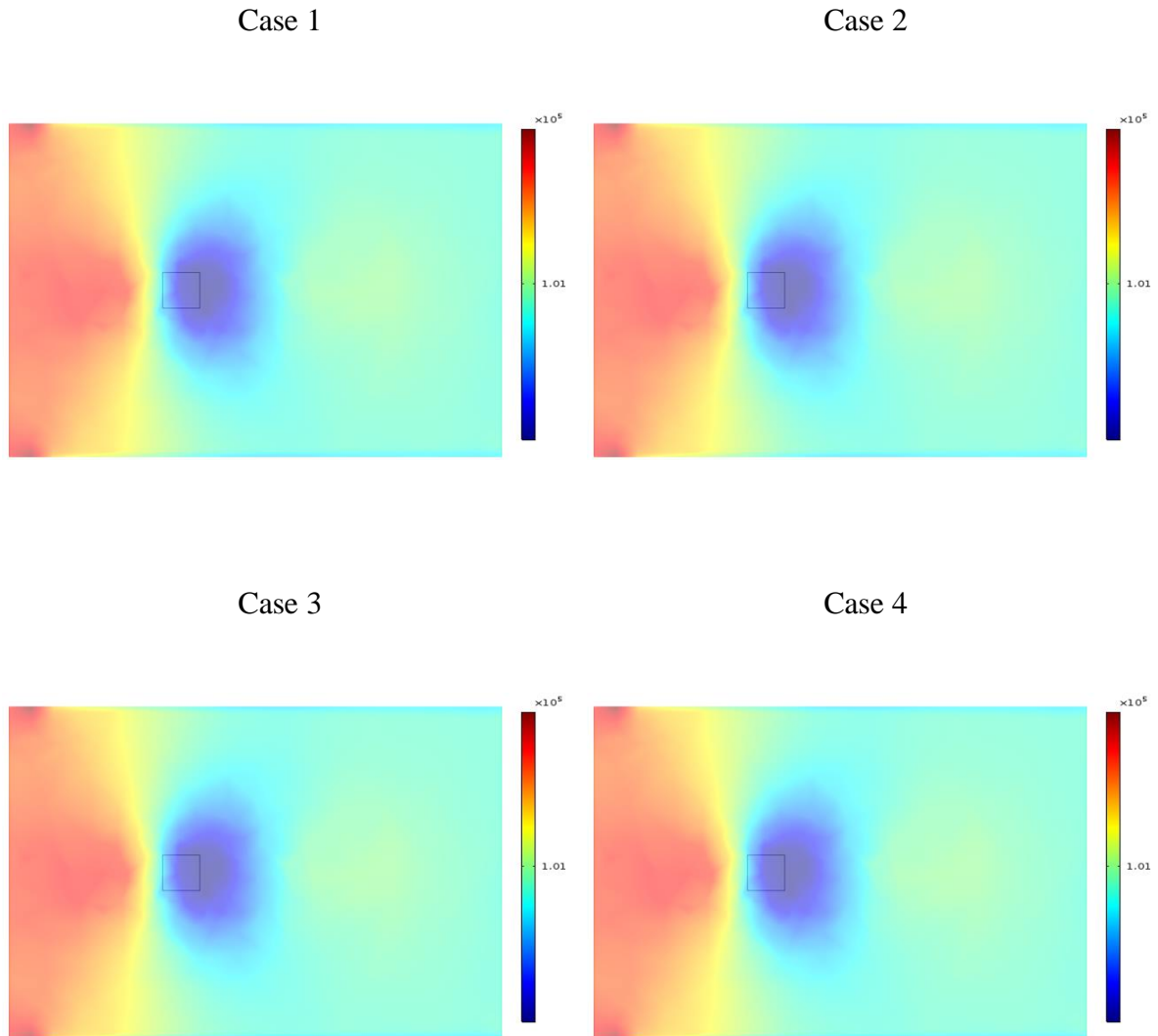


Figure 3.50: Pressure distribution for all cases in xy plane at $t = 15$ s

3.2.3 Ventilation Rate

The calculation of the air flow rate provided by natural ventilation is usually accomplished by means of a simple relationship. For single-sided wind driven natural ventilation, the ventilation rate can be calculated as:

$$Q_{ss} = 0.025 \cdot A \cdot U_h$$

where A (m^2) is the opening area and U_h (m/s) is the reference wind velocity, measured at the building height. Table 3.1- 3.4 show numerical values of ventilation rate for all cases. Each table gives various flow rates for all four cases, and it is clear that the highest flow rate has occurred in the windward double openings (case 3).

Table 3.1: Ventilation rate for windward single opening (case 1)

	Time (s)	Ventilation Rate (m^3/s)
Windward Single Opening (case 1)	0.5	0.001169323400930352
	1	0.00215737146319126
	1.5	0.0017386873443760718
	2	0.0016763775215648529
	2.5	0.0016612309026117573
	3	0.0016788052143203607
	3.5	0.0016835601626219857
	4	0.0016865050375278116
	4.5	0.0016910077322976186
	5	0.0016927282368809785
	10	0.00168646025217215
	15	0.001685447401799411

Table 3.2: Ventilation rate for leeward single opening (case 2)

	Time (s)	Ventilation Rate (m^3/s)
Leeward Single Opening (case 2)	0.5	0.001572861881721248
	1	0.0023904343933533077
	1.5	0.0014460274201696644
	2	0.0013839273537283676
	2.5	0.0017448775435086694
	3	0.0016642435646309467
	3.5	0.0015551481244800232
	4	0.0014823815888515247
	4.5	0.0014109570697389984
	5	0.0013370066091951292
	10	9.52853378292106E-4
	15	9.232986347756224E-4

Table 3.3: Ventilation rate for windward double openings (case 3)

	Time (s)	Ventilation Rate (m^3/s)
Windward Double Openings (case 3)	0.5	5.942208533804205E-4
	1	0.0025876663757664516
	1.5	0.002670913114062119
	2	0.0027732010456357195
	2.5	0.002795352072869878
	3	0.0027768186570730105
	3.5	0.0027849933077490905
	4	0.002782478492625072
	4.5	0.0027806589090020747
	5	0.002776899591343757
	10	0.0027688471378035473
	15	0.0027703088596360355

Table 3.4: Ventilation rate for leeward double openings (case 4)

	Time (s)	Ventilation Rate (m^3/s)
Leeward Double Openings (case 4)	0.5	0.0031249174599475987
	1	0.0024985061097254468
	1.5	0.002231001736400236
	2	0.0019788576587311873
	2.5	0.0018180161537821806
	3	0.0017271969218653148
	3.5	0.0016536441015765062
	4	0.0016106951570946744
	4.5	0.0015767428885600865
	5	0.0015580092572904218
	10	0.0014763407989667372
	15	0.0014544266540096995

Natural Ventilation with the Influence of Solar Radiation

The Earth's climate depends on the delicate balance among incoming solar radiation, outgoing thermal radiation and the composition of Earth's atmosphere. Even small changes in these parameters can affect the entire climate. Around 30 percent of the solar energy that strikes Earth reflected into space. So, the evaluation of the effectiveness of a particular single-sided ventilation design, various parameters must be considered, which are significant to evaluate thermal comfort. Among these factors, air temperature and velocity are considered here. The information about the flow pattern, airflow rate, temperature profile, and radiosity are provided in this chapter.

4.1 Introduction

The Sun, or Sol, is the star at the center of the solar system, which is the most important source of energy for life on the Earth. The solar energy incident on a surface oriented normal to the sun's rays, at the outer edge of the earth's atmosphere when the earth is at its mean distance from the sun is called the solar constant. The value of this solar constant is 1000 w/m^2 on a clear day at solar noon in the summer months. The main goal of building design for the tropical climate is the reduction of direct heat gain by radiation and to reduce internal surface temperature. The building should be designed with protected openings and walls to reduce the energy for high-rise apartments through an improved building envelope design [51]. They had identified six passive thermal design strategies, namely, insulation, thermal mass, the color of external walls, glazing systems, window size, and shading devices. About 30% reduction in solar absorptance can achieve 12% saving in annual is required for cooling energy. They concluded that 12% saving on cooling energy could be obtained from using white or light color external wall finishes. However, most residential buildings in Dhaka are already light-colored, with only a very few exceptions. The choice of building color depends mostly on architects and in a few cases, on clients. In order to evaluate the effectiveness in particular single-sided ventilation design, various parameters must be considered. These performance parameters are determined by the thermal and flow boundary conditions, such as the size and geometry of a space, heat sources, and outdoor weather conditions. These parameters are significant to the evaluation of natural ventilation since thermal comfort is the major criterion that must be satisfied for effective natural ventilation design. Natural ventilation systems do not only

provide fresh air but also affect the indoor thermal environment a lot. To ensure the quality of the indoor environment, the temperature is the vital component for thermal comfort since the research focuses on the thermal comfort of the citizen of Dhaka city.

4.2 Results and Discussion

Heat balance in a living-room is very important from the energy consumption angle, and available solar radiation has an essential influence on it. On sunny days, owing to the considerable solar heat transfer through the opening/s required temperature in the room can be maintained with less heat from the air exchange system. The rotation of the Earth is also responsible for hourly variations in sunlight. In the early morning and late afternoon, the sun is low in the sky. Its rays travel further through the atmosphere than at noon when the sun is at its highest point. The location of Bangladesh is in both the eastern and northern hemispheres. In this study, the ambient temperature and a clear sunny day at noon have been considered. The calculations have been performed for a computational domain with a cubic room filled with air. Solar radiation through the opening/s is modeled as a heat source on the inner window's surface. For gray bodies, that is, surfaces for which the absorptivity and emissivity are independent of wavelength, considerable simplifications can be made. The net heat transfer is the difference between the radiation leaving from the surface and the radiation incident upon this surface.

4.2.1 Velocity Distribution

Air velocity is a vital factor that determines the level of indoor thermal comfort. Since this research is time dependent so the velocity components U and V along streamwise and vertical direction respectively are calculated with time. The velocities are changed from time to time. After a few seconds, approximately 3 seconds, the changes are almost the same. Numerically, the air velocities are slightly different from Figure 3.2 – Figure 3.49.

4.2.2 Temperature Distribution

Temperature is the main component for thermal comfort. The information about temperature profile in cubic buildings as well as computational domain are provided in this section. Since the fluctuation of the air velocity is comparatively stable after 3 seconds, so the temperature distribution has been considered from 3 seconds. The graphs in Figures 4.1-4.3 display the temperature distribution profile for all (four) cases in section A, section B and section C respectively at time $t = 3$ second. An interesting observation is that air temperature is

fluctuating so much for windward opening/s (case 1 and case 3) in section A because hot air which exists outside the room is entered easily into the room but the room temperature is comparatively cool. This cold temperature influences the outside temperature when air comes out of the room. In similar manner, Figure 4.4-4.18 show the section wise temperature distribution profile for all cases at time $t = 5, 10, 15, 30, 60$ seconds, respectively. From these figures, it is clear that the air temperature fluctuation is decreasing in section A when time is increasing gradually. Figure 4.19 shows the temperature distribution in one frame to predict temperature for outside and inside of the room. For all cases, the outside temperature of the room is around 306 K where the room temperature is fluctuating from 293 K to 301 K. Figure 4.20 and Figure 4.21 show the three dimensional view of surface temperatures for all cases in the computational domain and a cubic room, respectively. In addition, Figure 4.22 and Figure 4.23 show the isothermal surfaces for all cases in the computational domain and a cubic room, respectively. In all cases, the low temperature exists in the floor. When time is increasing, the roof of the cubic building is heated gradually for a certain period which gives rise to the room temperature. However, the ASHRAE Standard [52] states that occupants may feel uncomfortable due to contact with floor surfaces that are too warm or too cool, giving an allowable range of floor temperatures between 292 K and 303 K. In this study, only solar radiation effect is regarded but no other heat source or mechanical system are accounted here. Since room temperature is a vital factor so average volume temperature is needed. Furthermore, Table 4.1 shows the details average volume temperature for all cases at different times. The air temperature inside the room maintains the ASHRAE standard in all cases in the context of the weather in Dhaka city. The average volume temperature for double windward openings and double leeward openings are much closed. At different times, the average volume temperature for double leeward opening is comparatively less than the double windward openings.

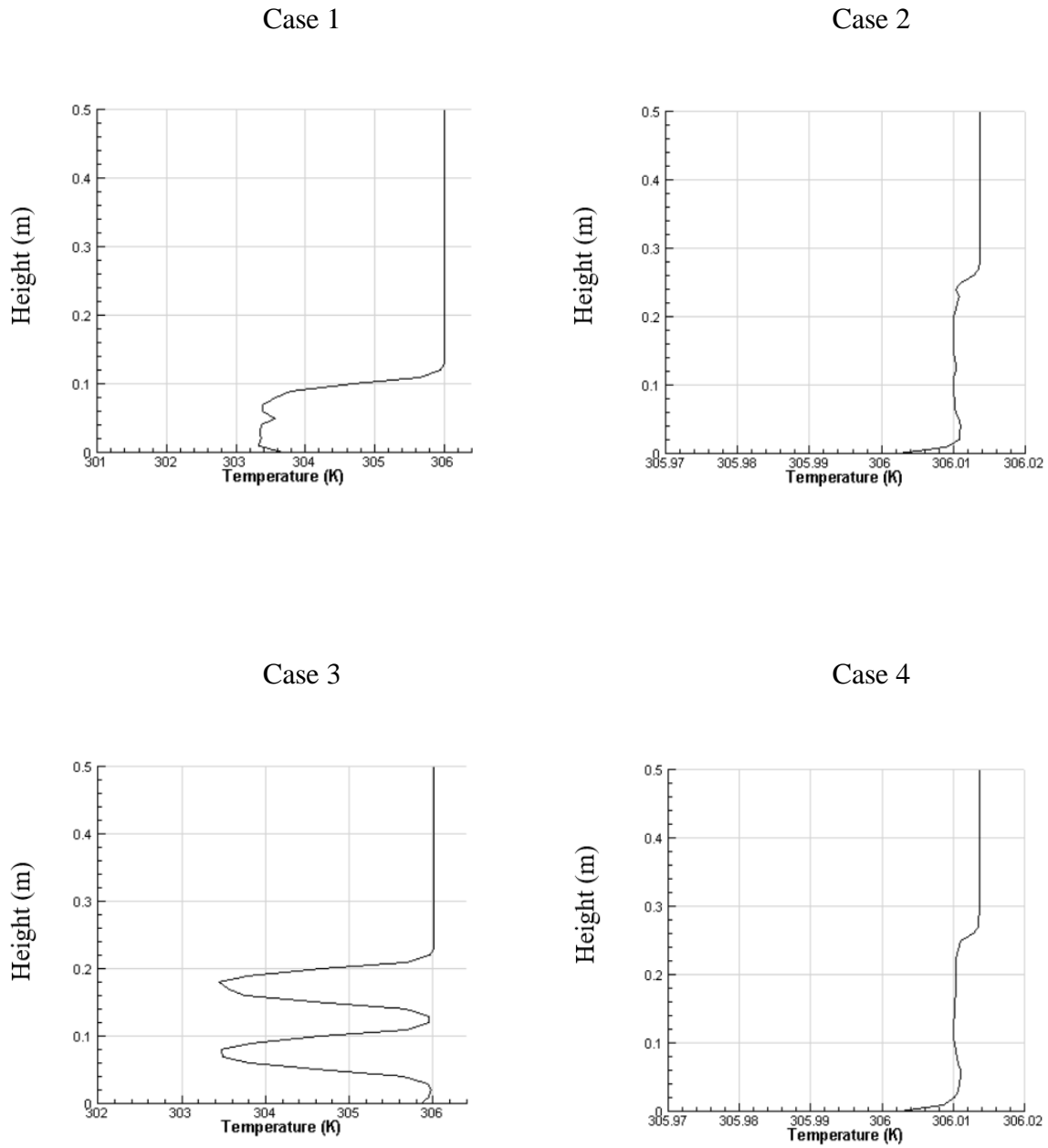
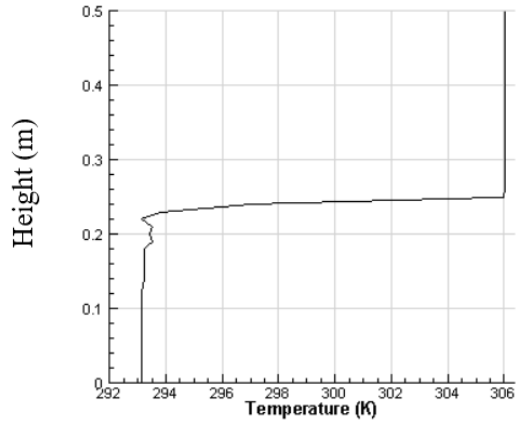
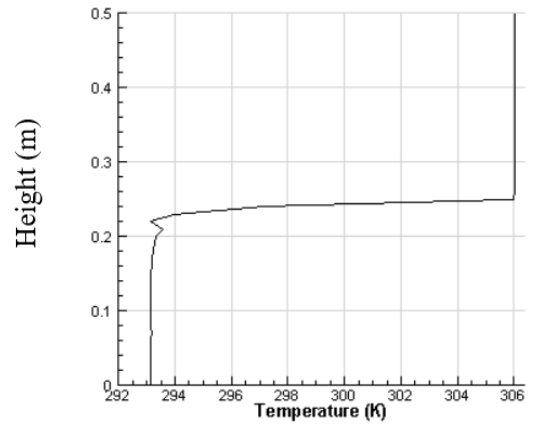


Figure 4.1: Temperature distribution in section A for four cases at $t = 3$ s

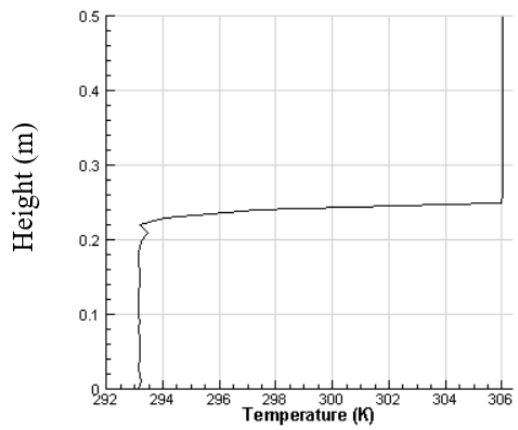
Case 1



Case 2



Case 3



Case 4

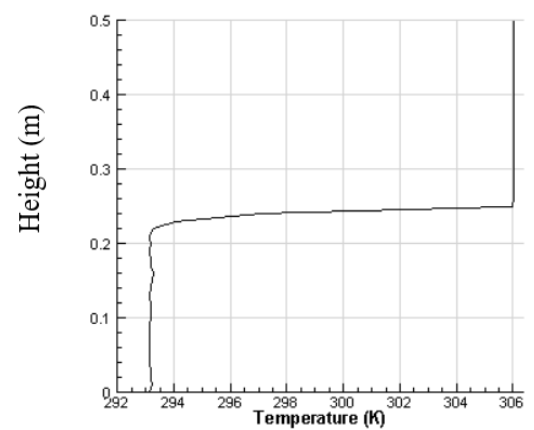


Figure 4.2: Temperature distribution in section B for four cases at $t = 3$ s

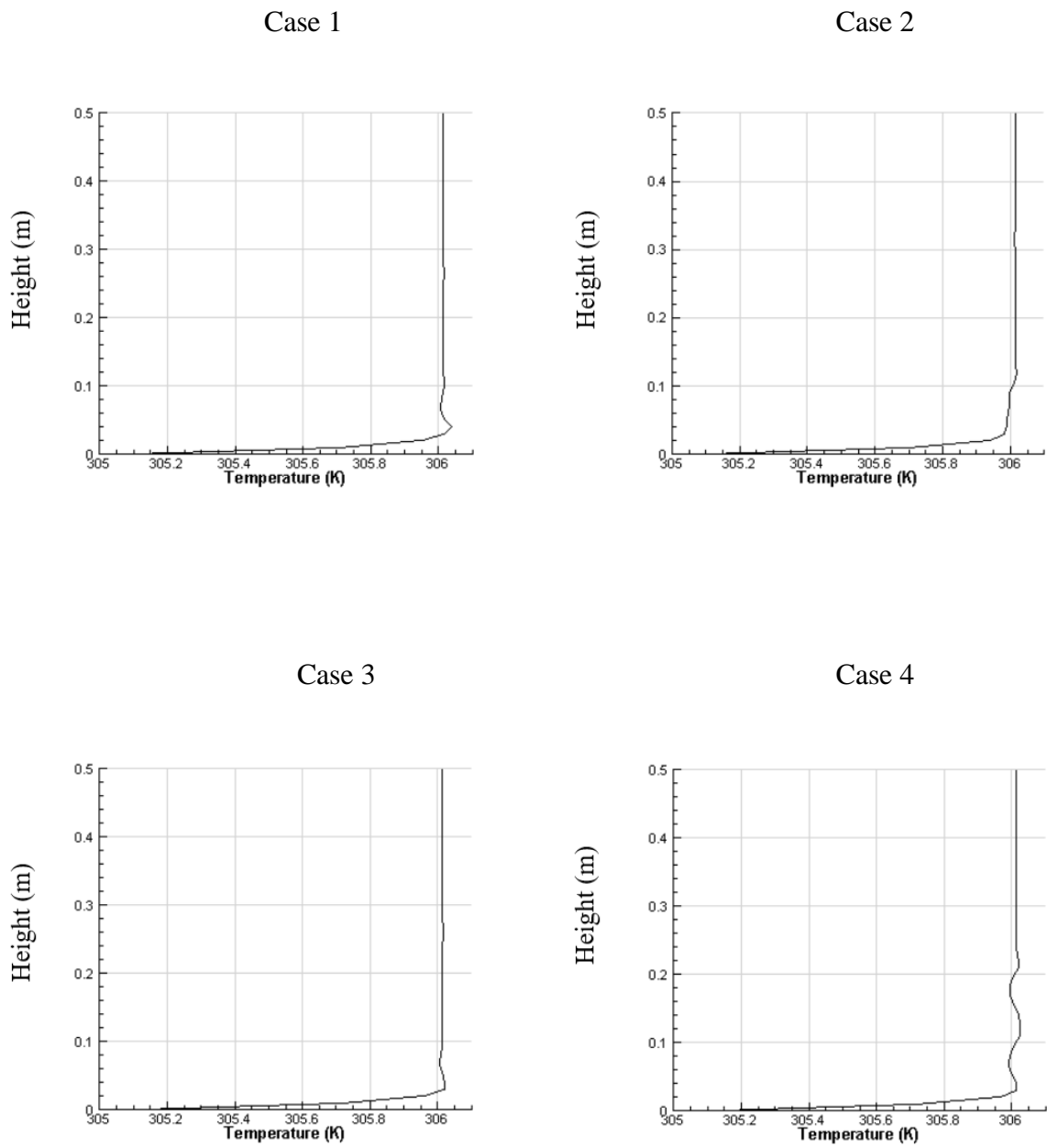
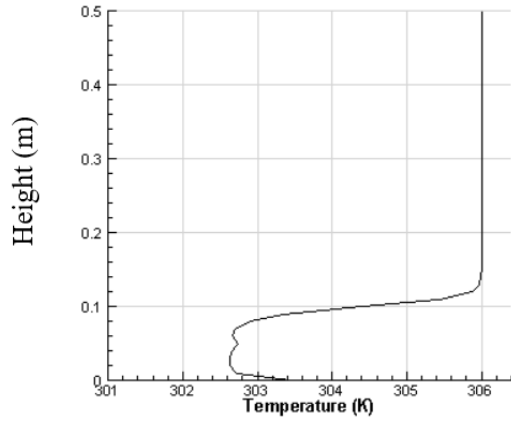
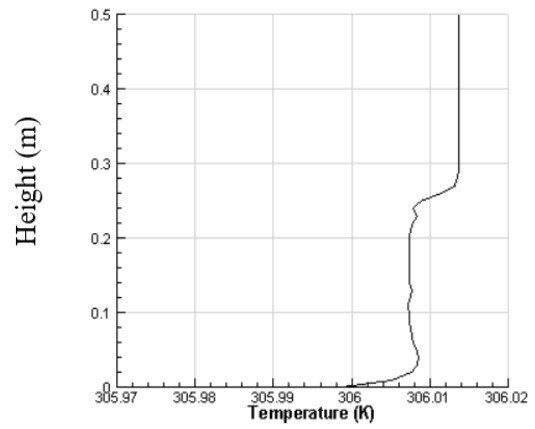


Figure 4.3: Temperature distribution in section C for four cases at $t = 3$ s

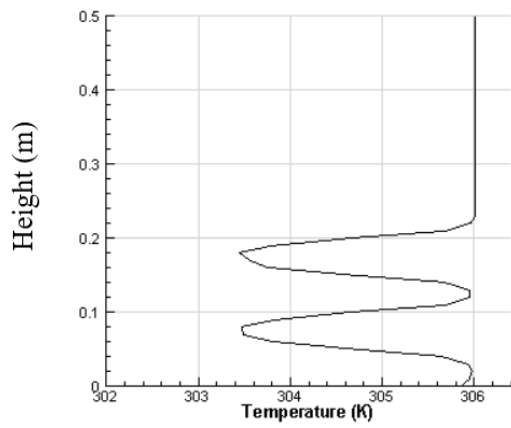
Case 1



Case 2



Case 3



Case 4

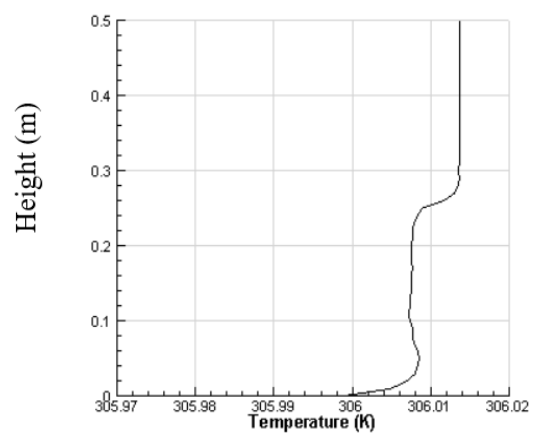
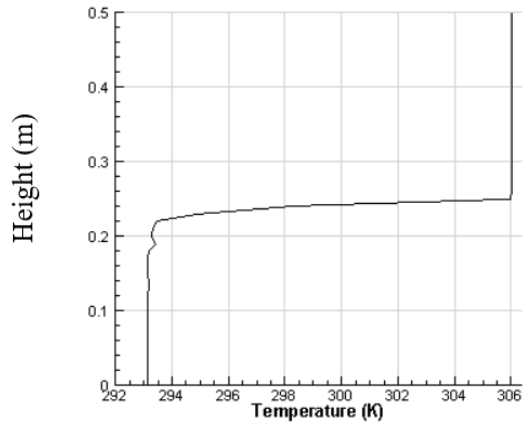
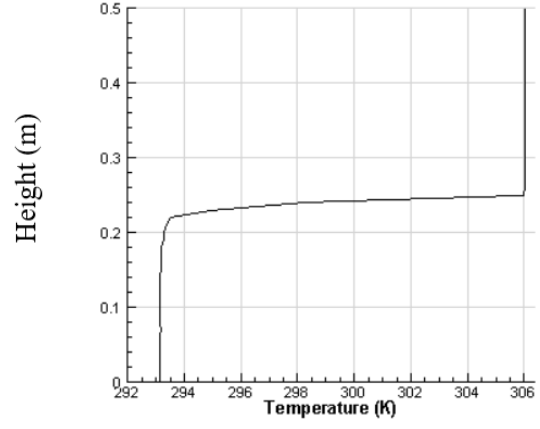


Figure 4.4: Temperature distribution in section A for four cases at $t = 5$ s

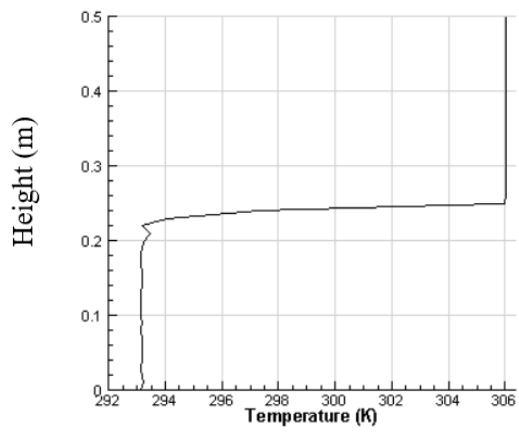
Case 1



Case 2



Case 3



Case 4

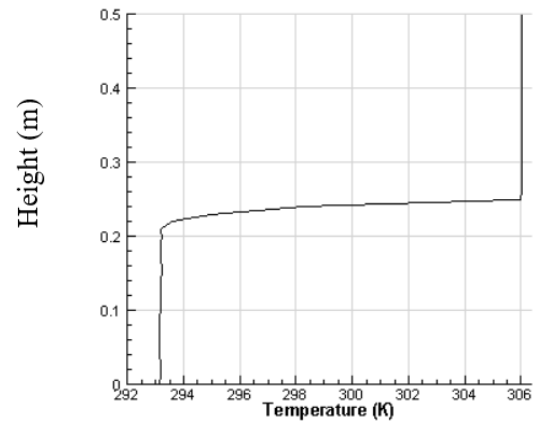
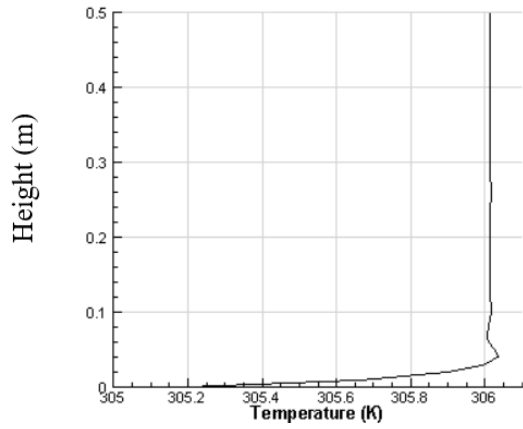
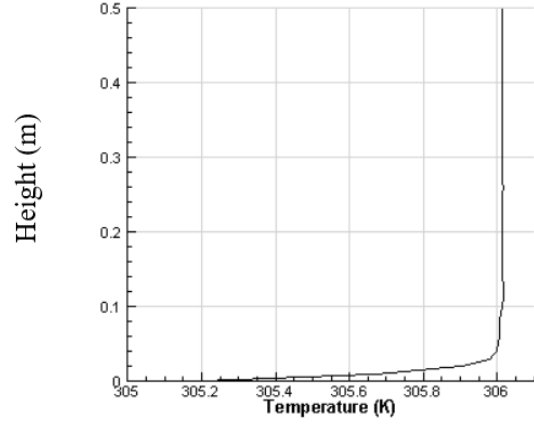


Figure 4.5: Temperature distribution in section B for four cases at $t = 5$ s

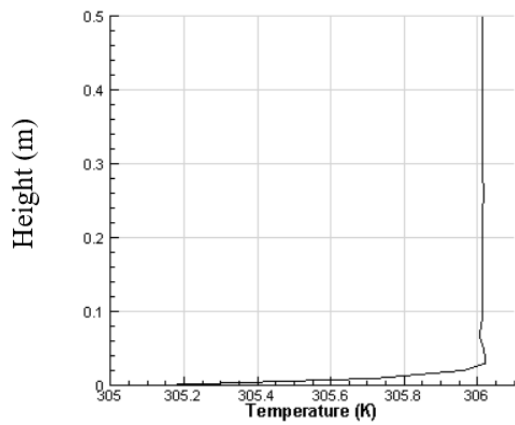
Case 1



Case 2



Case 3



Case 4

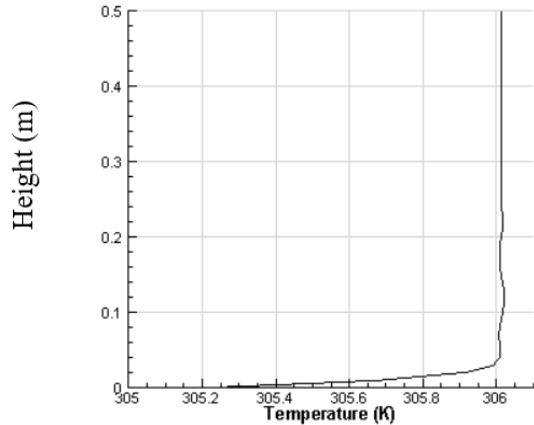
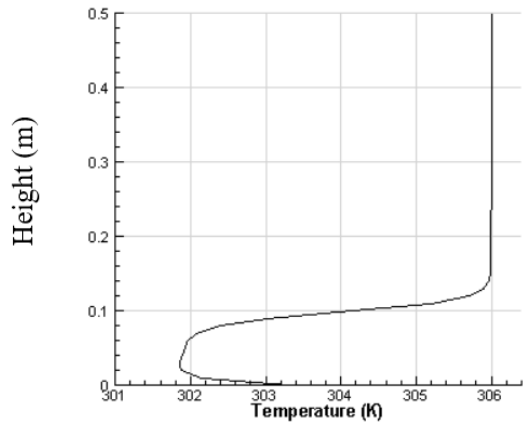
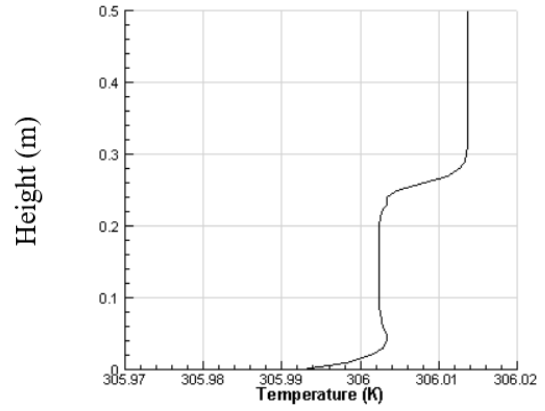


Figure 4.6: Temperature distribution in section C for four cases at $t = 5$ s

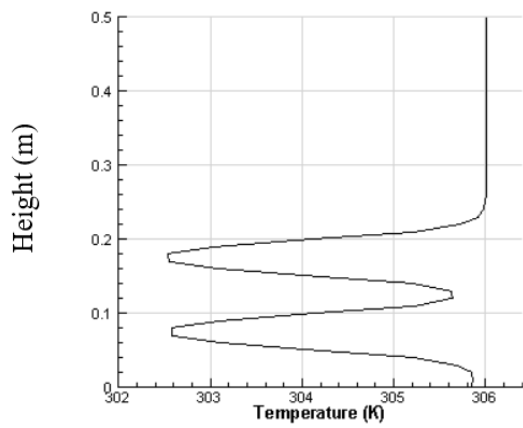
Case 1



Case 2



Case 3



Case 4

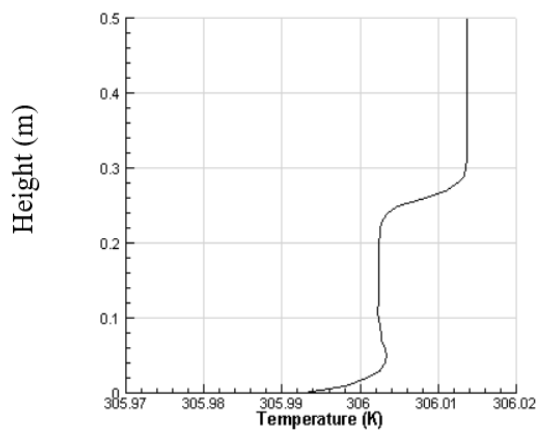
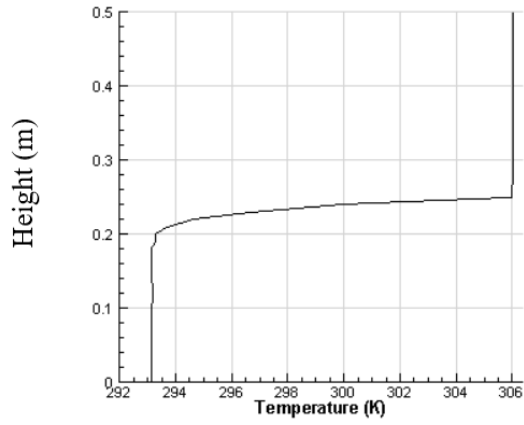
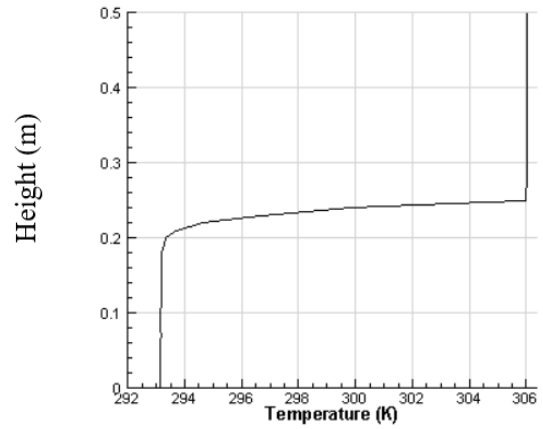


Figure 4.7: Temperature distribution in section A for four cases at $t = 10$ s

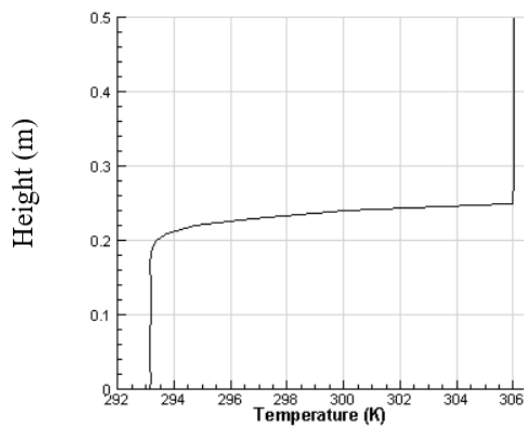
Case 1



Case 2



Case 3



Case 4

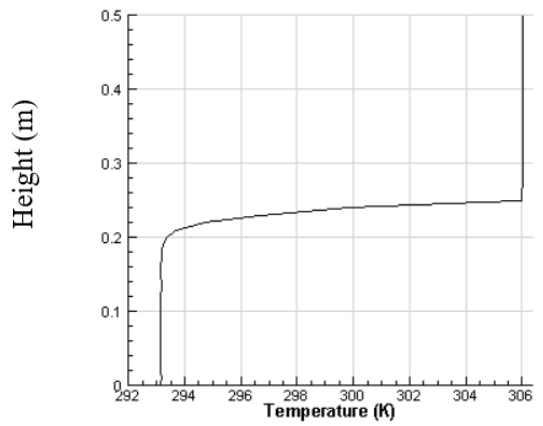
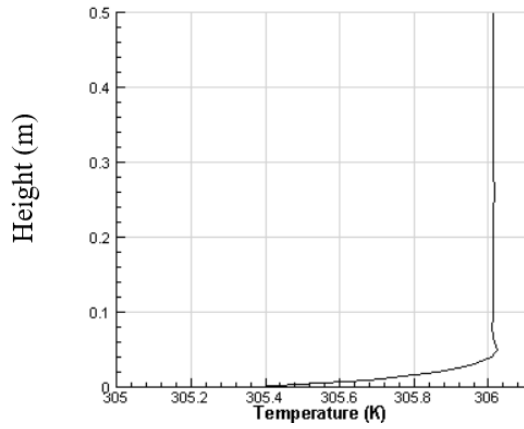
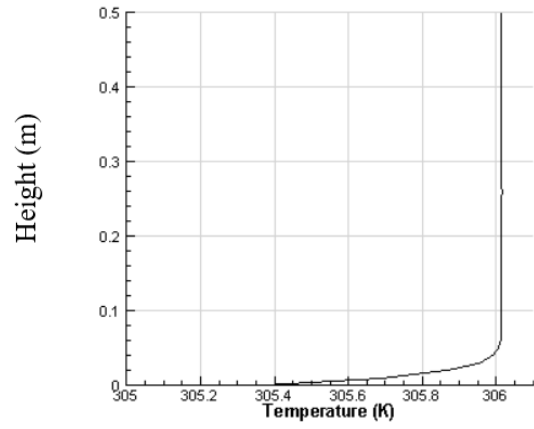


Figure 4.8: Temperature distribution in section B for four cases at $t = 10$ s

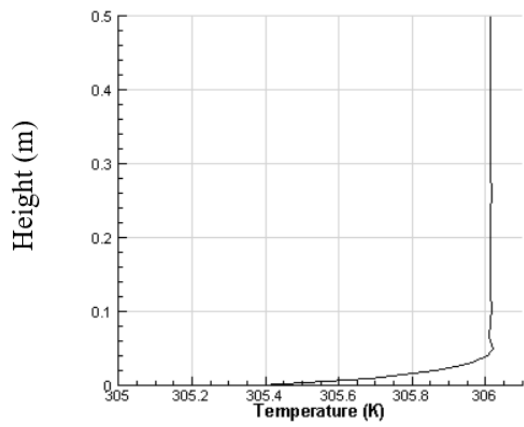
Case 1



Case 2



Case 3



Case 4

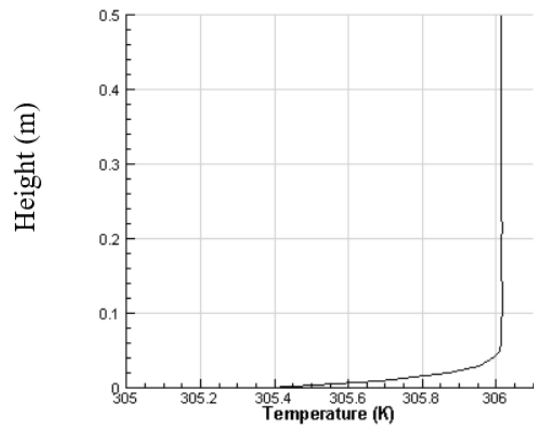


Figure 4.9: Temperature distribution in section C for four cases at $t = 10$ s

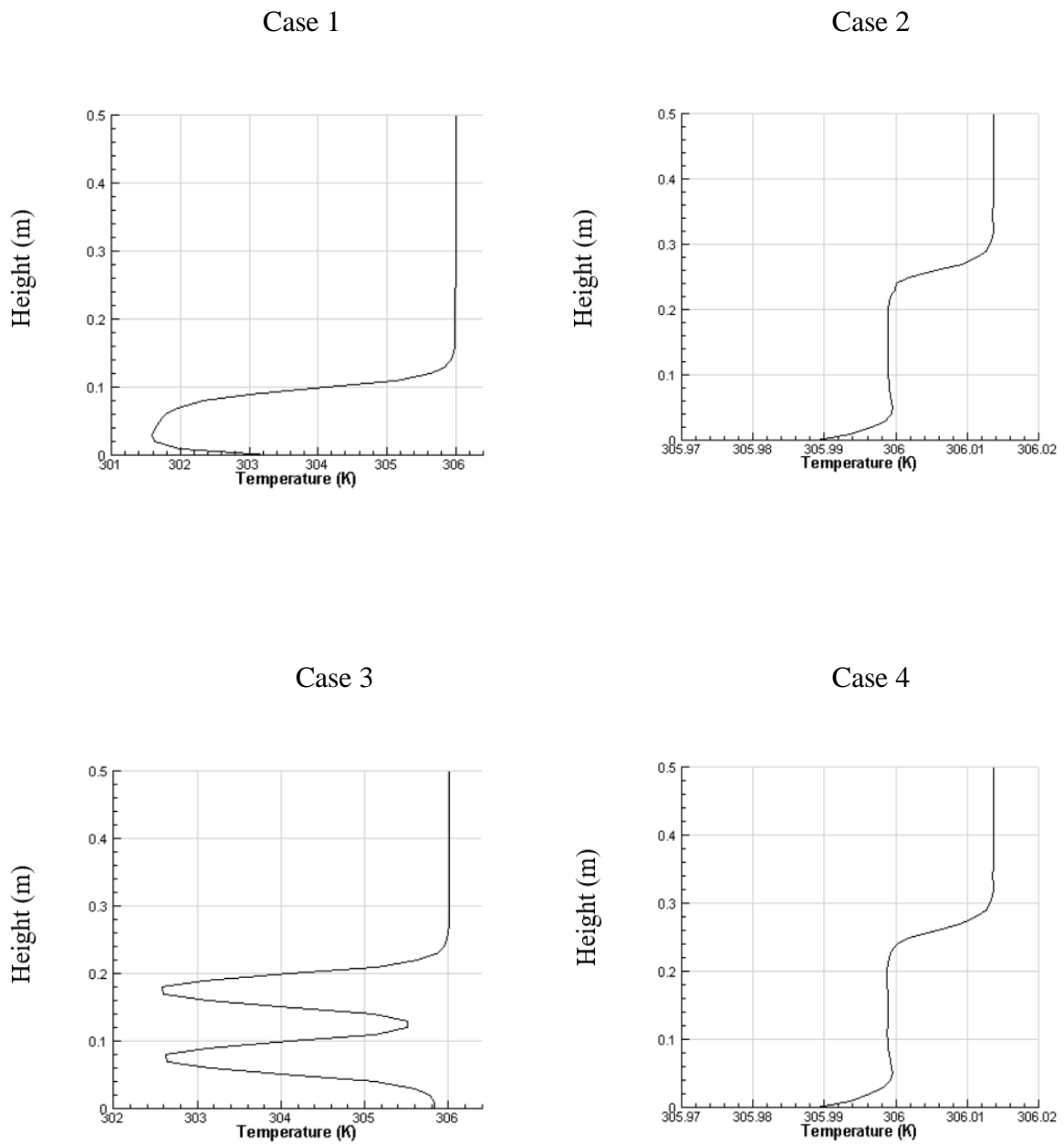
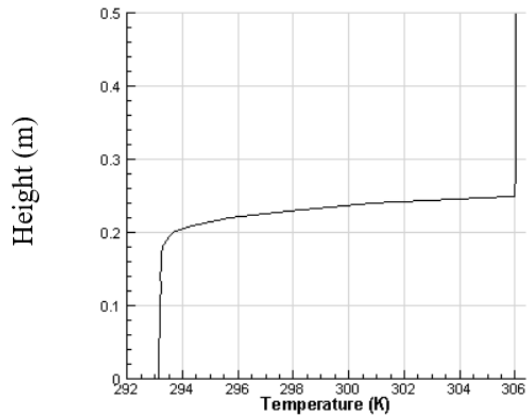
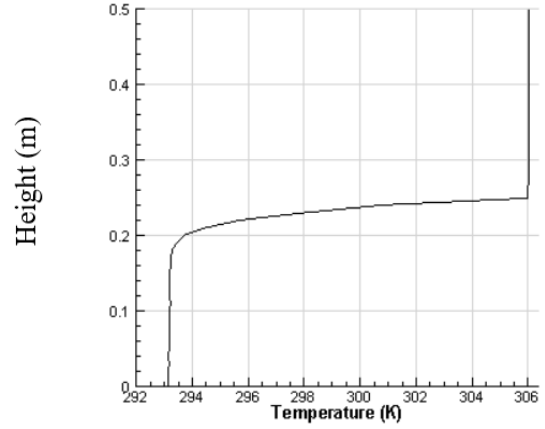


Figure 4.10: Temperature distribution in section A for four cases at $t = 15$ s

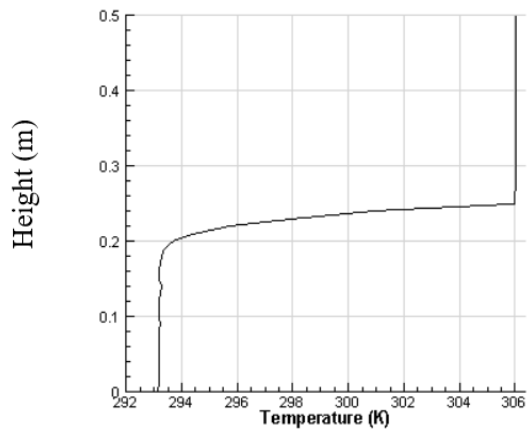
Case 1



Case 2



Case 3



Case 4

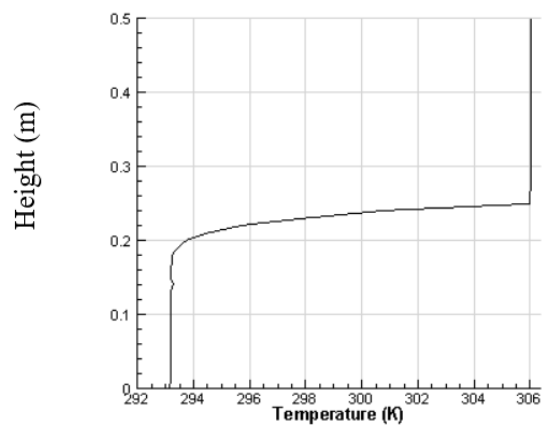
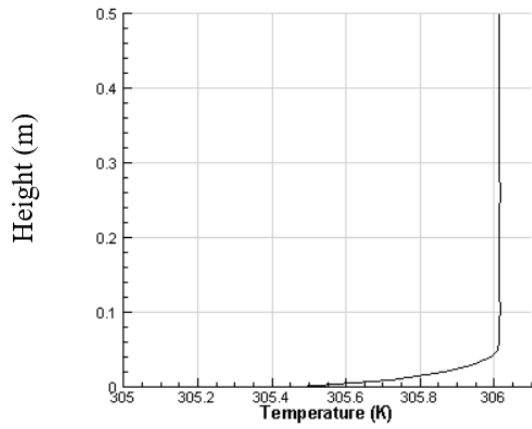
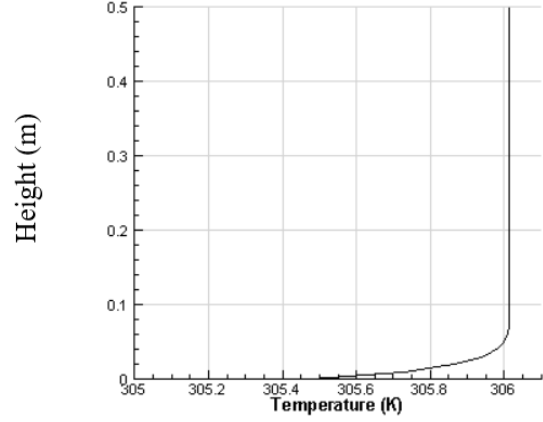


Figure 4.11: Temperature distribution in section B for four cases at $t = 15$ s

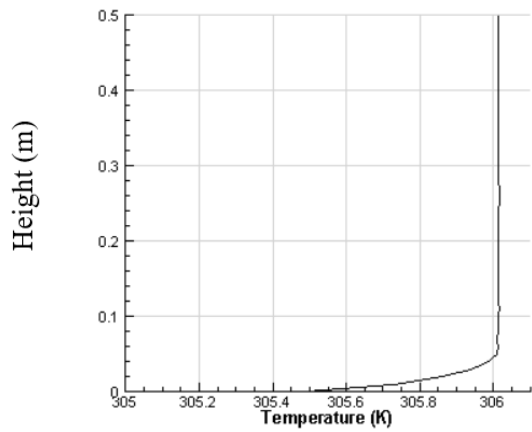
Case 1



Case 2



Case 3



Case 4

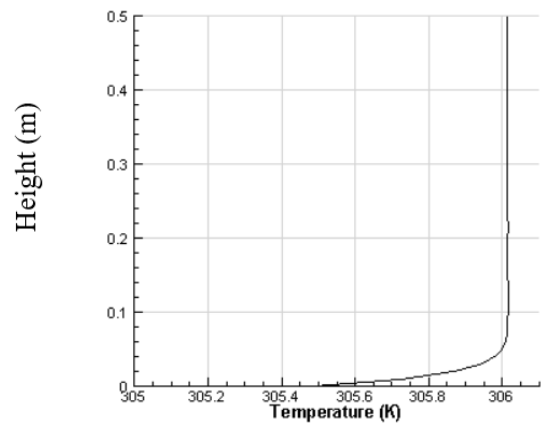


Figure 4.12: Temperature distribution in section C for four cases at $t = 15$ s

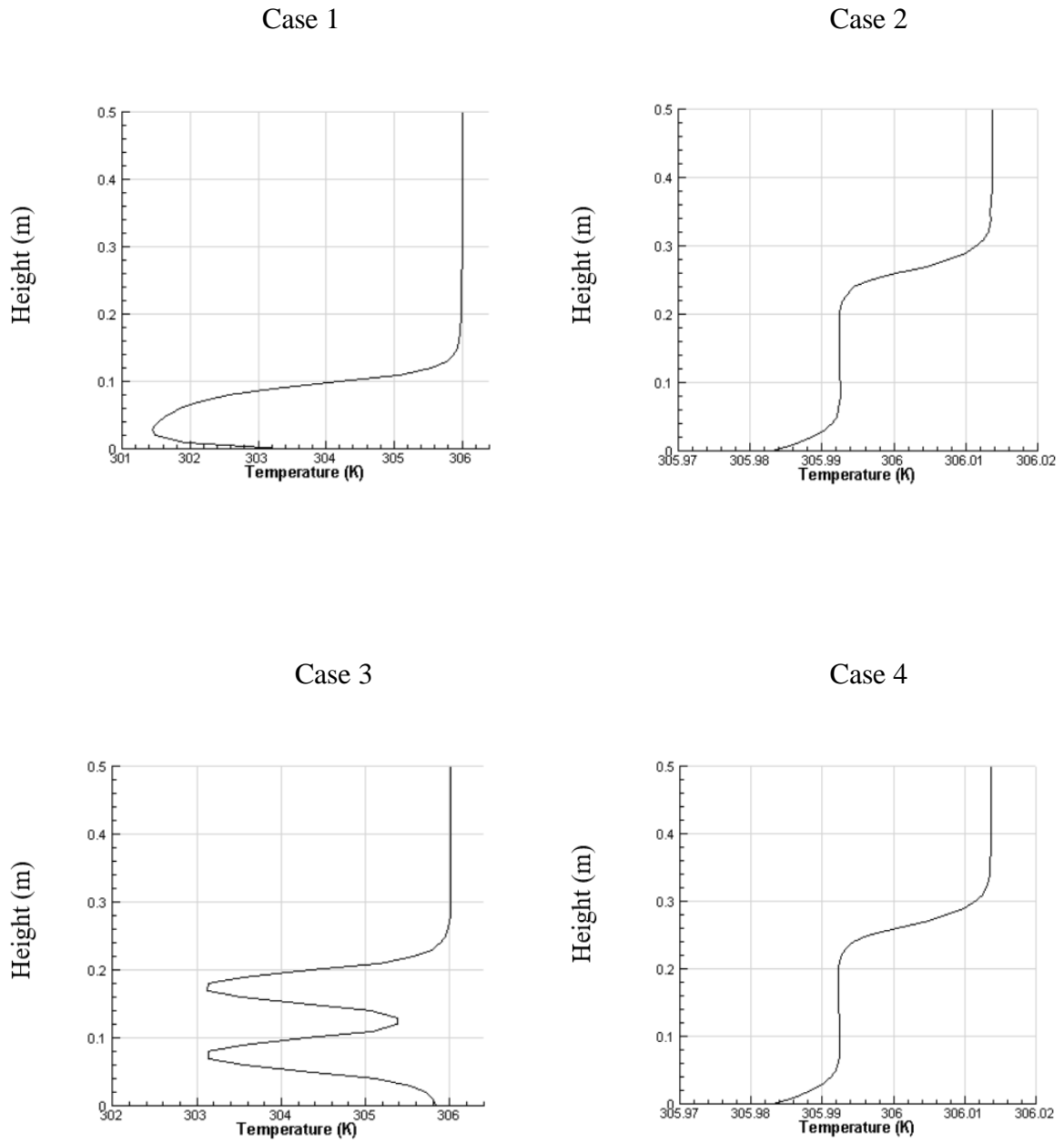
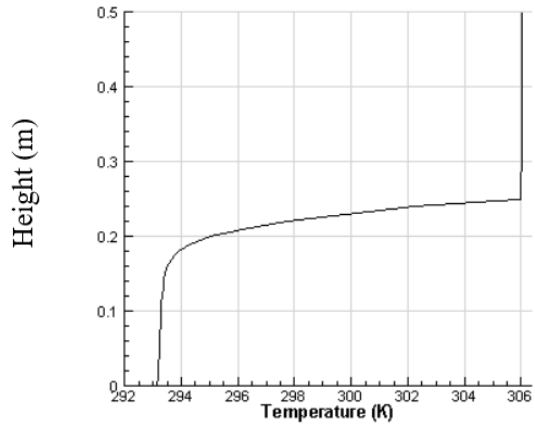
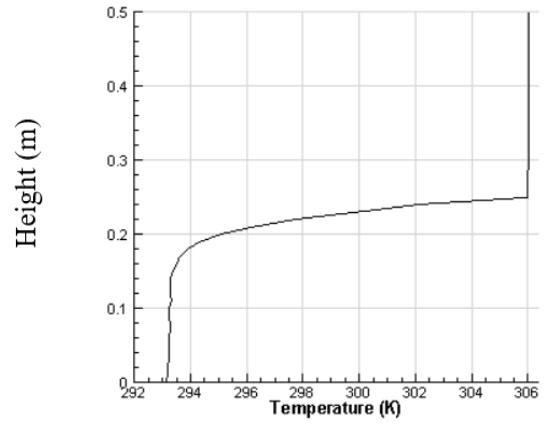


Figure 4.13: Temperature distribution in section A for four cases at $t = 30$ s

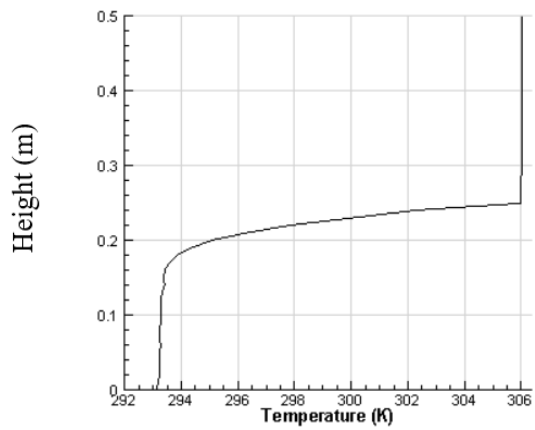
Case 1



Case 2



Case 3



Case 4

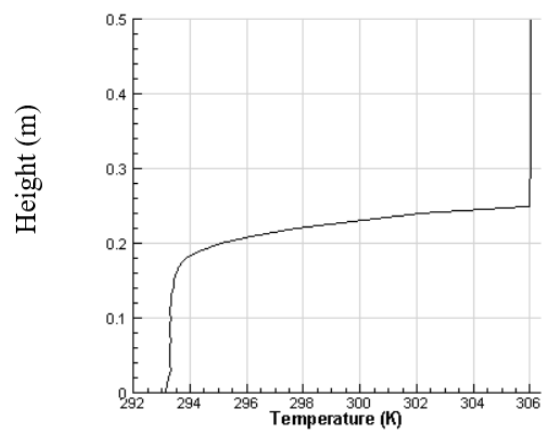


Figure 4.14: Temperature distribution in section B for four cases at $t = 30$ s

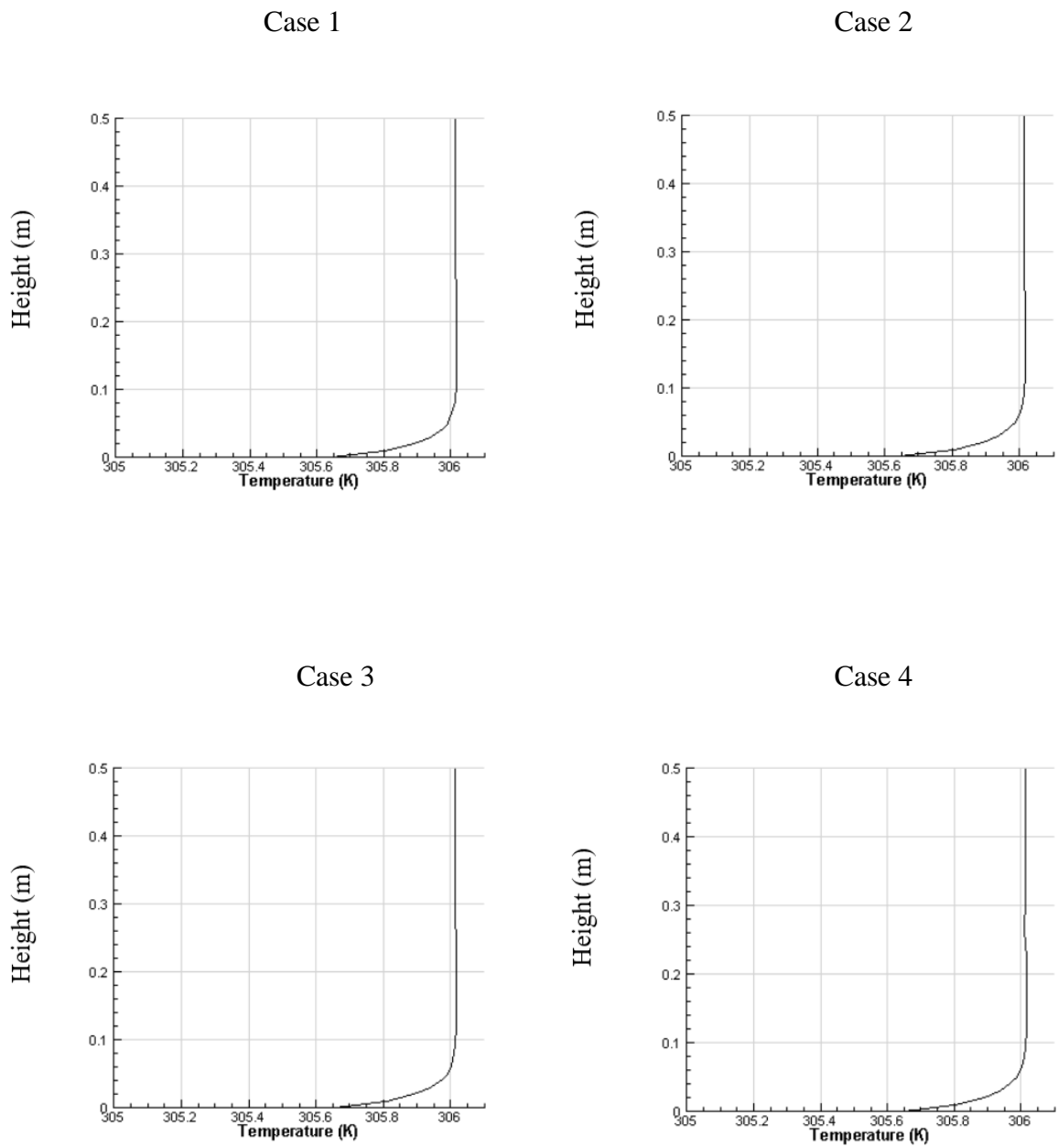


Figure 4.15: Temperature distribution in section C for four cases at $t = 30$ s

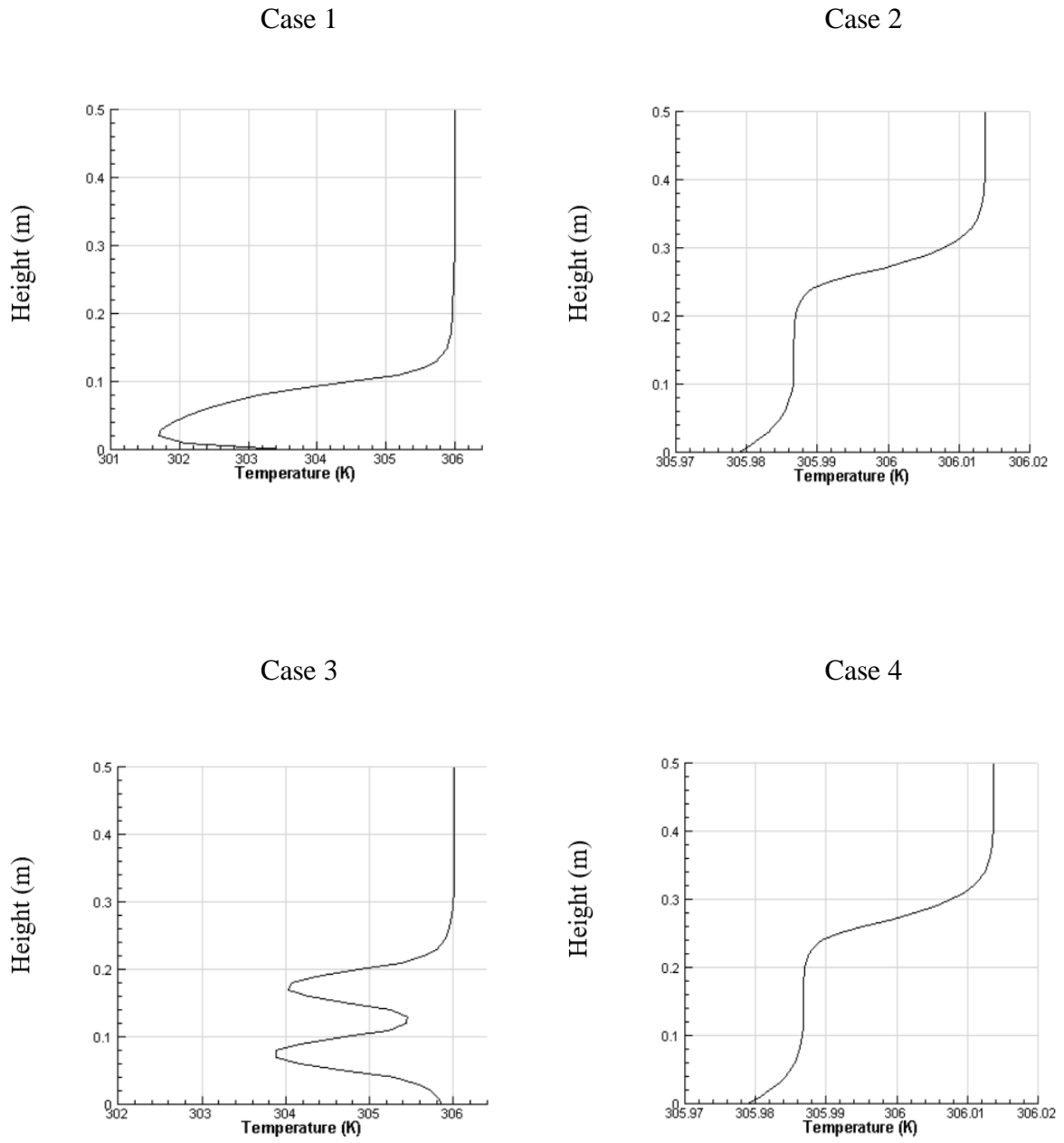
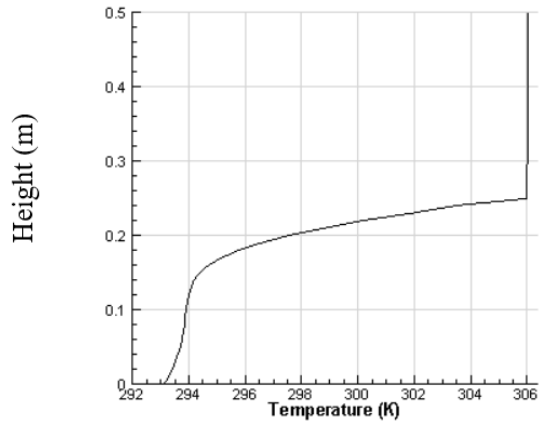
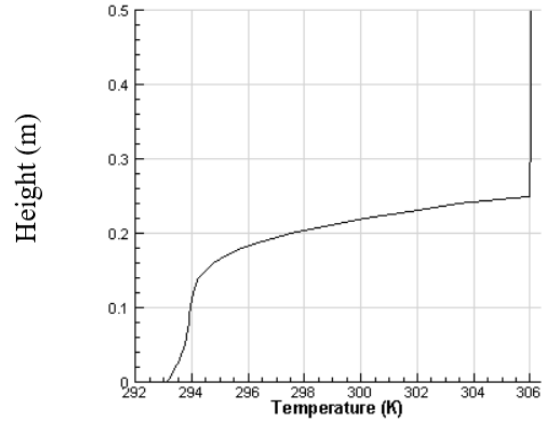


Figure 4.16: Temperature distribution in section A for four cases at $t = 60$ s

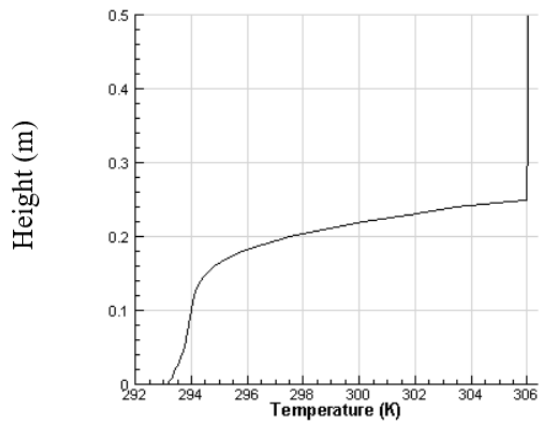
Case 1



Case 2



Case 3



Case 4

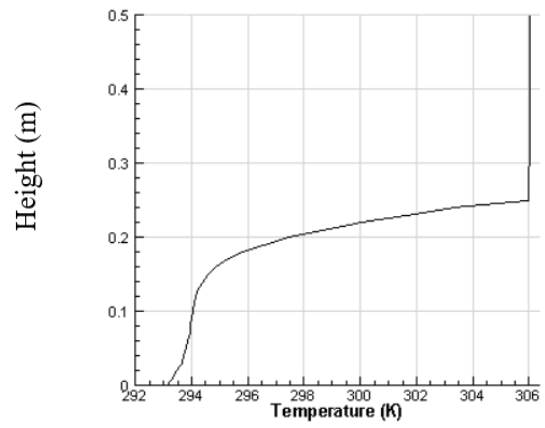
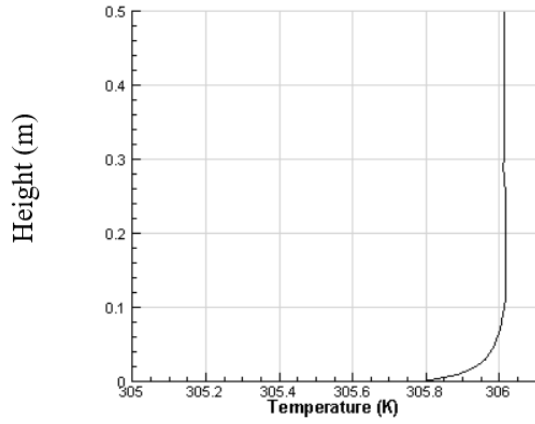
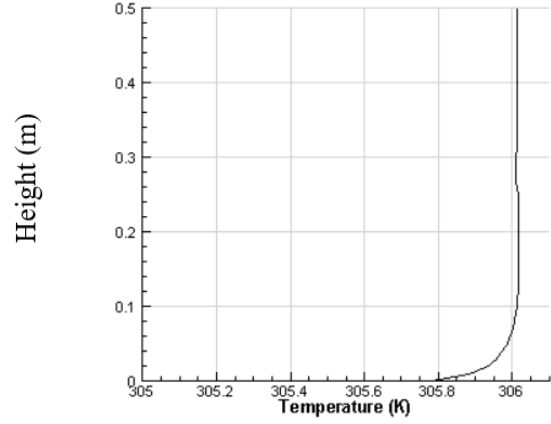


Figure 4.17: Temperature distribution in section B for four cases at $t = 60$ s

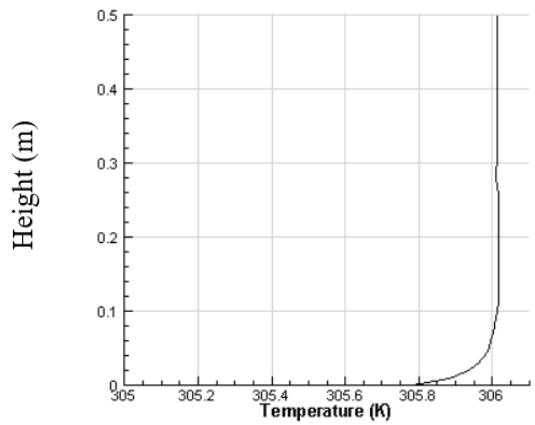
Case 1



Case 2



Case 3



Case 4

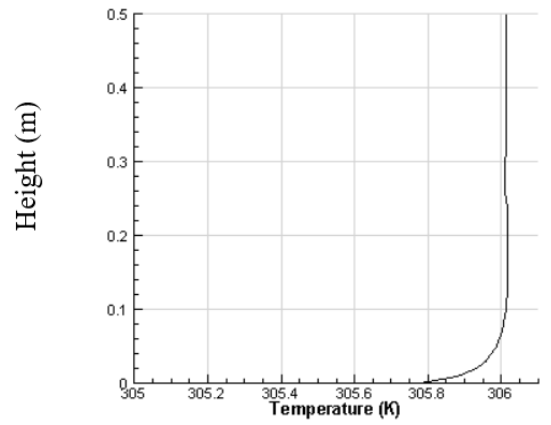
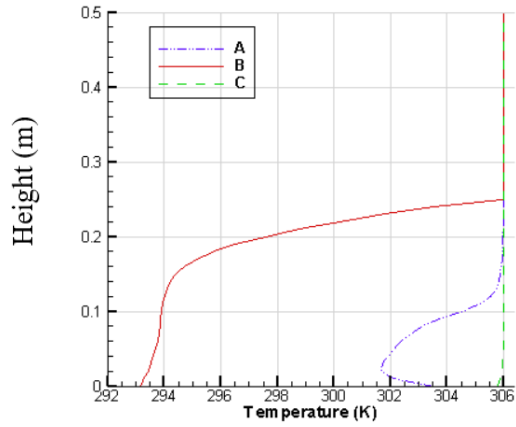
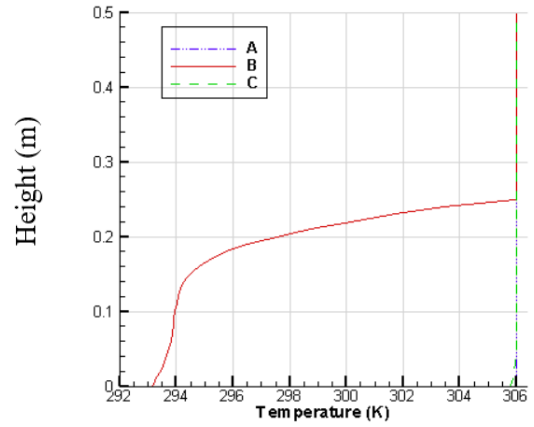


Figure 4.18: Temperature distribution in section C for four cases at $t = 60$ s

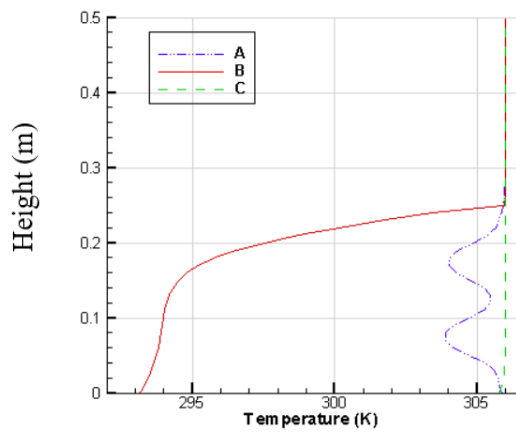
Case 1



Case 2



Case 3



Case 4

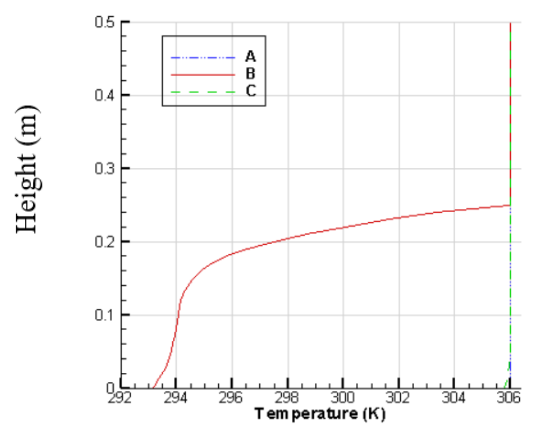
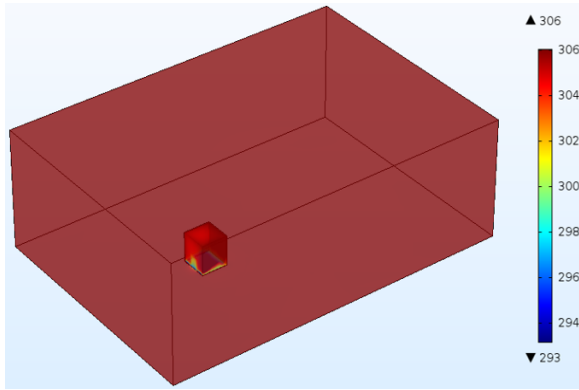
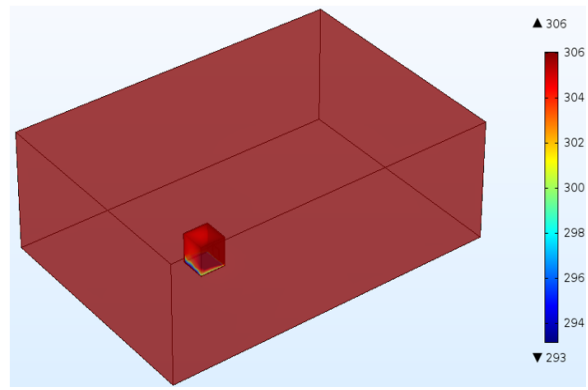


Figure 4.19: Temperature distribution in section A (Dash Dot Dot), section B (Solid line), section C (Dashed) for all cases at $t = 60$ s

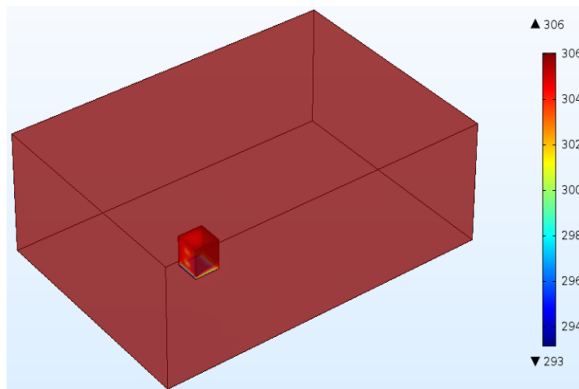
Case 1



Case 2



Case 3



Case 4

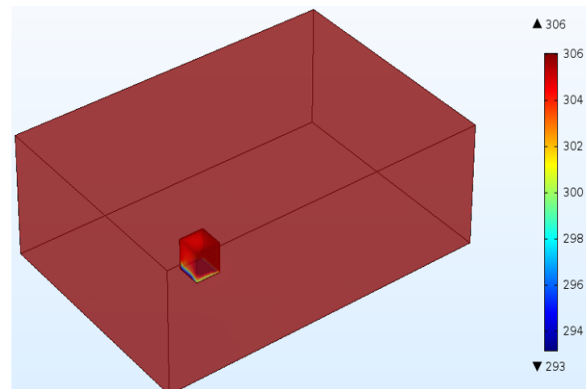
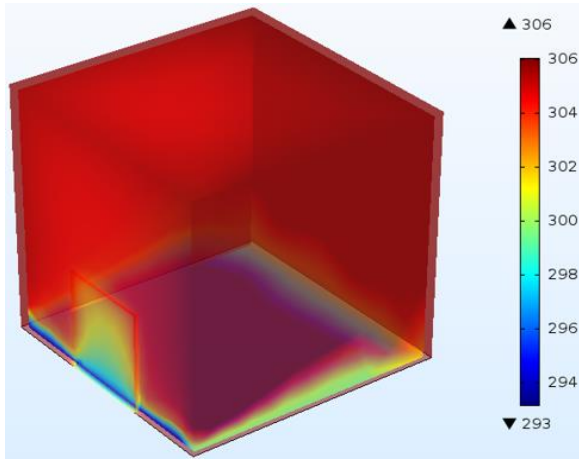
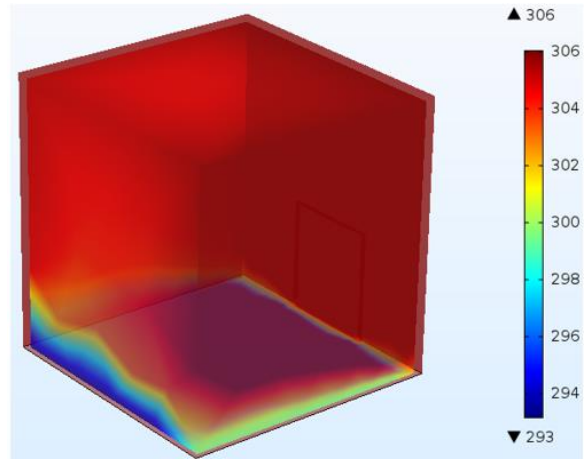


Figure 4.20: Surface temperature in computational domain for all cases at $t = 60$ s

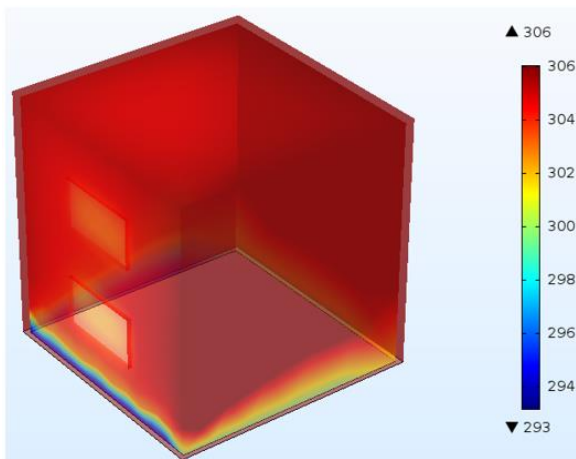
Case 1



Case 2



Case 3



Case 4

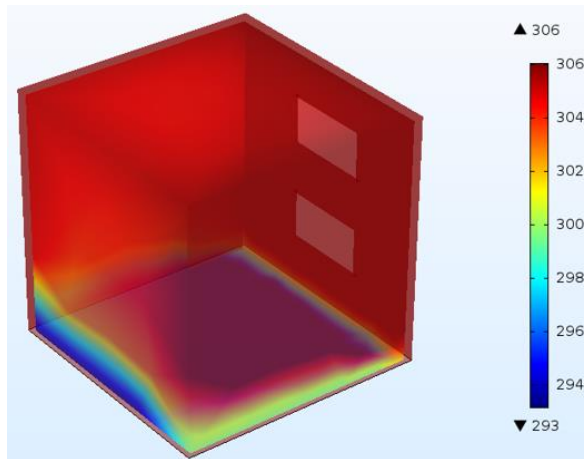
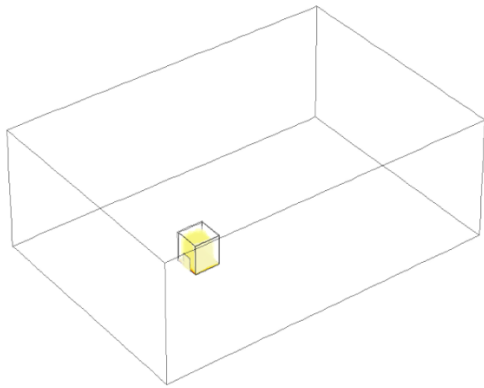
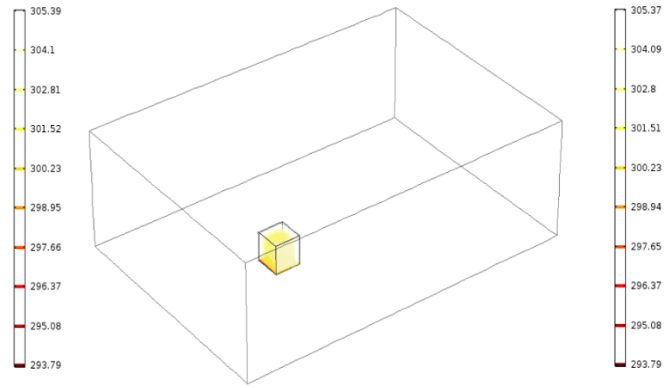


Figure 4.21: Surface temperature in building for all cases at $t = 60$ s

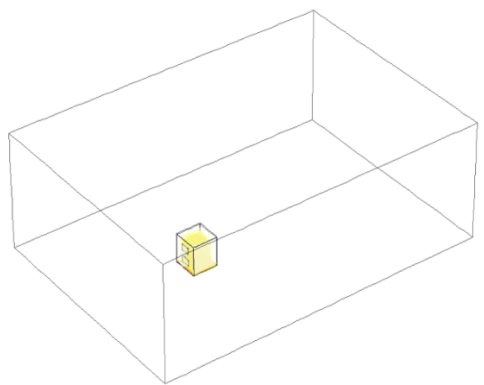
Case 1



Case 2



Case 3



Case 4

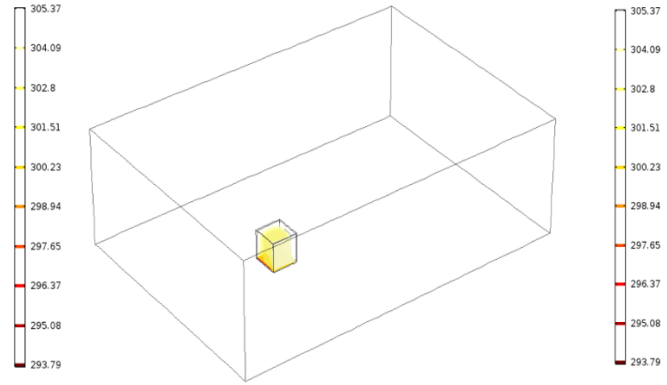
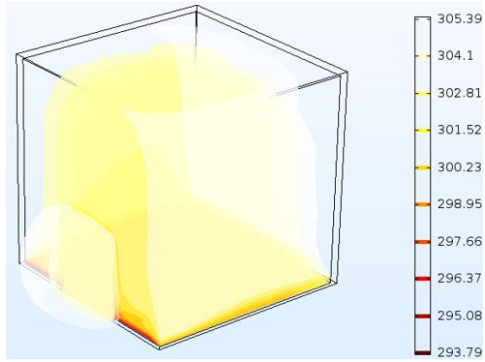
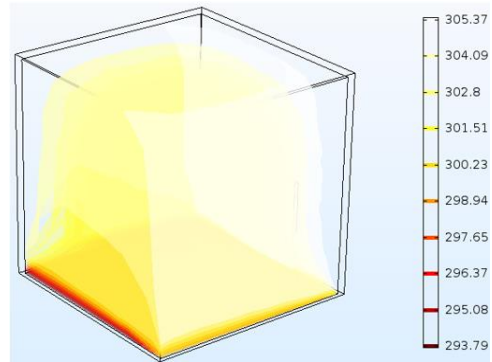


Figure 4.22: Isosurface in computational domain for all cases at $t = 60$ s

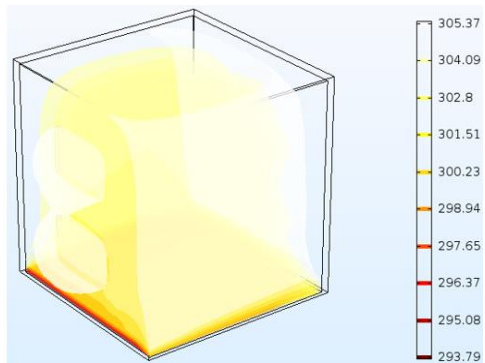
Case 1



Case 2



Case 3



Case 4

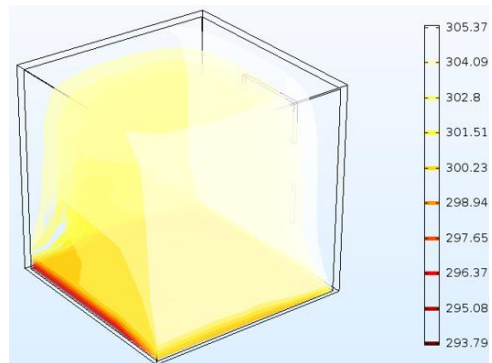


Figure 4.23: Isosurface in building for all cases at $t = 60$ s

Table 4.1: Volume Average Temperature (K) in the room at noon

	Single Windward	Single Leeward	Double Windward	Double Leeward
Time (s)	Volume Average Temperature (K)	Volume Average Temperature (K)	Volume Average Temperature (K)	Volume Average Temperature (K)
0	293.1665153111536	293.18174960041455	293.17168052796677	293.18300562478396
1	293.9613825543134	293.9600632787281	293.9600889957652	293.959124988735
2	294.38051822993526	294.3702032464736	294.37139551031925	294.3683067480971
3	294.71329656805614	294.6975990748435	294.7029917386626	294.69537457907046
4	294.99175488942893	294.9745605327375	294.9858627519709	294.97584017956785
5	295.2323724872882	295.2185600840253	295.23416905832045	295.22371503045946
10	296.16405172047865	296.16919579197037	296.1808355666653	296.1693480829345
15	296.83537782303085	296.8679075643108	296.88219722534825	296.8629045676422
20	297.3975576703203	297.4265846632843	297.4355579168931	297.4177950278883
25	297.87536435503836	297.9106007368323	297.9186604274133	297.89115199151223
30	298.2864242397725	298.34279080886563	298.3454945004384	298.3253753505509
35	298.66956047346315	298.7319275911715	298.7233060147472	298.70275992936376
40	299.02320160651385	299.07952348260005	299.05962003772163	299.02322046558044
45	299.346715644291	299.38372647803305	299.35917578173536	299.3147110040187
50	299.6410673612026	299.6594423893658	299.617672671279	299.586566409273
55	299.9037825857323	299.91068998844463	299.8595290487824	299.83802292759003
60	300.1220073021492	300.14086309775655	300.0855404953805	300.0713749351044

4.2.3 Ventilation Rate

Bangladesh is situated in both the eastern and northern hemisphere. So wind speed and wind direction is an important part for room temperature. Since this research is time dependent and also related to solar radiation so sunlight is necessary. In this study, a clear sunny day at noon is considered to calculate ventilation rate for a cubic room which is filled with air. The air flow rate for all cases are shown in Table 4.2. It is observed that, maximum and minimum ventilation rate are occurred in double windward openings and single leeward opening, respectively which are almost same as like as without effect of solar radiation. From this table it is clear that, double windward openings allows more air enter into the room than other opening/s and that's why more ventilation rate is accounted.

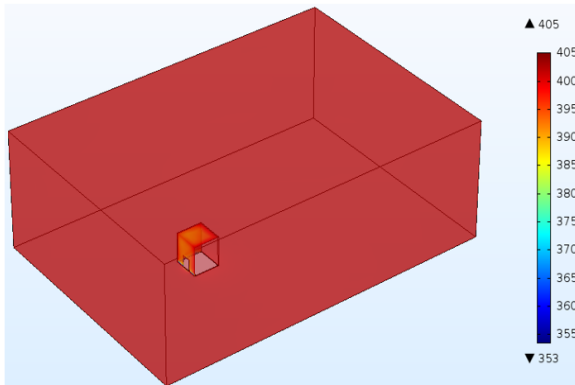
Table 4.2: Ventilation Rate for all cases at noon

	Case 1	Case 2	Case 3	Case 4
Time (s)	Ventilation Rate (m^3/s)	Ventilation Rate (m^3/s)	Ventilation Rate (m^3/s)	Ventilation Rate (m^3/s)
0.5	0.001172362091630969	0.001588568747730777	5.929694635613781E-4	0.00311752064128231
1	0.0021523975895172635	0.002401046306592673	0.0024766831973071697	0.002471364826565973
2	0.0016644301956356708	0.0013614476038673114	0.0027603430637148972	0.0019632210535251997
3	0.001673525177070272	0.0016730396613218012	0.0027843596723634728	0.0017177769997127471
4	0.001684390221120229	0.0014896484742816711	0.002780235099777419	0.0016179132917337206
5	0.0016855951893372787	0.001344218561947467	0.002779153858817295	0.0015709284222085319
10	0.0016825200188929558	9.517759770380223E-4	0.002767465206791116	0.0014756337433138532
15	0.0016863443957448243	9.249387418066147E-4	0.002769231763890396	0.0014625003332388333
20	0.0016894599237958553	9.238199687239082E-4	0.002769775767277836	0.001461104799895161
25	0.0016897975411500029	9.239219911865622E-4	0.00276955827910904	0.0014630345123159258
30	0.0016891182236171071	9.248463795067472E-4	0.00276930838288902	0.0014656838747378854
35	0.00168824519834264	9.265029230234043E-4	0.0027693633798010777	0.0014652166574941781
40	0.0016875982179310768	9.285882072373227E-4	0.002769808557825505	0.0014635545087114139
45	0.001687337104339046	9.301195131982697E-4	0.002770362783791998	0.0014638631899478818
50	0.001687485108790172	9.306673207659015E-4	0.002770124803310397	0.0014642612201423845
55	0.0016880443200622743	9.303725778035198E-4	0.002769628382766246	0.0014643110738635163
60	0.0016891437767264086	9.295641557399951E-4	0.002769219786673876	0.0014639224853118312

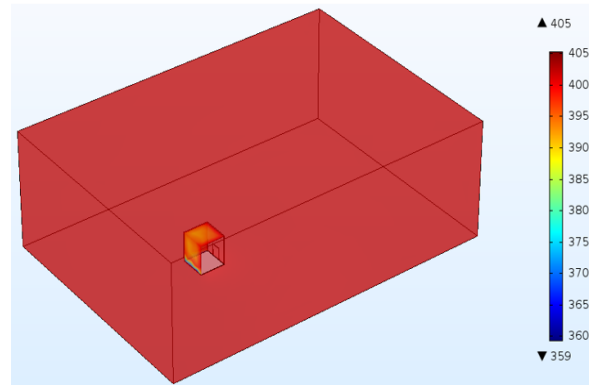
4.2.4 Radiosity

Radiosity is the summation of the reflected and the emitted radiation. Since, all objects except the transparent window are modelled as grey bodies so radiosity is another parameter which is defined as the rate at which radiation leaves a given surface per unit area. In this study, the lower surface of the computational domain and building are considered as sand and concrete materials, respectively. Figure 4.24 and Figure 4.25 show the surface radiosity for all cases of computational domain and a cubic room, respectively. Figures show that the range of the radiosity is 353 to 405 for the room as well as computational domain at noon. In a cubic room, two walls and the floor are free from surface radiosity because these walls are free from sunlight.

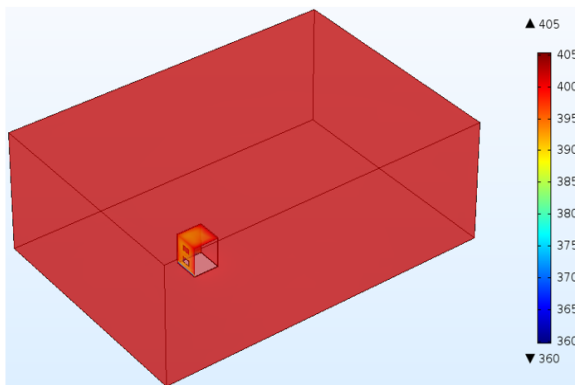
Case 1



Case 2



Case 3



Case 4

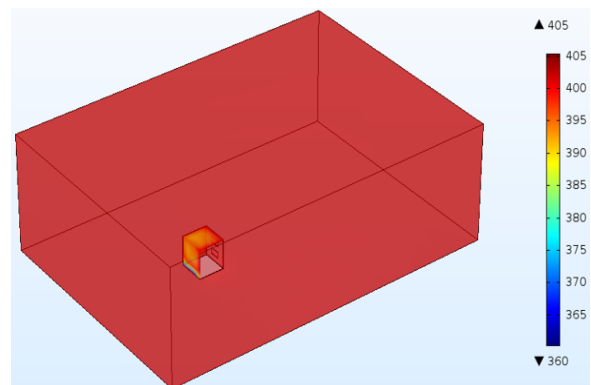
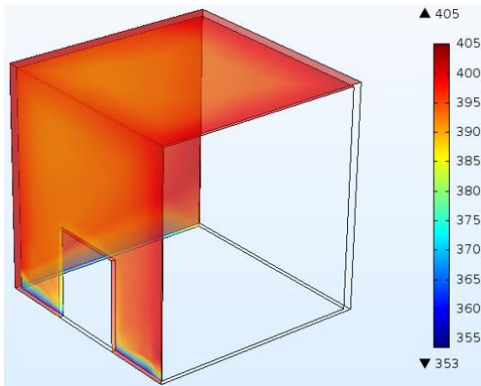
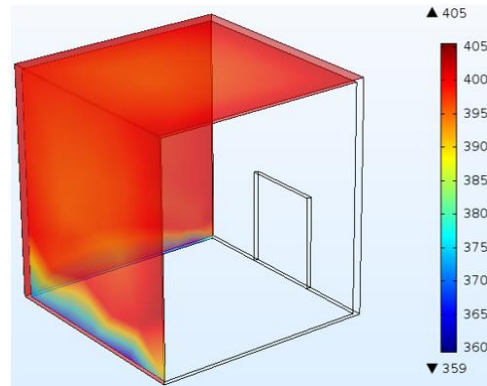


Figure 4.24: Surface radiosity in computational domain for all cases at $t = 60$ s

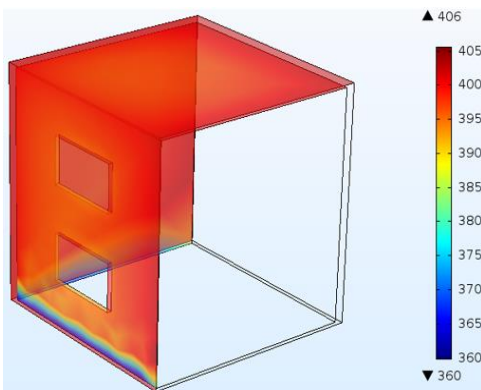
Case 1



Case 2



Case 3



Case 4

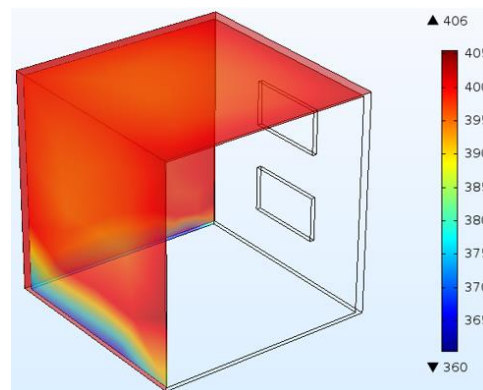


Figure 4.25: Surface radiosity in building for all cases at $t = 60$ s

People believe that the indoor environment is safe, and also the air they breathe is free from pollutants. It also essentially refers to the air quality within and around buildings, which is related to the health and comfort of building occupants. Natural ventilation is a critical strategy in the move towards energy efficient building design. Single-sided ventilation is a significant type of natural ventilation, since single-sided building forms are so prevalent, especially in the Dhaka city. The summary of this research is discussed in this chapter. A lot of outcomes have been found, but at the same time, a lot of new scopes have appeared that need to be analyzed in the future.

5.1 Conclusion

The global warming is occurred due to many reasons but air pollution is one of them. Natural Ventilation is a useful system to reduce the energy consumption and CO_2 emissions (the extraction and burning of fossil fuels) in official or residential building. Solar radiation is an important factor for the natural ventilation system, which varies during the day and each season. Indoor air quality and thermal comfort are important health safety measures to room occupants. The present investigation is focused on natural ventilation with the influence of solar radiation and without effect of solar radiation for single/double opening/s at the windward wall and the leeward wall of single-sided building. According to wind direction, four physical models are used in this research. The information about the air flow rate, flow pattern and temperature distribution are provided to observe the impact of solar radiation on natural ventilation.

From the tabular and graphical comparisons of the results of numerical computations, the findings are as follows:

- Three measurement lines are consider to observe the behavior of flow pattern. Since the problem is time dependent so the velocity of air is fluctuating with time to time. The maximum and the minimum velocity of the air is 0.5 m/s and 0 m/s respectively.
- The fluctuation of ventilation rate is from $0.0009\text{ m}^3/\text{s}$ to $0.0034\text{ m}^3/\text{s}$ that shows how much air enter into the room by the opening/s. It is observed that, maximum and minimum ventilation rates are occurred in double windward openings and single

leeward opening respectively which are almost same as like as without effect of solar radiation. So, it is clear that, the double windward openings allows more air enter into the room than other opening/s and that's why more ventilation rate is accounted.

- After the effect of sunlight, the room temperature is less than 301 K when the outside of the room temperature is fluctuating from 301 K to 306 K . Though the volume average temperature in leeward double openings is comparatively low from other cases but the ventilation rate is not in satisfactory level that means the fresh air can't enter into the room at well.
- Radiosity is another parameter which is defined as the rate at which radiation leaves a given surface per unit area. The range of the radiosity is 353 w/m^2 to 405 w/m^2 for the room as well as computational domain at noon. In a cubic room, two walls and the floor are free from surface radiosity because these walls are situated in opposite side of the sunlight.

All the output values of the model (in 4 cases) are satisfied with the ASHRAE standard. So, on the basis of the air quality and the volume average temperature, it can be concluded that the double openings in windward wall is more comfortable than the other opening/s.

5.2 Future Work

This outcome can open a new dimension in the field of an energy-efficient building to live healthily and reduce the consumption of the mechanical system and also help the designer to design buildings for considering the environmental parameters to build an energy-efficient city.

The present study can be extended by considering the following cases:

- Natural ventilating buildings highly depend on weather, which is often unpredictable. So, more research is required to the wind direction in all-weather condition.
- Physics models like cross ventilation, stack ventilation, mixed-mood ventilation may be considered for different location and different ambient temperature.

- RNG model and Large-eddy simulation can be used for comparative study.

- Building layouts and size are an important factor for air flow. Also, the thickness and materials of external wall can play a vital role to reduce the solar radiation heat gain.

- The projection effect can be used to design buildings by providing vertical windows on the equator-facing side of the building: this maximizes insolation in the winter months when the Sun is low in the sky and minimizes it in the summer when the Sun is high.

- This work can be extended by considering furniture, internal heat source like TV, Refrigerator, burner etc. in the room to analyze the airflow changes. Heat flux and natural convection are needed to consider for better result.

References

- [1] Boer, Y., Opening Keynote Statement, The United Nations Climate Change Conference, UNFCCC, Indonesia, Dec. 2007.
- [2] UNDP, “Human Development Report 2007/2008 - Fighting climate change: Human solidarity in a divided world”, United Nations Development Program, USA, 2007.
- [3] Adri, N., “Climate-Induced Migration in Bangladesh: Issues and concerns”, BIDS critical conversations, 2017.
- [4] Bahauddin, K. M., “Climate Change-induced Migration in Bangladesh: Realizing the Migration Process, Human Security and Sustainable Development”, Policy Brief for GSDR, 2016.
- [5] International Energy Agency, World Energy Outlook 2013.
- [6] Bangladesh Power Development Board, Annual Report 2018-2019.
- [7] Alam, M. S., Kabir, E., Rahman, M. M. and Chowdhury, M. A. K., “Power sector reform in Bangladesh: Electricity distribution system”, *Energy*, vol. 29(11), pp. 1773-1783, 2004.
- [8] Siddiqui, T., “Impact of Climate Change: Migration as one of the Adaptation Strategies Refugee and Migratory Movements Research Unit (RMMRU)”, Working paper series no. 18, 2010.
- [9] Reza, S. I., “Housing Crisis”, The Financial Express, Dhaka [Online], Dec. 2008.
- [10] Dhaka Power Distribution Company Limited (DPDC), Annual report 2019.
- [11] Hancock, J. M., “Dhaka Electric Supply Company Hosts Final USEA/USAID Utility Partnership Exchange Program with U.S. Distribution Utilities”, Retrieved 15 Dec. 2008, from http://www.usea.org/Programs/EPP/EPP_News/DESCO_12_2006.pdf.
- [12] Vangtook, P. and Chirattananon, S., “Application of Radiant Cooling as a Passive Cooling Option in Hot Humid Climate”, *Building and Environment*, vol. 42(2), pp. 543-556, 2007.
- [13] Zain, Z. M., Taib, M. N. and Baki, S. M. S., “Hot and Humid Climate: Prospect for Thermal Comfort in Residential Building”, *Desalination*, vol. 209(1-3), pp. 261-268, 2007.
- [14] Khan, S. I., Mahfuz, M. U., Aziz, T., and Zobair, N. M., “Prospect of Hybrid Wind System in Bangladesh,” in *Second International Conference on Electrical and Computer Engineering ICECE 2002*, pp. 212-215, Dec. 2002.

- [15] Ahmed, Z. N., *The Effects of Climate on the Design and Location of Windows in Bangladesh*, Ph.D. Thesis, Department of Building Science, Sheffield University, 1987.
- [16] Ahsan, T., *Passive Design Features for Energy-Efficient Residential Buildings in Tropical Climates: the context of Dhaka, Bangladesh*, Master's Thesis in Environmental Strategies Research, Department of Urban Planning and Environment Division of Environmental Strategies Research – fms, Stockholm, 2009.
- [17] Rahman, M. S., Saha, S. K., Khan, M. R. H., Habiba, U., and Chowdhury, S. M. H., "Present Situation of Renewable Energy in Bangladesh: Renewable Energy Resources Existing in Bangladesh", *Global Journal of Researches in Engineering Electrical and Electronics Engineering*, vol. 13(5), 2013.
- [18] Energy Information Administration, *International Energy Outlook 2019 with projections to 2050*.
- [19] Tamami, K., "Fundamentals of Building Heat Transfer", *Journal of Research of the National Bureau of Standards*, vol. 82(2), pp. 97-106, 1977.
- [20] Jiang, Y., Alexander, D., Jenkins, H., Arthur, R., and Chen, Q., "Natural ventilation in buildings: measurements in a wind tunnel and numerical simulation with large-eddy simulation", *Journal of Wind Engineering and Industrial Aerodynamics*, vol. 91(3), pp. 331–353, 2003.
- [21] Allocca, C., Chen, Q., and Glicksman, L. R., "Design analysis of single-sided natural ventilation," *Energy and Buildings*, vol. 35(8), pp. 785-795, 2003.
- [22] Jiang, Y., and Chen, Q., "Buoyancy-driven single-sided natural ventilation in buildings with large openings", *International Journal of Heat and Mass Transfer*, vol. 46(6), pp. 973–988, 2003.
- [23] Seifert, J., Li, Y., Axley, J., and Rösler, M., "Calculation of wind-driven cross ventilation in buildings with large openings", *Journal of Wind Engineering and Industrial Aerodynamics*, vol. 94(12), pp. 925-947, 2006.
- [24] Evola, G., and Popov, V., "Computational Analysis of wind Driven natural ventilation in buildings", *Energy and Buildings*, vol. 38, pp. 491-501, 2006.
- [25] Larsen, T. S., and Heiselberg, P., "Single-sided natural ventilation driven by wind pressure and temperature difference," *Energy and Buildings*, vol. 40(6), pp. 1031-1040, 2008.

- [26] Bangalee, M. Z. I., Lin, S. Y., and Miao, J. J., “Wind driven natural ventilation through multiple windows of a building: A Computational Approach”, *Energy and Building*, vol. 45, pp. 317-325, 2012.
- [27] Montazeri, H., and Blocken, B., “CFD simulation of wind-induced pressure coefficients on buildings with and without balconies: Validation and sensitivity analysis”, *Building and Environment*, vol. 60, pp. 137-149, 2013.
- [28] Idris, A., and Huynh, B. P., “Analysis of single-sided ventilated room with different location of windows opening using CFD”, *Congress of Numerical Methods in Engineering – CMN*, Bilbao, Spain, 25-28 June, 2013.
- [29] Gendelis, S., and Jakovics, A., “Influence of solar radiation and ventilation conditions on heat balance and thermal comfort conditions in living-rooms,” in *5th Baltic Heat Transfer Conference*, Saint-Petersburg, Russia, pp. 634-643, 2007.
- [30] Ahmmad, M. R., “Statistical Analysis of the Wind Resources at the Importance for Energy Production in Bangladesh”, *International Journal of u- and e- Service, Science and Technology*, vol. 7, pp. 127-136, 2014.
- [31] Hossain, M., Bhuiya, M. R., and Al-Mamun, M. M., “An analysis of the temperature change of Dhaka city,” in *5th International Conference on Environmental Aspects of Bangladesh*, pp. 46-48, 2014.
- [32] Hasan, M. R., *Computational study of natural ventilation air flow and heat transfer calculation for a room of different flow path and window configurations in Bangladesh*, M. Phil Thesis, Department of Mathematics, Bangladesh University of Engineering and Technology, 2019.
- [33] Jones, D. L., and Hudson, J. (1998), *Architecture and the Environment: Bioclimatic Building Design*, Laurence King, London.
- [34] Allard, F. (1998), *Natural Ventilation in Buildings: A Design Handbook*, James & James Ltd, London.
- [35] Eftekhari, M. M., Marjanovic, L. D., and Pinnock, D. J., “Air flow distribution in and around a single-sided naturally ventilated room,” *Building and Environment*, vol. 38(3), pp. 389-397, 2003.
- [36] Ayad, S. S., “Computational study of natural ventilation”, *Journal of Wind Engineering and Industrial Aerodynamics*, vol. 82, pp. 49-68, 1999.
- [37] Chen, Q., and Srebric, J., “Application of CFD tools for indoor and outdoor environment design”, *International Journal on Architectural Science*, vol. 1(1), pp. 14-29, 2000.

- [38] Allocca, C., Chen, Q., and Glicksman, L. R., “Design analysis of single-sided natural ventilation,” *Energy and Buildings*, vol. 35(8), pp. 785-795, 2003.
- [39] Gan, G., “Effective depth of fresh air distribution in rooms with single-sided natural ventilation,” *Energy and Buildings*, vol. 31(1), pp. 65-73, 2000.
- [40] Visagavel, K., and Srinivasan, P. S. S., “Analysis of single side ventilated and cross ventilated rooms by varying the width of the window opening using CFD”, *Solar Energy*, vol. 83(1), pp. 2-5, 2009.
- [41] Chen, Q., “Using computational tools to factor wind into architectural environment design”, *Energy and Buildings*, vol. 36(12), pp. 1197-1209, 2004.
- [42] Spengler, J. D., Samet, J. M., and McCarthy, J. F., “Indoor Air Quality Handbook,” in Q. Chen and L. R. Glicksman, *Application of computational fluid dynamics for indoor air quality studies*, chap. 59, McGRAW-HILL, 2001.
- [43] Yakhot, V., Orszag, S. A., Thangam, S., Gatski, T. B., and Speziale, C. G., “Development of turbulence models for shear flows by a double expansion technique”, *Physics of Fluids A Fluid Dynamics*, vol. 4(7), pp. 1510-1520, 1992.
- [44] Welty, J. R., Wicks, C. E., Wilson, R. E., and Rorrer, G. L. (2000), *Fundamentals of Momentum, Heat, and Mass Transfer*, 5th Edition, John Wiley & Sons, USA.
- [45] Cengel, Y. A. (2007), *Heat and Mass Transfer: Fundamentals & Applications*, 3rd Edition, McGraw-Hill, New York.
- [46] Holman, J. P. (2010), *Heat Transfer*”, 10th Edition, McGraw-Hill, New York.
- [47] Rahman, M. H., and Islam, A. K. M. S., “CFD Modelling of Natural and Forced Ventilation system in a conventional kitchen in Bangladesh,” in *The 13th Asian Congress of Fluid Mechanics*, pp. 460-464, 17-19 December 2010.
- [48] Tham, K. W., “Indoor air quality and its effects on humans – A review of challenges and developments in the last 30 years”, *Energy and Buildings*, vol. 130, pp. 637–650, 2016.
- [49] Jones, A. P., “Indoor air quality and health”, *Atmospheric Environment*, vol. 33, pp. 4535–4564, 1999.
- [50] Sundell, J., “On the history of indoor air quality and health”, *Indoor Air*, vol. 14 (s7), pp. 51–58, 2004.
- [51] Cheung, C. K., Fuller, R. J., and Luther, M. B., “Energy-efficient envelope design for high-rise apartments”, *Energy and Buildings*, vol. 37, pp. 37–48, 2005.
- [52] ASHRAE (2010), *ASHRAE Standard: Thermal Environment Standards for Human Occupancy*, Atlanta, GA 30329.